

# Computer assisted proofs for transverse collision and near collision orbits in the restricted three body problem

Maciej J. Capiński<sup>1</sup>

*AGH University of Science and Technology, al. Mickiewicza 30, 30-059 Kraków, Poland*

Shane Kepley

*Vrije Universiteit Amsterdam, De Boelelaan 1105, 1081 HV Amsterdam, Netherlands*

J.D. Mireles James<sup>2</sup>

*Florida Atlantic University, 777 Glades Road, Boca Raton, Florida, 33431*

---

## Abstract

This paper considers two point boundary value problems for conservative systems defined in multiple coordinate systems, and develops a flexible a posteriori framework for computer assisted existence proofs. Our framework is applied to the study collision and near collision orbits in the circular restricted three body problem. In this case the coordinate systems are the standard rotating coordinates, and the two Levi-Civita coordinate systems regularizing collisions with each of the massive primaries. The proposed framework is used to prove the existence of a number of orbits which have long been studied numerically in the celestial mechanics literature, but for which there are no existing analytical proofs at the mass and energy values considered here. These include transverse ejection/collisions from one primary body to the other, Strömberg's asymptotic periodic orbits (transverse homoclinics for  $L_{4,5}$ ), families of periodic orbits passing through collision, and orbits connecting  $L_4$  to ejection or collision.

*Keywords:* Celestial mechanics, collisions, transverse homoclinic, computer assisted proofs.

*2010 MSC:* 37C29, 37J46, 70F07.

---

## 1. Introduction

The present work develops computer assisted arguments for proving theorems about collision and near collision orbits in conservative systems. Using these arguments, we

---

<sup>1</sup>M. C. was partially supported by the NCN grants 2019/35/B/ST1/00655 and 2021/41/B/ST1/00407.

<sup>2</sup>J.D.M.J. was partially supported by NSF Grant DMS 1813501

*Email addresses:* `maciej.capinski@agh.edu.pl` (Maciej J. Capiński), `s.kepley@vu.nl` (Shane Kepley), `jmirelesjames@fau.edu` (J.D. Mireles James)

*Preprint submitted to Elsevier*

*March 23, 2023*

answer several open questions about the dynamics of the planar circular restricted three body problem (CRTBP), a simplified model of three body motion popular since the pioneering work of Poincaré [1, 2, 3]. Our approach combines classical Levi-Civita regularization with a multiple shooting scheme for two point boundary value problems (BVPs) describing orbits which begin and end on parameterized curves/symmetry sets in an energy level. After numerically computing an approximate solution to the BVP, we use a Newton-Krawczyk theorem to establish the proof of the existence of a true solution nearby. The a posteriori argument makes extensive use of validated Taylor integrators for vector fields and variational equations. See also Remark 10 for several additional remarks about the relationship between the present work and the existing literature.

The PCRTBP, defined formally in Section 3, describes the motion of an infinitesimal particle like a satellite, asteroid, or comet moving in the field of two massive bodies which orbit their center of mass on Keplerian circles. The massive bodies are called the primaries, and one assumes that their orbits are not disturbed by the addition of the massless particle. Changing to a co-rotating frame of reference results in autonomous equations of motion, and choosing normalized units of distance, mass, and time reduces the number of parameters in the problem to one: the mass ratio of the primaries. The system has a single first integral referred to as the Jacobi constant, usually written as  $C$ .

It is important to remember that for systems with a conserved quantity, periodic orbits occur in one parameter families – or tubes – parameterized by “energy” or conserved quantity. We note also that the CRTBP has an equilibrium solution, also called a Lagrange point or libration point, called  $L_4$  in the upper half plane forming an equilateral triangle with the two primaries. (Similarly,  $L_5$  forms an equilateral triangle in the lower half plane). We are interested in the following questions for the CRTBP.

- **Q1:** *Do there exist orbits of the infinitesimal body, which collide with one primary in forward time, and the other primary in backward time?* We refer to such orbits as primary-to-primary ejection-collisions.
- **Q2:** *Do there exist orbits of infinitesimal body which are asymptotic to the  $L_4$  in backward time, but which collide with a primary in forward time?* (Or the reverse - from ejection to  $L_4$ ). We refer to these as  $L_4$ -to-collision orbits (or ejection-to- $L_4$  orbits).
- **Q3:** *Do there exist orbits of the infinitesimal body which are asymptotic in both forward and backward time to  $L_4$ ?* Such orbits are said to be homoclinic to  $L_4$ .
- **Q4:** *Do there exist tubes of large amplitude periodic orbits for the infinitesimal body, which accumulate to an ejection-collision orbit with one of the primaries?* Such tubes are said to terminate at an ejection-collision orbit.
- **Q5:** *Do there exist tubes of periodic orbits for the infinitesimal body which accumulate to a pair of ejection-collision orbits going from one primary to the other and back?.* Such tubes are said to terminate at a consecutive ejection-collision.

The questions 1 and 4 are known to have affirmative answers in various perturbative situations, but they are open for many mass ratios and/or values of the Jacobi constant. There is also numerical evidence suggesting the existence of  $L_4$  homoclinic orbits, and consecutive ejection-collisions. However, questions 2,3, and 5 are not perturbative, and

until now they remain open. We review the literature in more detail in Section 1.1. The following theorems, for non-perturbative mass and energy parameters of the planar CRTBP, constitute the main results of the present work.

**Theorem 1.** *Consider the PCRTBP with mass ratio  $1/4$  and Jacobi constant  $C = 3.2$ . There exist at least two transverse ejection-collision orbits which transit between the primary bodies. One of these is ejected from the large primary and collides with the smaller, and the other is ejected from the smaller primary and collides with the larger. Both orbits make this transition in finite time as measured in the original/synodic coordinates. (See page 39 for the precise statement).*

**Theorem 2.** *Consider the PCRTBP with equal masses and Jacobi constant  $C_{L_4} = 3$ . There exists at least one ejection-to- $L_4$  orbit, and at least one  $L_4$ -to-collision. These orbits take infinite (forward or backward) time to reach  $L_4$ . (See page 41 for the precise statement.) Analogous orbits exist for  $L_5$  by symmetry.*

**Theorem 3.** *Consider the PCRTBP with equal masses and Jacobi constant  $C_{L_4} = 3$ . There exist at least three distinct transverse homoclinic orbits to  $L_4$ . (See page 43 for the precise statement). Analogous orbits exist for  $L_5$  by symmetry considerations. These orbits take infinite time to accumulate to  $L_4$ . As a corollary of transversality, (see also Remark 7) there exist chaotic subsystems in some neighborhood of each homoclinic orbit.*

**Theorem 4.** *Consider the PCRTBP with Earth-Moon mass ratio. There exists a one parameter family of periodic orbits which accumulate to an ejection-collision orbit originating from and terminating with the Earth. The ejection collision orbit has Jacobi constant  $C \approx 1.434$ , and has “large amplitude”, in the sense that it passes near collision with the Moon. This ejection-collision occurs in finite time in synodic/unregularized coordinates. (See page 45 for the precise statement.)*

**Theorem 5.** *Consider the PCRTBP with equal masses. There exists a family of periodic orbits which accumulate to a consecutive ejection-collision orbit involving both primaries. Each of the ejection-collisions occurs in finite time in synodic/unregularized coordinates. The Jacobi constant of the consecutive ejection-collision orbit is  $C \approx 2.06$ . (See page 47 for the precise statement.)*

Each of the theorems is interesting in its own right, as we elaborate on in the remarks below. Nevertheless, we note that the mass ratios and energies in the theorems have been chosen primarily to illustrate that our approach can be applied in many different settings. Similar theorems could be proven at other parameter values, or in other problems involving collisions, using the methodology developed here. We also remark that our results make no claims about global uniqueness. There could be many other such orbits for the given parameter values. However, due to the transversality, such orbits cannot be arbitrarily close to the orbits whose existence we prove.

**Remark 6 (Ballistic transport).** Theorem 1 establishes the existence of ballistic transport, or zero energy transfer, from one primary to the other in finite time (think of this as a “free lunch” trip between the primaries). In physical terms, ballistic transport allows debris to diffuse between a planet and its moon, or between a star and one of its planets,

using only the natural dynamics of the system. This phenomena is observed for example when Earth rocks, ejected into space after a meteor strike, are later discovered on the Moon [4] (or vice versa). Martial applications of low energy Moon-to-Earth transfer are discussed in [5, 6]. Mathematically rigorous existence proofs for primary-to-primary ejection-collision orbits have until now required both small mass ratio and high velocity – that is, negative enough Jacobi constant. See [7].

In a similar fashion, Theorem 2 establishes the existence of zero energy transfers involving  $L_4$  and a primary, and could for example be used to design space missions which visit the triangular libration points.

**Remark 7 (Termination orbits).** Theorems 3, 4, 5 involve the termination of tubes of periodic orbits. Indeed, a corollary of Theorem 3 is that there are families/tubes of periodic orbits accumulating to each of our  $L_4$  homoclinics. This follows from a theorem of Henrard [8]. Another corollary is that, near each of the orbits of Theorem 3, there is an invariant chaotic subsystem in the  $L_4$  energy level. This is due to a theorem of Devaney [9].

Numerical evidence for the existence of  $L_4$  homoclinics in the equal mass CRTBP appears already in the work of Strömngren in the 1920’s [10, 11]. See [12, 13, 14] for more discussion. Such orbits were once called *asymptotic periodic orbits*, in light of the fact that they are closed loops with infinite period. Despite of the fact that they appeared in the literature more than a hundred years ago, the present work provides – to the best of our knowledge – the first mathematically rigorous existence proof of transverse  $L_4$  homoclinics in the CRTBP.

In Theorems 4 and 5, we first prove the existence of the ejection-collision orbits, and then directly establish the existence of one parameter families of periodic orbits terminating at these ejection-collision orbits by an application of the implicit function theorem.

Termination orbits have a long history in celestial mechanics, and are of fundamental importance in equivariant bifurcation theory. We refer the interested reader to the discussion of “Strömngren’s termination principle” in Chapter 9 of [14], and to the works of [15, 16, 17] on equivariant families in the Hill three body and restricted three body problems. See also the works of [18, 19] on global continuation families in the restricted  $N$ -body problem.

**Remark 8 (Final fate of the velocity variables).** Chazy’s 1922 paper [20] proved an important classification result describing the possible asymptotic behavior of the position variables of three body orbits defined for all time. In the context of the CRTBP, Chazy’s result says that orbits are either hyperbolic (massless particle goes to infinity with non-zero final velocity), parabolic (massless particle goes to infinity with zero final velocity), bounded (massless particle remains in a bounded region for all time), or oscillatory (the lim sup of the distance from the origin is infinite, while the lim inf is finite – that is, the massless particle makes infinitely many excursions between neighbourhoods of the origin and infinity). An analogous complete classification theorem for the velocity variables does not exist, however we note that our Theorems 2 and 3 and establish the existence of orbits with interesting asymptotic velocities. For example the  $L_4$  to collision orbits of Theorem 2 have zero asymptotic velocity and reach infinite velocity in forward time (or vice versa), while the homoclinics of Theorem 3 have zero forward and backward asymptotic velocity.

**Remark 9 (Moulton’s  $L_4$  periodic orbits).** The family of periodic orbits whose existence is established in Theorem 5 is of Moulton’s  $L_4$  type, in the sense of [21]. That is, these are periodic orbits which when projected into the  $(x, y)$  plane (i.e. the configuration space) have non-trivial winding about  $L_4$ . See also Chapter 9 of [14], or the works of [13, 12] for a more complete discussion of the history (and controversy) surrounding Moulton’s orbits. The present work provides, to the best of our knowledge, the first proof that Moulton type  $L_4$  periodic orbits exist.

The remainder of the paper is organized as follows. The next three subsections briefly discuss some literature on regularization of collision, numerical computational methods, and computer assisted methods of proof in celestial mechanics. We conclude them with Remark 10 which places our work in the context of the discussed works. These sections can be skimmed by the reader who wishes to dive right into the mathematical setup, which is described in Section 2. There we describe the problem setup in terms of an appropriate multiple shooting problem, and establish tools for solving it. In particular, we define the unfolding parameters which we use to isolate transverse solutions in energy level sets and use this notion to formulate Theorem 16 and Lemma 19 which we later use for our computer assisted proofs. The role of the unfolding parameter is to add a missing variable, which is needed for solving the problems by means of zero finding with a Newton method. The unfolding parameter is an artificial variable added to the equations. It is added though in a way that ensures that we can recover the solution of the original problem from the appended one. (See Remark 14 for more detailed comments.) In Section 3 we describe the planar CRTBP and its Levi-Civita regularization. Sections 4, 5, and 6 describe respectively the formulation of the multiple shooting problem for primary-to-primary ejection-collision orbits,  $L_4$  to ejection/collision orbits,  $L_4$  homoclinic orbits, and periodic ejection-collision families. Section 7 describes our computer assisted proof strategy and illustrates how this strategy is used to prove our main theorems. Some technical details are given in the appendices. The codes implementing the computer assisted proofs discussed in this paper are available at the homepage of the first author MC.

## Literature review

### 1.1. Geometric approach to collision dynamics

Suppose one were to choose, more or less arbitrarily, an initial configuration of the gravitational  $N$ -body problem. A fundamental question is to ask “does this initial configuration lead to collision between two or more of the bodies in finite time?” The question is delicate, and remains central to the theory even after generations of serious study. Saari for example has shown that the set of orbits which reach collision in finite time (the *collision set*) has measure zero [22, 23], so that  $N$ -body collisions are in some sense physically unlikely. On the other hand, results due to Kaloshin, Guardia, and Zhang prove that the collision set can be  $\gamma$ -dense in open sets [24]. Though this notion of density is technical, the result shows that the embedding of the collision set may be topologically complicated.

One of the main tools for studying collisions is to introduce coordinate transformations which regularize the singularities. The virtue of a regularizing coordinate change, from a geometric perspective, is that it transforms the singularity set in the original coordinates

into a nicer geometric object. For example, after Levi-Civita regularization in the planar CRTBP, the singularity sets (restricted to a particular fixed energy level) are transformed into circles [25]. We review the Levi-Civita coordinates for the CRTBP in Section 3, and refer the interested reader to Chapter 3 of [14], to the notes of [26, 27], and to the works of [28, 27, 29, 30, 31] for much more complete overview of the pre-McGehee literature on different regularization techniques.

Advecting the regularized singularity set under the backward flow for a time  $T$  leads to a smooth manifold of initial conditions whose orbits collide with the primary in forward time  $T$  or less. This is referred to as a local collision manifold. Running time backwards leads to a local ejection manifold. Studying intersections between ejection and collision manifolds, and their intersections with other invariant objects, provides invaluable insights.

One of the first works to combine this geometric picture of collisions with techniques from the qualitative theory of dynamical systems is the paper by McGehee [29]. Here, a general method for regularizing singularities is developed and used to study triple collisions in an isocoles three body problem. As an illustration of the power of the method, the author proves the existence of an infinite set of initial conditions whose orbits achieve arbitrarily large velocities after near collision.

Building on these results, Devaney proved the existence of infinitely many ejection-collision orbits in the same model, when one of the masses is small [32]. Further insights, based on similar techniques, are found in the works of Simo, ElBialy, and Lacomba and Losco, and Moeckel [33, 34, 35, 35, 36]. Using similar methods, Alvarez-Ramírez, Barrabés, Medina, and Ollé obtain numerical and analytical results for a related symmetric collinear four-body problem in [37]. In [31], Belbruno developed a new regularization technique for the spatial CRTBP and used it to prove the existence of families of periodic orbits which terminate at ejection-collision when the mass ratio is small enough. This is a perturbative analog of our Theorem 4 (but in the spatial problem).

The paper [7] by Llibre is especially relevant to the present study, as the author establishes a number of theorems about ejection-collision orbits in the planar CRTBP. Taylor expansions for the local ejection/collision manifolds in Levi-Civita coordinates are given and used to show that the local collision sets are homeomorphic to cylinders for all values of energy and any mass ratio. Then, for mass ratio sufficiently small, the author proves that the ejection/collision manifolds intersect twice near the large primary. This gives the existence of a pair of ejection-collision orbits which depart from and return to the large body. For Jacobi constant sufficiently negative and mass ratio sufficiently small, he also proves the existence of an ejection from the large body which collides with the small body in finite time. This is a perturbative analogue of our Theorem 1. We note that the large primary to small primary ejection-collisions in [7] are “fast”, in the sense that the relative velocity between the infinitesimal body and the large primary is never zero. Compare this to the orbits of our Theorem 1, which twice attain zero relative velocity with respect to the large primary (the orbits make a “loop”).

A follow up paper by Lacomba and Llibre [38] shows that the ejection-collision orbits of [7] are transverse, and as a corollary the authors prove that the CRTBP has no  $C^1$  extendable regular integrals. Heuristically speaking, this says that the Jacobi integral is the only conserved quantity in the CRTBP and hence the system is not integrable. Transversality is proven analytically for small values of the mass ratio in the CRTBP, and studied numerically for Hill’s problem. In [39], Delgado proves the transversality

result for the Hill's problem, using a perturbative argument for  $1/C$  small (large Jacobi constant). We remark that the techniques developed in the present work could be applied to the Hill problem for non-perturbative values of  $C$ . We also mention the work of Pinyol [40], which uses similar techniques to prove the existence of ejection-collision orbits for the elliptic CRTBP.

A number of results for collision and near collision orbits have been established using KAM arguments in Levi-Civita coordinates. For example in [41] and for the planar CRTBP, Chenciner and Llibre prove the existence of invariant tori which intersect the regularized collision circle transversally. The argument works for  $1/C$  small enough and for any mass ratio. The dynamics on the invariant tori are conjugate to irrational rotation, so that their existence implies that there are infinitely many orbits which pass arbitrarily close to collision infinitely many times. Returning to the original coordinates, the authors refer to these as punctured invariant tori (punctured by the collision set). Punctured tori in an averaged four body problem (weakly coupled double Kepler problem) are studied by Féjóz in [42], and this work is extended by the same author to the CRTBP, for a parameter regime where the system can be viewed as a perturbation of two uncoupled Kepler problems [43]. See also the work of Zhao [44] for a proof that there exists a positive measure set of punctured tori in the spatial CRTBP.

In [45], Bolotin and Mackay use variational methods to prove the existence of chaotic collision and near collision dynamics in the planar CRTBP. The argument studies some normally hyperbolic invariant manifolds whose stable/unstable manifolds, in regularized coordinates, intersect one another near the local ejection/collision manifolds. The small parameter in this situation is the mass ratio, and the results hold in an explicit closed interval of energies. The same authors extend the result to the spatial CRTBP in [46], and Bolotin obtains the existence of chaotic near collision dynamics for the elliptic CRTBP in [47].

A more constructive (non-variational) approach to studying chaotic collision and near collision dynamics is found in Font, Nunes, and Simó [48]. Here, the authors prove the existence of chaotic invariant sets containing orbits which make infinitely many near collisions with the smaller body in the planar CRTBP. Again,  $\mu$  is taken as the small parameter and the authors compute perturbative expansions for some Poincaré maps in Levi-Civita coordinates. Using these expansions they directly prove the existence of horseshoe dynamics. Since the argument is constructive, they are also able to show, via careful numerical calculations, that the expansions provide useful predictions for  $\mu$  as large as  $10^{-3}$ . In a follow up paper [49], the same authors numerically compute all the near collision periodic orbits in a fixed energy level satisfying certain bounds on the return time, and present numerical evidence for the existence of chaotic dynamics between these.

In the paper [50], Ollé, Rodríguez, and Soler introduce the notion of an  $n$ -ejection-collision orbit. This is an orbit which is ejected from larger primary body, and which makes an excursion where it achieves a relative maximum distance from the large primary  $n$ -times before colliding with it: such orbits look like flowers with  $n$  petals and the primary body at the center. Finding  $n$ -ejection-collision orbits necessitates studying the local ejection/collision manifolds at a greater distance from the regularized singularity set than in previous works. The authors also numerically study the bifurcation structure of these families for  $1 \leq n \leq 10$  over a range of energies.

In a follow-up paper [51], the same authors prove the existence of four families of



$n$ -ejection-collision orbits for any value of  $n \geq 1$ , for  $\mu$  small enough, and for values of the Jacobi constant sufficiently large. The argument exploits an analytic solution of the variational equations in a neighborhood of the regularized singularity set in the Levi-Civita coordinates. They also perform large scale numerical calculations which suggest that the  $n$ -ejection-collision orbits persist at all values of the mass ratio, and for large ranges of the Jacobi constant. Another paper by the same authors numerically studies the manifold of ejection orbits, for both the large and small primary bodies, over the whole range of mass ratios and for a number of different values of the Jacobi constant [52]. The authors also propose a geometric mechanism for finding ejection orbits which transit from one primary to the neighborhood of the other. More precisely, they numerically compute intersections between the ejection manifold and the stable manifold of a periodic orbit in the  $L_1$  Lyapunov family at the appropriate energy level, and study the resulting dynamics.

In the paper [53], Seara, Ollé, Rodríguez, and Soler dramatically extend the results of [51]. First, they show that the existence of an  $n$ -ejection-collision is equivalent to an orbit with  $n$ -zeros of the angular momentum: a scalar quantity. Using this advance they are able to remove the small mass condition, and prove that for either primary, at any value of the mass ratio, and for any  $n \geq 1$ , there exist four  $n$ -ejection-collision orbits. The argument is based on an application of the implicit function theorem, with the  $1/C$  as the small parameter. The authors also make a detailed numerical study of this enlarged family of  $n$ -ejection-collision orbits, taking  $\mu \rightarrow 1$ . Using insights obtained from these numerical explorations, they propose an analytical hypotheses which allows them to prove existence results for  $n$ -ejection-collision orbits for the Hill problem, again for large enough energies. We remark that, since  $n$ -ejection-collision orbits can be formulated as solutions of two point boundary value problems beginning and ending on the regularized collision circle, an interesting project could be to prove the existence of such orbits for smaller values of  $C$  using the techniques developed in the present work.

## 1.2. Numerical calculations, computational mathematics, and celestial mechanics

Computational and observational tools for predicting the motions of celestial bodies have roots in antiquity, so that even a terse overview is beyond the scope of the present study. Nevertheless, we remark that the numerical methods like integration techniques for solving initial value problems, and bisection/Newton schemes for solving nonlinear systems of equations have been applied to the study of the CRTBP at least since G.H. Darwin's 1897 treatise on periodic orbits [54]. The reader interested in the history of pen-and-paper calculations for the CRTBP will find the work of Moulton's group in Chicago, as well as Stromgren's group in Copenhagen, from the 1910's to the 1930's of great interest. Detailed discussion of their accomplishments are found in [10, 21], and in Chapter 9 of Szebehely's Book [14].

The historic work of the mathematicians/human computers at the NACA, and subsequent NASA space agencies, had a profound effect on the shape of twentieth century affairs, as chronicled in a number of books and films. See for example [55, 56, 57, 58, 59]. The ascension of digital computing and the dawn of the space race in the 1950's and 1960's led to an explosion of computational work in celestial mechanics. Again, the literature is vast and we refer to the books of Szebehely [14], Celletti and Perozzi [60], and Belbruno [61] for more thorough discussion of historical developments and the surrounding literature.



In the context of the present work, it is important to discuss the idea of recasting transport problems into two point boundary value problems (BVPs). The main idea is to project the boundary conditions for an orbit segment onto a representation of the local stable/unstable manifold of some invariant object (both linear and higher order expansions of the stable/unstable manifolds are in frequent use). Then a homoclinic or heteroclinic connection is reconceptualized as an orbit beginning on the unstable and terminating on the stable manifold, giving a clear example of a BVP.

The papers by Beyn, Friedman, Doedel, Kunin [62, 63, 64, 65, 66] lay the foundations for such BVP methods. A BVP approach for computing periodic orbits in conservative systems is developed by Muñoz-Almaraz, Freire, Galán, Doedel, and Vanderbauwhede in [67]. In particular, they introduce an unfolding parameter for the periodic orbit problem, an idea we make extensive use of in Section 2. Connections between periodic orbits are studied by Doedel, Kooi, Van Voorn, and Kuznetsov in [68, 69], and Calleja, Doedel, Humphries, Lemus-Rodríguez and Oldeman apply these techniques to the CRTBP in [70].

BVP methods for computing connections between invariant objects are central to the geometric approach to space mission design described in the four volume set of books by Gómez, Jorba, Simó, and Masdemont [71, 72, 73, 74], and also in the book of Koon, Lo, Marsden, and Ross [75]. A focused (and shorter) research paper describing the role of connecting orbits in the spatial CRTBP is found in the paper [76] by Gómez, Koon, Lo, Marsden, Masdemont, and Ross, and explicit discussion of the role of invariant manifolds in space missions which visit the moons of Jupiter is found in the paper [77], by Koon, Marsden, Ross, and Lo. A sophisticated multiple shooting scheme for computing families of connecting orbits between periodic orbits in Lyapunov families is developed in by Barrabés, Mondelo, and Ollé in [78], and extended by the same authors to the general Hamiltonian setting in [79]. Recent extensions are found in the work of Kumar, Anderson, and de la Llave [80, 81] on connecting orbits between invariant tori in periodic perturbations of the CRTBP, and by Barcelona, Haro, and Mondelo [82] for studying families of connecting orbits between center manifolds. A broad overview of numerical techniques for studying transport phenomena in  $N$ -body problems is found in the review by Dellnitz, Junge, Koon, Lekien, Lo, Marsden, Padberg, Preis, Ross, and Thiere [83].

We must insist that the references given in this subsection in no way constitute a complete list. Our aim is only to stress the importance of BVP techniques, and to suggest their rich history of application in the celestial mechanics literature, while possibly directing the reader to more definitive sources.

### *1.3. Computer assisted proof in celestial mechanics*

Constructive, computer assisted proofs are a valuable tool in celestial mechanics, as they facilitate the study  $N$ -body dynamics far from any perturbative regime, and in the absence of any small parameters or variational structure. Computer assisted arguments usually begin with careful numerical calculation of some dynamically interesting orbits. From this starting point, one tries to construct a posteriori arguments which show that there are true orbits with the desired dynamics nearby. Invariant objects like equilibria, periodic orbits, quasi-periodic solutions (invariant tori), local stable/unstable manifolds, and connecting orbits between invariant sets can be either reformulated as solutions of appropriate functional equations, or expressed in terms of topological/geometric conditions in certain regions of phase space. Given a numerical candidate which approximately

satisfies either the functional equation or the geometric conditions, fixed point or degree theoretical arguments are used to prove the existence of true solutions nearby. As an example, the Newton-Krawczyk Theorem 30 from Section 7 is a tool for verifying the existence of a unique non-degenerate zero of a nonlinear map given a good enough approximate root. The theorem is proved using the contraction mapping theorem, and the interested reader will find many similar theorems discussed in the references below.

To get a sense of the power of computer assisted methods of proof in celestial mechanics, we refer the reader to the works of Arioli, Barutello, Terracini, Kapela, Zgliczyński, Simó, Burgos, Calleja, García-Azpeitia, Lessard, Mireles James, Walawska, and Wilczak [84, 85, 86, 87, 88, 89, 90, 91, 92] on periodic orbits, the works of Arioli, Wilczak, Zgliczyński, Capiński, Kepley, Mireles James, Galante, and Kaloshin [93, 94, 95, 96, 97] on transverse connecting orbits and chaos, the works of Capiński, Guardia, Martín, Sera, Zgliczyński, Roldan, Wodka, and Gidea [98, 99, 100, 101] on oscillations to infinity, center manifolds, and Arnold diffusion, and to the works of Celletti, Chierchia, de la Llave, Rana, Figueras, Haro, Luque, Gabern, Jorba, Caracciolo, and Locatelli [102, 103, 104, 105, 106] on quasi-periodic orbits and KAM phenomena. We remark that while this list is by no means complete, consulting these papers and the papers cited therein will give the reader a reasonable impression of the state-of-the-art in this area. More general references on computer assisted proofs in dynamical systems and differential equations are found in the review articles by Lanford, Koch, Schenkel, Wittwer, van den Berg, Lessard, and Gómez-Serrano [107, 108, 109, 110], and in the books by Tucker, and Nakao, Plum, and Watanabe [111, 112].

We also mention the recent review article by Kapela, Mrozek, Wilczak, and Zgliczyński [113], which describes the use of the CAPD library for validated numerical integration of ODEs and their variational equations. The CAPD library is a general purpose toolkit, and can be applied to any problem where explicit formulas for the vector field are known in closed form. We make extensive use of this library throughout the present work. Additional details about CAPD algorithms are found in the papers by Zgliczyński, and Wilczak [114, 115], but the reader who is interested in the historical development of these ideas should consult the references of [113]. Methods for computing validated enclosures of stable/unstable manifolds attached to equilibrium solutions for some restricted three and four body problems are discussed in [96, 116]. and these methods are used freely in the sequel.

**Remark 10 (Relevance of the present work).** In light of the discussion contained in Sections 1.1, 1.2, and 1.3 a few, somewhat more refined comments about the novelty of the present work are in order. First, note that our results make essential use of the geometric formulation of collision dynamics discussed in Section 1.1. An important difference of perspective is that, since we work without small parameters, we formulate multiple shooting problems describing orbits with boundary conditions on the regularized collision set, rather than working with perturbative expansions for the local ejection/collision manifolds and studying intersections between them. Once we have a good enough numerical approximation of the solution of a BVP we validate the existence of a true solution via a standard a posteriori argument.

In this sense our work exploits the BVP approach for studying dynamical objects discussed in Section 1.2. Our shooting templates, discussed (see Section 2), are general enough to allow for any number of coordinate swaps in any order, and allow us to

shoot from stable/unstable manifolds, regularized collision sets, or discrete symmetry subspaces. In this way we have one BVP framework which covers all the theorems considered in this paper. We note that the setup applies also to higher dimensional problems involving stable/unstable manifolds of other geometric objects, as seen for example in [117]. Our setup incorporates an unfolding parameter approach to BVPs for conservative systems – as discussed in [118, 67, 119] for periodic orbits. An important feature of our setup is that the existence of a non-degenerate solution of the BVP implies transversality relative to the energy submanifold. One virtue of the abstract framework presented in Section 2 is that we prove transversality results and properties of the unfolding parameter only once, and they apply to all problems considered later in the text – rather than having to establish such results for each new problem considered.

Still, this shooting template framework is just a convenience. The main contribution of the present work is a flexible computer assisted approach to proving theorems about collision dynamics in celestial mechanics problems. We remark that, until now, collisions have been viewed largely as impediments to the implementation of successful computer assisted proofs. The present work demonstrates that well known tools from regularization theory can be combined with existing validated numerical tools and a posteriori analysis to prove interesting theorems about collisions in non-perturbative settings. As applications, we prove a number of new results for the CRTBP.

## 2. Problem setup

Consider an ODE with one or more first integrals or constants of motion. For such systems, the level sets of the integrals give rise to invariant sets. Indeed, the level sets are invariant manifolds except at critical points of the conserved quantities. In this section we describe a shooting method for two point boundary value problems between submanifolds of the level set. To be more precise, we consider two manifolds, parameterized (locally) by some functions, which are contained in a level set. We present a method which allows us to find points on these manifold which are linked by a solution of an ODE. This in particular implies that the two manifolds intersect. Our method will allow us to establish transversality of the intersection within the level set.

We consider an ODE

$$x' = f(x), \tag{1}$$

where  $f : \mathbb{R}^d \rightarrow \mathbb{R}^d$ . Assume that the flow  $\phi(x, t)$  induced by (1) has an integral of motion expressed as

$$E : \mathbb{R}^d \rightarrow \mathbb{R}^k,$$

which means that

$$E(\phi(x, t)) = E(x), \tag{2}$$

for every  $x \in \mathbb{R}^d$  and  $t \in \mathbb{R}$ . Fix  $c \in \mathbb{R}^k$  and define the level set

$$M := \{x \in \mathbb{R}^d : E(x) = c\}, \tag{3}$$

and assume that  $M$  is (except possibly at some degenerate points) a smooth manifold. Consider two open sets  $D_1 \subset \mathbb{R}^{d_1}$  and  $D_2 \subset \mathbb{R}^{d_2}$  and two chart maps

$$P_i : D_i \rightarrow M \subset \mathbb{R}^d \quad \text{for } i = 1, 2, \tag{4}$$

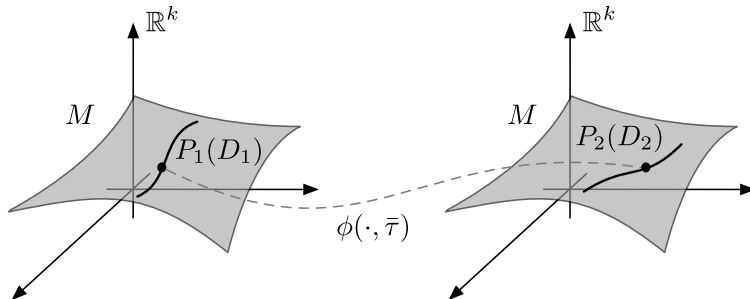


Figure 1: The left and right plots are in  $\mathbb{R}^d$  with a  $d - k$  dimensional manifold  $M$  depicted in gray. The manifolds  $P_i(D_i) \subset M$ , for  $i = 1, 2$ , are represented by curves inside of  $M$ . We seek  $\bar{x}_1 \in D_1, \bar{x}_2 \in D_2$  and  $\bar{\tau} \in \mathbb{R}$  such that  $\phi(P_1(\bar{x}_1), \bar{\tau}) = P_2(\bar{x}_2)$ . The two points  $P_i(\bar{x}_i)$ , for  $i = 1, 2$ , are represented by dots.

parameterizing submanifolds of  $M$ .

**Remark 11.** One can for example think of the  $P_1$  and  $P_2$  as parameterizations of the exit or entrance sets on some local unstable and stable manifolds, respectively, of some invariant object. However in some of the applications to follow  $P_{1,2}$  will parameterize collision sets in regularized coordinates or some surfaces of symmetry for  $f$ .

We seek points  $\bar{x}_i \in D_i$  for  $i = 1, 2$  and a time  $\bar{\tau} \in \mathbb{R}$  such that

$$\phi(P_1(\bar{x}_1), \bar{\tau}) = P_2(\bar{x}_2). \quad (5)$$

Note that if  $P_1$  and  $P_2$  parameterize some  $\phi$ -invariant manifolds, then Equation (5) implies that these manifolds intersect. The setup is depicted in Figure 1.

**Remark 12.** Denote by  $x_1, x_2$  the points  $x_1 \in \mathbb{R}^{d_1}$  and by  $x_2 \in \mathbb{R}^{d_2}$ : this avoids confusion with  $x \in \mathbb{R}^d$ .

We introduce a general scheme which allows us to:

1. Establish the intersection of the manifolds parameterized by  $P_1$  and  $P_2$  by means of a suitable Newton operator.
2. Establish that the intersection is transverse relative to the level set  $M$ .
3. Provide a setup flexible enough for multiple shooting between charts in different coordinates.

Our methodology is applied to establish connections between stable/unstable and collision manifolds in the PCRTBP.

### 2.1. Level set shooting

We now provide a more detailed formulation of problem (5) which allows us to describe connections between multiple level sets in distinct coordinate systems (instead of just one coordinate system as discussed in Section 3). This allows us to study applications

to collision dynamics as boundary value problems joining points in different coordinate systems. Let  $U_1, U_2 \subset \mathbb{R}^d$  be open sets and consider smooth functions  $E_1, E_2$

$$E_i : U_i \rightarrow \mathbb{R}^k \quad \text{for } i = 1, 2,$$

for which  $DE_i(x)$  is of rank  $k$  for every  $x \in U_i$ , for  $i = 1, 2$ . We fix  $c_1, c_2 \in \mathbb{R}^k$  and define the following the level sets

$$M_i = \{x \in U_i : E_i(x) = c_i\} \quad \text{for } i = 1, 2,$$

and assume that  $M_i \neq \emptyset$  for  $i = 1, 2$ . Observe that the  $M_i$  are smooth  $d - k$  dimensional manifolds by the assumption that  $DE_i$  are of rank  $k$ , for  $i = 1, 2$ .

Consider now a smooth function  $R : U_1 \times \mathbb{R} \times \mathbb{R}^k \rightarrow \mathbb{R}^d$ . We introduce the following notation for coordinates

$$(x, \tau, \alpha) \in \mathbb{R}^d \times \mathbb{R} \times \mathbb{R}^k, \quad y \in \mathbb{R}^d,$$

and define a parameter dependent family of maps  $R_{\tau, \alpha} : U_1 \rightarrow \mathbb{R}^d$  by

$$R_{\tau, \alpha}(x) := R(x, \tau, \alpha),$$

and assume that for each  $(x, \tau, \alpha) \in \mathbb{R}^{d+k+1}$ , the  $d \times d$  matrix

$$\frac{\partial}{\partial x} R(x, \tau, \alpha),$$

is invertible, so that  $R_{\tau, \alpha}(x)$  is a local diffeomorphism on  $\mathbb{R}^d$ .

The following definition makes precise our assumptions about when  $R_{\tau, \alpha}(x)$  takes values in  $M_2$ .

**Definition 13.** *We say that  $\alpha$  is an unfolding parameter for  $R$  if the following two conditions are satisfied for every  $x \in M_1$ .*

1. *If  $R_{\tau, \alpha}(x) \in M_2$ , then  $\alpha = 0$ .*
2. *If  $R_{\tau, 0}(x) \in U_2$ , then  $R_{\tau, 0}(x) \in M_2$ .*

To emphasize that we are interested in points mapped from  $M_1$  to  $M_2$ , we say that  $\alpha$  is an unfolding parameter for  $R$  from  $M_1$  to  $M_2$ .

Assume from now on that  $\alpha$  is an unfolding parameter for  $R$ . We consider two open sets  $D_1 \subset \mathbb{R}^{d_1}$  and  $D_2 \subset \mathbb{R}^{d_2}$  where  $d_1, d_2 \in \mathbb{N}$  and two smooth functions

$$P_i : D_i \rightarrow M_i, \quad \text{for } i = 1, 2,$$

each of which is a diffeomorphism onto its image. Define

$$F : D_1 \times D_2 \times \mathbb{R} \times \mathbb{R}^k \rightarrow \mathbb{R}^d$$

by the formula

$$F(x_1, x_2, \tau, \alpha) := R_{\tau, \alpha}(P_1(x_1)) - P_2(x_2). \quad (6)$$

We require that

$$d_1 + d_2 + 1 + k = d, \quad (7)$$

and seek  $\bar{x}_1, \bar{x}_2, \bar{\tau}$  such that

$$F(\bar{x}_1, \bar{x}_2, \bar{\tau}, 0) = R_{\bar{\tau}, 0}(P_1(\bar{x}_1)) - P_2(\bar{x}_2) = 0, \quad (8)$$

with  $DF(\bar{x}_1, \bar{x}_2, \bar{\tau}, 0)$  an isomorphism. In fact, we do more than simply solve (8). For some open interval  $I \subset \mathbb{R}$  containing  $\bar{\tau}$  we establish a transverse intersection between the smooth manifolds  $R(P_1(D_1), I, 0)$  and  $P_2(D_2)$  at  $\bar{y} := P_2(\bar{x}_2) \in M_2$ .

**Remark 14 (Role of the unfolding parameter).** The setup above, and in particular the roles of the parameters  $\alpha$  and  $\tau$ , might first appear puzzling. In the applications we have in mind,  $\tau$  is the time associated with the flow map of an ODE. The unfolding parameter  $\alpha$  deals with the fact that we solve a problem restricted to the level sets  $M_i$  for  $i = 1, 2$ . Consider for example shooting from a 1D arc to a 1D arc in a 4D conservative vector field, where the arcs are in the same level set of the conserved quantity (think of the arc as an outflowing segment on the boundary of a local 2D stable/unstable manifold, or part of the collision set). Since we are working in a 3D level set, the 2D surfaces formed by advecting the arcs can intersect transversally relative to the level set. However, since the arcs are parameterized by one variable functions, and the time of flight  $\tau$  is unknown, taking into account the dimension of the vector field, we have 4 equations in 3 unknowns. Adding an unfolding parameter to the problem balances the equations, but it must be done carefully, so that the new variable does not change the solution set for the problem. The idea was first exploited for periodic orbits of conservative systems in [67, 118]. We adapt the idea to the shooting templates developed for the present work, and this is the purpose of the variable  $\alpha$ .

An alternative formulation would be to fix the energy and use its formula to eliminate one of the variables in the equations of motion, or to work with coordinates in which we can write  $M_i$  as graphs of some functions and use these functions and appropriate projections to enforce the constraints. Another possibility is to throw away one of the equations in the BVP formulation when applying Newton, and to check a-posteriori that this equation is satisfied [120, 121]. Yet another approach would be to directly apply a Newton scheme for the unbalanced BVP, exploiting the Moore-Penrose pseudoinverse at each step. While such approaches lead to excellent numerical methods, one encounters difficulties when translating them into computer assisted arguments. We believe that the unfolding parameter is a good solution in this setting, as it leads to balanced equations with isolated solutions suitable for verification using fixed point theorems.

We now give an example which informs the intuition.

**Example 15. (Canonical unfolding.)** Consider the ODE in Equation (1) and  $E : \mathbb{R}^d \rightarrow \mathbb{R}$  satisfying Equation (2). Suppose  $c \in \mathbb{R}$  is fixed and denote its associated level set by  $M := \{E = c\}$  (In this example we have  $k = 1$  and  $E_1 = E_2 = E$ .) Assume there are smooth functions  $P_1, P_2$  as in (4) and that  $d_1 + d_2 + 2 = d$ . We construct a shooting operator for Equation (5) by choosing  $R$  as follows. Consider the  $\alpha$ -parameterized family of ODEs

$$x' = f(x) + \alpha \nabla E(x).$$

Let  $\phi_\alpha(x, t)$  denote the induced flow and note that  $\phi_0 = \phi$  is the flow induced by Equation (1). Defining the shooting operator by the formula

$$R(x, \tau, \alpha) := \phi_\alpha(x, \tau), \quad (9)$$

we see that solving Equation (5) is equivalent to solving Equation (8).

Observe that  $\alpha$  is unfolding for  $R$  because  $E$  is an integral of motion for  $\phi$  from which it follows that

$$\begin{aligned} \frac{d}{dt} E(R_{\tau, \alpha}(x)) &= \frac{d}{dt} E(\phi_\alpha(x, t)) \\ &= \nabla E(\phi_\alpha(x, t)) \cdot (f(\phi_\alpha(x, t)) + \alpha \nabla E(\phi_\alpha(x, t))) \\ &= \alpha \|\nabla E(\phi_\alpha(x, t))\|^2, \end{aligned}$$

where  $\cdot$  denotes the standard scalar product. Here we have used the fact that Equation (2) implies  $\nabla E(x) \cdot f(x) = 0$  but also  $\nabla E(\phi_\alpha(x, t)) \neq 0$  since  $\nabla E$  is assumed to have rank 1 everywhere.

Returning to the general setup we have the following theorem.

**Theorem 16.** *Assume that  $\alpha$  is an unfolding parameter for  $R$  and  $F$  is defined as in Equation (6). If*

$$F(\bar{x}_1, \bar{x}_2, \bar{\tau}, \bar{\alpha}) = 0, \quad (10)$$

then  $\bar{\alpha} = 0$ . Moreover, if  $DF(\bar{x}_1, \bar{x}_2, \bar{\tau}, 0)$  is an isomorphism, then there exists an open interval  $I \subset \mathbb{R}$  of  $\bar{\tau}$  such that the manifolds  $R(P_1(D_1), I, 0)$  and  $P_2(D_2)$  intersect transversally in  $M_2$  at  $\bar{y} := P_2(\bar{x}_2)$ . Specifically, we have the splitting

$$T_{\bar{y}}R(P_1(D_1), I, 0) \oplus T_{\bar{y}}P_2(D_2) = T_{\bar{y}}M_2, \quad (11)$$

and moreover,  $\bar{y}$  is an isolated transverse point.

**Proof.** Recalling the definition of  $F$  in Equation (6) and the hypothesis of Equation (10), we have that  $\bar{x} = P_1(\bar{x}_1) \in M_1$  and  $\bar{y} = P_2(\bar{x}_2) \in M_2$ . The fact that  $\alpha$  is an unfolding parameter for  $R$ , combined with  $R(\bar{x}, \bar{\tau}, \bar{\alpha}) = \bar{y}$ , implies that  $\bar{\alpha} = 0$ . Since  $F(\bar{x}_1, \bar{x}_2, \bar{\tau}, 0) = 0$ , we see that  $R(P_1(D_1), I, 0)$  and  $P_2(D_2)$  intersect at  $\bar{y}$ .

Our hypotheses on  $P_{1,2}$  and  $R$  imply that  $R(P_1(D_1), I, 0)$  and  $P_2(D_2)$  are submanifolds of  $M_2$  so evidently

$$T_{\bar{y}}R(P_1(D_1), I, 0) \oplus T_{\bar{y}}P_2(D_2) \subset T_{\bar{y}}M_2.$$

However, from the assumption in Equation (7) we have  $d - k = d_1 + d_2 + 1$  and therefore it suffices to prove that  $T_{\bar{y}}R(P_1(D_1), I, 0) \oplus T_{\bar{y}}P_2(D_2)$  is  $d - k$  dimensional.

Suppose  $\{e_1, \dots, e_{d_1}\}$  is a basis for  $\mathbb{R}^{d_1}$  and  $\{\tilde{e}_1, \dots, \tilde{e}_{d_2}\}$  is a basis for  $\mathbb{R}^{d_2}$ . Define

$$\begin{aligned} v_i &:= \frac{\partial R}{\partial x_1}(\bar{x}_1, \bar{\tau}, 0) DP_1(\bar{x}_1) e_i \quad \text{for } i = 1, \dots, d_1 \\ v_i &:= DP_2(\bar{x}_2) \tilde{e}_{i-d_1} \quad \text{for } i = d_1 + 1, \dots, d_1 + d_2 \\ v_{d_1+d_2+1} &:= \frac{\partial R}{\partial \tau}(\bar{x}_1, \bar{\tau}, 0). \end{aligned}$$

After differentiating Equation (6) we obtain the formula

$$DF = \begin{pmatrix} \frac{\partial F}{\partial x_1} & \frac{\partial F}{\partial x_2} & \frac{\partial F}{\partial \tau} & \frac{\partial F}{\partial \alpha} \end{pmatrix} = \begin{pmatrix} \frac{\partial R}{\partial x_1} DP_1 & -DP_2 & \frac{\partial R}{\partial \tau} & \frac{\partial R}{\partial \alpha} \end{pmatrix},$$



and since  $DF$  is an isomorphism at  $(\bar{x}_1, \bar{x}_1, \bar{\tau}, 0)$ , it follows that the vectors  $v_1, \dots, v_{d_1+d_2+1}$  span a  $d_1 + d_2 + 1 = d - k$  dimensional space. Observe that

$$\begin{aligned} T_{\bar{y}}R(P(D_1), I, 0) &= \text{span}(v_1, \dots, v_{d_1}, v_{d_1+d_2+1}), \\ T_{\bar{y}}P_2(D_2) &= \text{span}(v_{d_1+1}, \dots, v_{d_1+d_2}), \end{aligned}$$

proving the claim in Equation (11). Moreover, since

$$\dim R(P_1(D_1), I, 0) + \dim P_2(D_2) = (d_1 + 1) + d_2 = d - k = \dim M_2,$$

it follows that  $\bar{y}$  is an isolated transverse intersection point which concludes the proof.  $\blacksquare$

We finish this section by defining an especially simple ‘‘dissipative’’ unfolding parameter which works in the setting of the PCRTBP.

**Example 17.** (*Dissipative unfolding.*) Let  $x, y \in \mathbb{R}^{2k}$ , let  $\Omega : \mathbb{R}^{2k} \rightarrow \mathbb{R}$  and  $J \in \mathbb{R}^{2k \times 2k}$  be of the form

$$J = \begin{pmatrix} 0 & \text{Id}_k \\ -\text{Id}_k & 0 \end{pmatrix},$$

where  $\text{Id}_k$  is a  $k \times k$  identity matrix. Let us consider an ODE of the form

$$(x', y') = f(x, y) := \left( y, 2Jy + \frac{\partial}{\partial x} \Omega(x) \right).$$

One can check that  $E(x, y) = -\|y\|^2 + 2\Omega(x)$  is an integral of motion. Consider the parameterized family of ODEs

$$(x', y') = f_\alpha(x, y) := f(x, y) + (0, \alpha y), \quad (12)$$

and let  $\phi_\alpha((x, y), t)$  denote the flow induced by Equation (12). Define the shooting operator defined by

$$R((x, y), \tau, \alpha) := \phi_\alpha((x, y), \tau). \quad (13)$$

As in Example 15, one can check the equivalence between Equations (5) and (8). The fact that  $\alpha$  is unfolding for  $R$  follows as

$$\frac{d}{dt} E(\phi_\alpha((x, y), t)) = -2\alpha \|y\|^2.$$

## 2.2. Level set multiple shooting

Consider a sequence of open sets  $U_1, \dots, U_n \subset \mathbb{R}^d$  and a sequence of smooth maps

$$E_i : U_i \rightarrow \mathbb{R}^k \quad \text{for } i = 1, \dots, n$$

for which  $DE_i(x)$  is of rank  $k$  for every  $x \in U_i$ , for  $i = 1, \dots, n$ . Let  $c_1, \dots, c_n \in \mathbb{R}^k$  be a fixed sequence with corresponding level sets

$$M_i := \{x \in U_i : E_i(x) = c_i\} \quad \text{for } i = 1, \dots, n.$$

Let

$$R^i : U_i \times \mathbb{R} \times \mathbb{R}^k \rightarrow \mathbb{R}^d \quad \text{for } i = 1, \dots, n-1$$

be a sequence of smooth functions which defines a sequence of parameter dependent maps

$$R_{\tau,\alpha}^i : U_i \rightarrow \mathbb{R}^d, \\ R_{\tau,\alpha}^i(x) := R^i(x, \tau, \alpha), \quad \text{for } i = 1, \dots, n-1.$$

We assume that for each fixed  $\tau$  and  $\alpha$ , each of the maps is a local diffeomorphism on  $\mathbb{R}^d$ .

Let  $D_0 \subset \mathbb{R}^{d_0}$  and  $D_n \subset \mathbb{R}^{d_n}$  be open sets, and let

$$P_0 : D_0 \rightarrow M_0 \subset \mathbb{R}^d, \quad P_n : D_n \rightarrow M_n \subset \mathbb{R}^d,$$

be diffeomorphisms onto their image. Assume that

$$d_0 + d_n + 1 + k = d \tag{14}$$

and consider the function

$$\tilde{F} : \mathbb{R}^{nd} \supset D_0 \times \underbrace{\mathbb{R}^d \times \dots \times \mathbb{R}^d}_{n-1} \times D_n \times \mathbb{R} \times \mathbb{R}^k \rightarrow \underbrace{\mathbb{R}^d \times \dots \times \mathbb{R}^d}_n,$$

defined by the formula

$$\tilde{F}(x_0, \dots, x_n, \tau, \alpha) = \begin{pmatrix} P_0(x_0) - x_1 \\ R_{\tau,\alpha}^1(x_1) - x_2 \\ \vdots \\ R_{\tau,\alpha}^{n-2}(x_{n-2}) - x_{n-1} \\ R_{\tau,\alpha}^{n-1}(x_{n-1}) - P_n(x_n) \end{pmatrix} \tag{15}$$

We now define the following functions

$$R : U_1 \times \mathbb{R} \times \mathbb{R}^k \rightarrow \mathbb{R}^d, \\ F : D_0 \times D_n \times \mathbb{R} \times \mathbb{R}^k \rightarrow \mathbb{R}^d$$

by the formulas

$$R(x_1, \tau, \alpha) = R_{\tau,\alpha}(x_1) := R_{\tau,\alpha}^{n-1} \circ \dots \circ R_{\tau,\alpha}^1(x_1), \\ F(x_0, x_n, \tau, \alpha) := R_{\tau,\alpha}(P_0(x_0)) - P_n(x_n). \tag{16}$$

**Definition 18.** We say that  $\alpha$  is an unfolding parameter for the sequence  $R_{\tau,\alpha}^i$  if it is unfolding for  $R_{\tau,\alpha} = R_{\tau,\alpha}^{n-1} \circ \dots \circ R_{\tau,\alpha}^1$ .

We now formulate the following lemma.

**Lemma 19.** If  $\tilde{F}(\bar{x}_0, \dots, \bar{x}_n, \bar{\tau}, \bar{\alpha}) = 0$  and  $D\tilde{F}(\bar{x}_0, \dots, \bar{x}_n, \bar{\tau}, \bar{\alpha})$  is an isomorphism, then  $F(\bar{x}_0, \bar{x}_n, \bar{\tau}, \bar{\alpha}) = 0$  and  $DF(\bar{x}_0, \bar{x}_n, \bar{\tau}, \bar{\alpha})$  is an isomorphism.

**Proof.** The fact that  $F(\bar{x}_0, \bar{x}_n, \bar{\tau}, \bar{\alpha}) = 0$  follows directly from the way  $\tilde{F}$  and  $F$  are defined in Equations (15) and (16) respectively. Before proving that  $DF$  is an isomorphism, we set up some notation. We will write

$$dR^i := \frac{\partial R^i}{\partial x_i}(\bar{x}_i, \bar{\tau}, \bar{\alpha}) \quad \text{for } i = 1, \dots, n-1.$$

It will be convenient for us to swap the order of the coordinates, so we define

$$\hat{F}(x_1, \dots, x_n, x_0, \tau, \alpha) := \tilde{F}(x_0, x_1, \dots, x_n, \tau, \alpha), \quad (17)$$

and write

$$\hat{F} = (\hat{F}_1, \dots, \hat{F}_n) \quad \text{where} \quad \hat{F}_i : \mathbb{R}^{nd} \rightarrow \mathbb{R}^d, \text{ for } i = 1, \dots, n.$$

Finally, the last notation we introduce is  $z \in \mathbb{R}^d$  to combine the coordinates from the domain of  $F$  together

$$z = (z_1, \dots, z_d) = (x_n, x_0, \tau, \alpha) \in \mathbb{R}^{dn} \times \mathbb{R}^{d_0} \times \mathbb{R} \times \mathbb{R}^k = \mathbb{R}^d.$$

Note that  $z$  is also the variable corresponding to the last  $d$  coordinates from the domain of  $\hat{F}$  (see Equation (17)). Finally, we remark that all derivatives considered in the argument below are computed at the point  $(\bar{x}_0, \dots, \bar{x}_n, \bar{\tau}, \bar{\alpha})$ .

With the above notation we see that

$$D\hat{F} = \begin{pmatrix} -\text{Id} & 0 & \cdots & 0 & \frac{\partial \hat{F}_1}{\partial z} \\ dR^1 & -\text{Id} & \ddots & \vdots & \frac{\partial \hat{F}_2}{\partial z} \\ 0 & \ddots & \ddots & 0 & \vdots \\ \vdots & \ddots & dR^{n-2} & -\text{Id} & \frac{\partial \hat{F}_{n-1}}{\partial z} \\ 0 & \cdots & 0 & dR^{n-1} & \frac{\partial \hat{F}_n}{\partial z} \end{pmatrix},$$

and  $D\hat{F}$  is an isomorphism since  $D\tilde{F}$  is an isomorphism. To see this define a sequence of vectors  $v^1, \dots, v^d \in \mathbb{R}^{nd}$  of the form

$$v^i = \begin{pmatrix} v_1^i \\ \vdots \\ v_n^i \end{pmatrix} \in \mathbb{R}^d \times \dots \times \mathbb{R}^d = \mathbb{R}^{nd} \quad \text{for } i = 1, \dots, d,$$

with  $v_1^i, v_n^i \in \mathbb{R}^d$  chosen as

$$v_1^i = \frac{\partial \hat{F}_1}{\partial z_i}, \quad v_n^i = \left( 0 \quad \cdots \quad 0 \quad i \quad 0 \quad \cdots \quad 0 \right)^\top, \quad (18)$$

and  $v_2^i, \dots, v_{n-1}^i \in \mathbb{R}^d$  defined inductively as

$$v_k^i = dR^{k-1}v_{k-1}^i + \frac{\partial \hat{F}_k}{\partial z_i} \quad \text{for } k = 2, \dots, n-1. \quad (19)$$

Note that from the choice of  $v_n^i$  in (18) the vectors  $v^1, \dots, v^d$  are linearly independent.

By direct computation<sup>5</sup> it follows that

$$D\hat{F}v^i = \begin{pmatrix} 0 \\ dR^{n-1}v_{n-1}^i + \frac{\partial \hat{F}_n}{\partial z_i} \end{pmatrix} \quad \text{for } i = 1, \dots, d, \quad (20)$$

<sup>5</sup>From (15) and (19) follow the cancellations when multiplying the vector  $v^i$  by  $D\hat{F}$ .

where the zero is in  $\mathbb{R}^{(n-1)d}$ .

Looking at (15), since  $\hat{F}_1, \dots, \hat{F}_{n-1}$  do not depend on  $x_n$ , we see that for  $i \in \{1, \dots, d_n\}$  we have  $\frac{\partial \hat{F}_1}{\partial z_i} = \dots = \frac{\partial \hat{F}_{n-1}}{\partial z_i} = 0$ , so

$$\begin{aligned}
dR^{n-1}v_{n-1}^i + \frac{\partial \hat{F}_n}{\partial z_i} &= dR^{n-1} \left( dR^{n-2}v_{n-2}^i + \frac{\partial \hat{F}_{n-1}}{\partial z_i} \right) - \frac{\partial P_n}{\partial x_{n,i}} \quad (21) \\
&= dR^{n-1} (dR^{n-2}v_{n-2}^i + 0) - \frac{\partial P_n}{\partial x_{n,i}} \\
&= \dots \\
&= dR^{n-1} \dots dR^1 v_1^i - \frac{\partial P_n}{\partial x_{n,i}} \\
&= dR^{n-1} \dots dR^1 \frac{\partial \hat{F}_1}{\partial z_i} - \frac{\partial P_n}{\partial x_{n,i}} \\
&= -\frac{\partial P_n}{\partial x_{n,i}} \quad \text{for } i = 1, \dots, d_n.
\end{aligned}$$

Similarly, for  $j = i - d_n \in \{1, \dots, d_0\}$  from (15) we see that  $\frac{\partial \hat{F}_1}{\partial z_i} = \frac{\partial P_0}{\partial x_{0,j}}$  and  $\frac{\partial \hat{F}_2}{\partial z_i} = \dots = \frac{\partial \hat{F}_n}{\partial z_i} = 0$ , so

$$\begin{aligned}
dR^{n-1}v_{n-1}^i + \frac{\partial \hat{F}_n}{\partial z_i} &= dR^{n-1}dR^{n-2} \dots dR^1 \frac{\partial P_0}{\partial x_{0,j}} = \frac{\partial (R_{\bar{\tau}, \bar{\alpha}} \circ P_0)}{\partial x_{0,j}} \quad (22) \\
&\quad \text{for } i = d_n + 1, \dots, d_n + d_0.
\end{aligned}$$

The index  $i = d_n + d_0 + 1$  corresponds to  $\tau$ . Similarly to (21), by inductively applying the chain rule, it follows that

$$dR^{n-1}v_{n-1}^i + \frac{\partial \hat{F}_n}{\partial z_i} = \frac{\partial R}{\partial \tau} \quad \text{for } i = d_n + d_0 + 1. \quad (23)$$

Finally, for  $j = i - d_n - d_0 - 1 \in \{1, \dots, k\}$ , the variable  $z_i$  corresponds to  $\alpha_j$ , and also by applying the chain rule we obtain that

$$dR^{n-1}v_{n-1}^i + \frac{\partial \hat{F}_n}{\partial z_i} = \frac{\partial R}{\partial \alpha_j} \quad \text{for } i = d_n + d_0 + 2, \dots, d. \quad (24)$$

Combining Equations (20)–(24) we see that

$$\left( D\hat{F}v^1 \quad \dots \quad D\hat{F}v^d \right) = \begin{pmatrix} 0 & 0 & 0 & 0 \\ -\frac{\partial P_n}{\partial x_n} & \frac{\partial (R_{\bar{\tau}, \bar{\alpha}} \circ P_0)}{\partial x_0} & \frac{\partial R}{\partial \tau} & \frac{\partial R}{\partial \alpha} \end{pmatrix}. \quad (25)$$

Since  $v^1, \dots, v^d$  are linearly independent and since  $D\hat{F}$  is an isomorphism, the rank of the above matrix is  $d$ . Looking at Equation (15) we see that the lower part of the matrix in Equation (25) corresponds to  $DF$  which implies that  $DF$  is of rank  $d$ , hence is an isomorphism. ■

We see that we can validate assumptions of Theorem 16 by setting up a multiple shooting problem (15) and applying Lemma 19. To do so, one needs to additionally check whether  $\alpha$  is an unfolding parameter for the sequence  $R_{\tau, \alpha}^i$ .

### 3. Regularization of collisions in the PCRTBP

In this section we formally introduce the equations of motion for the PCRTBP as discussed in Section 1. We stress that all the material in this section, and in Subsections 3.1 and 3.2 are completely standard, and we follow the normalization conventions as in [14]. That being said, since we use this material to implement computer assisted proofs, it is important to explicitly state every formula correctly and to recall some important but well known facts. The reader who is familiar with the CRTBP and its Levi-Civita regularization may want to skim this section while jumping ahead to Section 4.

Recall that the problem describes a three body system, where two massive primaries are on circular orbits about their center of mass, and a third massless particle moves in their field. The equations of motion for the massless particle are expressed in a co-rotating frame with the frequency of the primaries. Writing Newton's laws in the co-rotating frame leads to

$$\begin{aligned}x'' &= 2y' + \partial_x \Omega(x, y), \\y'' &= -2x' + \partial_y \Omega(x, y),\end{aligned}\tag{26}$$

where

$$\begin{aligned}\Omega(x, y) &= (1 - \mu) \left( \frac{r_1^2}{2} + \frac{1}{r_1} \right) + \mu \left( \frac{r_2^2}{2} + \frac{1}{r_2} \right), \\r_1^2 &= (x - \mu)^2 + y^2, \quad \text{and} \quad r_2^2 = (x + 1 - \mu)^2 + y^2.\end{aligned}$$

Here  $x, y$  are the positions of the massless particle on the plane. The  $\mu$  and  $1 - \mu$  are the masses of the primaries (normalized so that the total mass of the system is 1). The rotating frame is oriented so that the primaries lie on the  $x$ -axis, with the center of mass at the origin. We take  $\mu \in (0, \frac{1}{2}]$  so that the large body is always to the right of the origin. The larger primary has mass  $m_1 = 1 - \mu$  and is located at the position  $(\mu, 0)$ . Similarly the smaller primary has mass  $m_2 = \mu$  and is located at position  $(\mu - 1, 0)$ . The top frame of Figure 2 provides a schematic for the positioning of the primaries and the massless particle.

Let  $U \subset \mathbb{R}^4$  denote the open set

$$U := \{(x, p, y, q) \in \mathbb{R}^4 \mid (x, y) \notin \{(\mu, 0), (\mu - 1, 0)\}\}.$$

The vector field  $f: U \rightarrow \mathbb{R}^4$  defined by

$$f(x, p, y, q) := \begin{pmatrix} 2q + x - \frac{(1-\mu)(x-\mu)}{((x-\mu)^2+y^2)^{3/2}} - \frac{\mu(x+1-\mu)}{((x+1-\mu)^2+y^2)^{3/2}} \\ -2p + y - \frac{(1-\mu)y}{((x-\mu)^2+y^2)^{3/2}} - \frac{\mu y}{((x+1-\mu)^2+y^2)^{3/2}} \end{pmatrix}\tag{27}$$

is equivalent to the second order system given in (26). Note that

$$\|f(x, p, y, q)\| \rightarrow \infty \quad \text{as either} \quad (x, y) \rightarrow (\mu, 0) \quad \text{or} \quad (x, y) \rightarrow (\mu - 1, 0).$$

Let  $\mathbf{x} = (x, p, y, q)$  denote the coordinates in  $U$  and denote by  $\phi(\mathbf{x}, t)$  the flow generated by  $f$  on  $U$ . The system (27) has an integral of motion  $E: U \rightarrow \mathbb{R}$  given by

$$E(\mathbf{x}) = -p^2 - q^2 + 2\Omega(x, y),\tag{28}$$

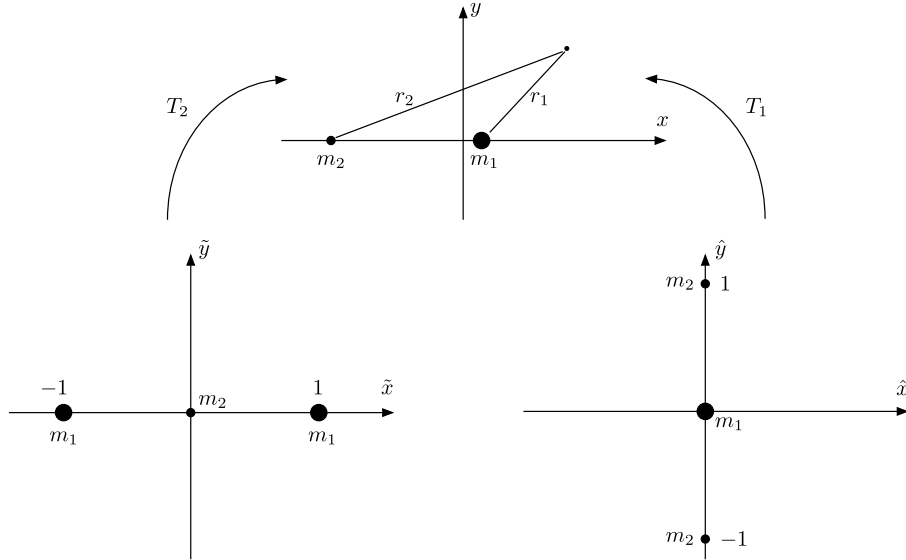


Figure 2: Three coordinate frames for the PCRTBP: the center top image depicts the classical PCRTBP in the rotating frame. The bottom left and right frames depict the restricted three body problem in Levi-Civita coordinates: regularization of collisions with  $m_2$  on the left and with  $m_1$  on the right. Observe that in these coordinates the regularized body has been moved to the origin. The Levi-Civita transformations  $T_1$  and  $T_2$  provide double covers of the original system, so that in the regularized frames there are singularities at the two copies of the remaining body.

which is referred to as the Jacobi integral.

We are interested in orbits with initial conditions  $\mathbf{x} \in U$  with the property that their positions limit to either  $m_1 := (\mu, 0)$  or  $m_2 := (\mu - 1, 0)$  in finite time. Such orbits, which reach a singularity of the vector field  $f$  in finite time, are called collisions. It has long been known that if we fix our attention to a specific level set of the Jacobi integral for some fixed  $c \in \mathbb{R}$ , then it is possible to make a change of coordinates which “removes” or regularizes the singularities. This idea is reviewed in the next sections.

### 3.1. Regularization of collisions with $m_1$

To regularize a collision with  $m_1$ , define the complex variables  $z = x + iy$ , and the new “regularized” variables  $\hat{z} = \hat{x} + i\hat{y}$ , related to  $z$  by the transformation

$$\hat{z}^2 = z - \mu.$$

One also rescales time in the regularized coordinates with the rescaled time  $\hat{t}$  related to the original time  $t$  by the formula

$$\frac{dt}{d\hat{t}} = 4|\hat{z}|^2.$$

Let  $U_1 \in \mathbb{R}^4$  denote the open set

$$U_1 = \{ \hat{\mathbf{x}} = (\hat{x}, \hat{p}, \hat{y}, \hat{q}) \in \mathbb{R}^4 : (\hat{x}, \hat{y}) \notin \{(0, -1), (0, 1)\} \}.$$

This set will be the domain of the regularized vector field which allows us to “flow through” collisions with  $m_1$  but not with  $m_2$ .

A lengthy calculation (see [14]), applying the change of coordinates and time rescaling just described to the vector field  $f$  defined in Equation (27) leads to the regularized Levi-Civita vector field  $f_1^c: U_1 \rightarrow \mathbb{R}^4$  with the ODE  $\hat{\mathbf{x}}' = f_1^c(\hat{\mathbf{x}})$  given by

$$\begin{aligned}
\hat{x}' &= \hat{p}, \\
\hat{p}' &= 8(\hat{x}^2 + \hat{y}^2)\hat{q} + 12\hat{x}(\hat{x}^2 + \hat{y}^2)^2 + 16\mu\hat{x}^3 + 4(\mu - c)\hat{x} \\
&\quad + \frac{8\mu(\hat{x}^3 - 3\hat{x}\hat{y}^2 + \hat{x})}{((\hat{x}^2 + \hat{y}^2)^2 + 1 + 2(\hat{x}^2 - \hat{y}^2))^{3/2}}, \\
\hat{y}' &= \hat{q}, \\
\hat{q}' &= -8(\hat{x}^2 + \hat{y}^2)\hat{p} + 12\hat{y}(\hat{x}^2 + \hat{y}^2)^2 - 16\mu\hat{y}^3 + 4(\mu - c)\hat{y} \\
&\quad + \frac{8\mu(-\hat{y}^3 + 3\hat{x}^2\hat{y} + \hat{y})}{((\hat{x}^2 + \hat{y}^2)^2 + 1 + 2(\hat{x}^2 - \hat{y}^2))^{3/2}},
\end{aligned} \tag{29}$$

where the parameter  $c$  in the above ODE is  $c = E(x, p, y, q)$ . The main observation is that the regularized vector field is well defined at the origin  $(\hat{x}, \hat{y}) = (0, 0)$ , and that the origin maps to the collision with  $m_1$  when we invert the Levi-Civita coordinate transformation.

Let  $\psi_1^c(\hat{\mathbf{x}}, \hat{t})$  denote the flow generated by  $f_1^c$ . The flow conserves the first integral  $E_1^c: U_1 \rightarrow \mathbb{R}$  given by

$$\begin{aligned}
E_1^c(\hat{\mathbf{x}}) &= -\hat{q}^2 - \hat{p}^2 + 4(\hat{x}^2 + \hat{y}^2)^3 + 8\mu(\hat{x}^4 - \hat{y}^4) + 4(\mu - c)(\hat{x}^2 + \hat{y}^2) \\
&\quad + 8(1 - \mu) + 8\mu \frac{(\hat{x}^2 + \hat{y}^2)}{\sqrt{(\hat{x}^2 + \hat{y}^2)^2 + 1 + 2(\hat{x}^2 - \hat{y}^2)}}.
\end{aligned} \tag{30}$$

Note that the parameter  $c$  appears both in the formulae for  $f_1^c$  and  $E_1^c$ . We write  $\psi_1^c$  to stress that the flow depends explicitly on the choice of  $c$ . We choose  $c \in \mathbb{R}$  and then, after regularization, have new coordinates which allow us to study collisions only in the level set

$$M := \{\mathbf{x} \in U : E(\mathbf{x}) = c\}. \tag{31}$$

We define the linear subspace  $\mathcal{C}_1 \subset \mathbb{R}^4$  by

$$\mathcal{C}_1 = \{(\hat{x}, \hat{p}, \hat{y}, \hat{q}) \in \mathbb{R}^4 \mid \hat{x} = \hat{y} = 0\},$$

The change of coordinates between the two coordinate systems is given by the transform  $T_1: U_1 \setminus \mathcal{C}_1 \rightarrow U$ ,

$$\mathbf{x} = T_1(\hat{\mathbf{x}}) := \begin{pmatrix} \hat{x}^2 - \hat{y}^2 + \mu \\ \frac{\hat{x}\hat{p} - \hat{y}\hat{q}}{2(\hat{x}^2 + \hat{y}^2)} \\ 2\hat{x}\hat{y} \\ \frac{\hat{y}\hat{p} + \hat{x}\hat{q}}{2(\hat{x}^2 + \hat{y}^2)} \end{pmatrix}, \tag{32}$$

and is a local diffeomorphism on  $U_1 \setminus \mathcal{C}_1$ . The following theorem collects results from [14], and relates the dynamics of the original and the regularized systems.



**Theorem 20.** Let  $c$  be the fixed parameter determining the level set  $M$  in Equation (31). Assume that  $\mathbf{x}_0 \in U$  satisfies  $E(\mathbf{x}_0) = c$ , and assume that  $\hat{\mathbf{x}}_0 \in U_1 \setminus \mathcal{C}_1$  is such that  $\mathbf{x}_0 = T_1(\hat{\mathbf{x}}_0)$ . Then the curve

$$\gamma(s) := T_1(\psi_1^c(\hat{\mathbf{x}}_0, s))$$

parameterizes the following possible solutions of the PCRTBP in  $M$ :

1. If for every  $\hat{t} \in [-\hat{T}, \hat{T}]$  we have  $\psi_1^c(\hat{\mathbf{x}}_0, \hat{t}) \in U_1 \setminus \mathcal{C}_1$ , then  $\gamma(s)$ , for  $s \in [-\hat{T}, \hat{T}]$  lies on a trajectory of the PCRTBP which avoids collisions. Moreover, the time  $t$  in the original coordinates that corresponds to the time  $\hat{t} \in [-\hat{T}, \hat{T}]$  in the regularised coordinates is recovered by the integral

$$t = 4 \int_0^{\hat{t}} (\hat{x}(s)^2 + \hat{y}(s)^2) ds, \quad (33)$$

i.e.

$$\phi(t, \mathbf{x}_0) = T_1(\psi_1^c(\hat{\mathbf{x}}_0, \hat{t})).$$

2. If for  $\hat{T} > 0$ , for every  $\hat{t} \in [0, \hat{T})$  we have  $\psi_1^c(\hat{\mathbf{x}}_0, \hat{t}) \in U_1 \setminus \mathcal{C}_1$  and  $\psi_1^c(\hat{\mathbf{x}}_0, \hat{T}) \in \mathcal{C}_1$ , then in the original coordinates the trajectory starting from  $\mathbf{x}_0$  reaches the collision with  $m_1$  at time  $T > 0$  given by

$$T = 4 \int_0^{\hat{T}} (\hat{x}(s)^2 + \hat{y}(s)^2) ds. \quad (34)$$

3. If for  $\hat{T} < 0$ , for every  $\hat{t} \in (\hat{T}, 0]$  we have  $\psi_1^c(\hat{\mathbf{x}}_0, \hat{t}) \in U_1 \setminus \mathcal{C}_1$  and  $\psi_1^c(\hat{\mathbf{x}}_0, \hat{T}) \in \mathcal{C}_1$ , then in the original coordinates the backward trajectory starting from  $\mathbf{x}_0$  reaches the collision with  $m_1$  at time  $T < 0$  expressed in Equation (34).

Orbits satisfying condition 2 from Theorem 20 are collision orbits, while orbits satisfying condition 3 from Theorem 20 are called ejection orbits. From Theorem 20 we see that for regularized orbits  $\psi_1^c(\hat{\mathbf{x}}_0, \hat{t})$  to have a physical meaning in the original coordinates we need to choose  $c = E(T_1(\hat{\mathbf{x}}_0))$  for the regularization energy. The following lemma, whose proof is a standard calculation (see [14]), addresses this choice.

**Lemma 21.** For every  $\hat{\mathbf{x}} \in U_1$ , we have

$$E(T_1(\hat{\mathbf{x}})) = c \quad \text{if and only if} \quad E_1^c(\hat{\mathbf{x}}) = 0. \quad (35)$$

The following corollary of Lemma 21 is a consequence of evaluating the expression for the energy at zero when the positions are zero.

**Corollary 22.** If we consider  $\hat{\mathbf{x}} = (\hat{x}, \hat{p}, \hat{y}, \hat{q})$  with  $\hat{x} = \hat{y} = 0$ , which corresponds to a collision with  $m_1$ , then from  $E_1^c(\hat{\mathbf{x}}) = 0$  we see that for a trajectory  $\psi_1^c(\hat{\mathbf{x}}, \hat{t})$  starting from a collision point  $\hat{\mathbf{x}} = (0, \hat{p}, 0, \hat{q})$  to have a physical meaning in the original coordinates it is necessary and sufficient that

$$\hat{q}^2 + \hat{p}^2 = 8(1 - \mu). \quad (36)$$

**Definition 23.** We refer to

$$\{\psi_1^c(\hat{\mathbf{x}}, \hat{t}) : \hat{q}^2 + \hat{p}^2 = 8(1 - \mu), \hat{t} \geq 0 \text{ and } \psi_1^c(\hat{\mathbf{x}}, [0, \hat{t}]) \cap \mathcal{C}_1 = \emptyset\}$$

as the ejection manifold from  $m_1$ , and

$$\{\psi_1^c(\hat{\mathbf{x}}, \hat{t}) : \hat{q}^2 + \hat{p}^2 = 8(1 - \mu), \hat{t} \leq 0 \text{ and } \psi_1^c(\hat{\mathbf{x}}, [\hat{t}, 0]) \cap \mathcal{C}_1 = \emptyset\}$$

as the collision manifold to  $m_1$ .

Note that both the collision and the ejection manifolds depend on the choice of  $c$ . That is, we have a family of collision/ejection manifolds, parameterized by the Jacobi constant  $c$ . For a fixed  $c$  the collision manifold, when viewed in the original coordinates, consists of points with energy  $c$ , whose forward trajectory reaches the collision with  $m_1$ . Similarly, for fixed  $c$ , the ejection manifold, in the original coordinates, consists of points with energy  $c$  whose backward trajectory collide with  $m_1$ . Thus, the circle defined in Corollary 22 is a sort of “fundamental domain” for ejections/collisions to  $m_1$  with energy  $c$ .

### 3.2. Regularization of collisions with $m_2$

To regularize at the second primary, we define the coordinates  $\tilde{z} = \tilde{x} + i\tilde{y}$  through  $\tilde{z}^2 = z + 1 - \mu$  and consider the time rescaling  $dt/d\tilde{t} = 4|\tilde{z}|^2$ . As in the previous section, define

$$\begin{aligned} U_2 &:= \{\tilde{\mathbf{x}} = (\tilde{x}, \tilde{p}, \tilde{y}, \tilde{q}) \in \mathbb{R}^4 \mid (\tilde{x}, \tilde{y}) \notin \{(-1, 0), (1, 0)\}\}, \\ \mathcal{C}_2 &:= \{\tilde{\mathbf{x}} = (\tilde{x}, \tilde{p}, \tilde{y}, \tilde{q}) \in \mathbb{R}^4 \mid \tilde{x} = \tilde{y} = 0\}, \end{aligned}$$

so that  $U_2$  consists of points in the regularized coordinates which do not collide with  $m_1$ , and  $\mathcal{C}_2$  consists of points which collide with  $m_2$ .

The regularized Levi-Civita vector field  $f_2^c : U_2 \rightarrow \mathbb{R}^4$  with the ODE  $\tilde{\mathbf{x}}' = f_2^c(\tilde{\mathbf{x}})$  is of the form (see [14])

$$\begin{aligned} \tilde{x}' &= \tilde{p}, \\ \tilde{p}' &= 8(\tilde{x}^2 + \tilde{y}^2)\tilde{q} + 12\tilde{x}(\tilde{x}^2 + \tilde{y}^2)^2 - 16(1 - \mu)\tilde{x}^3 + 4((1 - \mu) - c)\tilde{x} \\ &\quad + \frac{8(1 - \mu)(-\tilde{x}^3 + 3\tilde{x}\tilde{y}^2 + \tilde{x})}{((\tilde{x}^2 + \tilde{y}^2)^2 + 1 + 2(\tilde{y}^2 - \tilde{x}^2))^{3/2}}, \\ \tilde{y}' &= \tilde{q}, \\ \tilde{q}' &= -8(\tilde{y}^2 + \tilde{x}^2)\tilde{p} + 12\tilde{y}(\tilde{x}^2 + \tilde{y}^2)^2 + 16(1 - \mu)\tilde{y}^3 + 4((1 - \mu) - c)\tilde{y} \\ &\quad + \frac{8(1 - \mu)(\tilde{y}^3 - 3\tilde{x}^2\tilde{y} + \tilde{y})}{((\tilde{x}^2 + \tilde{y}^2)^2 + 1 + 2(\tilde{y}^2 - \tilde{x}^2))^{3/2}}, \end{aligned} \tag{37}$$

with the integral of motion

$$\begin{aligned} E_2^c(\tilde{\mathbf{x}}) &= -\tilde{p}^2 - \tilde{q}^2 + 4(\tilde{x}^2 + \tilde{y}^2)^3 + 8(1 - \mu)(\tilde{y}^4 - \tilde{x}^4) + 4((1 - \mu) - c)(\tilde{x}^2 + \tilde{y}^2) \\ &\quad + 8(1 - \mu)\frac{\tilde{x}^2 + \tilde{y}^2}{\sqrt{(\tilde{x}^2 + \tilde{y}^2)^2 + 1 + 2(\tilde{y}^2 - \tilde{x}^2)}} + 8\mu. \end{aligned} \tag{38}$$

We write  $\psi_2^c(\tilde{\mathbf{x}}, \tilde{t})$  for the flow induced by (37).

The change of coordinates from the regularized coordinates  $\tilde{\mathbf{x}}$  to the original coordinates  $\mathbf{x}$  is given by  $T_2 : U_2 \setminus \mathcal{C}_2 \rightarrow \mathbb{R}^4$  of the form

$$\mathbf{x} = T_2(\tilde{\mathbf{x}}) = \begin{pmatrix} \tilde{x}^2 - \tilde{y}^2 + \mu - 1 \\ \frac{\tilde{x}\tilde{p} - \tilde{y}\tilde{q}}{2(\tilde{x}^2 + \tilde{y}^2)} \\ 2\tilde{x}\tilde{y} \\ \frac{\tilde{y}\tilde{p} + \tilde{x}\tilde{q}}{2(\tilde{x}^2 + \tilde{y}^2)} \end{pmatrix}. \quad (39)$$

A theorem analogous to Theorem 20 characterizes solution curves in the two coordinate systems and the collisions with the second primary  $m_2$ . Also, analogously to Lemma 21 and Corollary 22 for every  $\tilde{\mathbf{x}} \in U_2$  we have

$$E(T_2(\tilde{\mathbf{x}})) = c \quad \text{if and only if} \quad E_2^c(\tilde{\mathbf{x}}) = 0, \quad (40)$$

and a trajectory  $\psi_2^c(\tilde{\mathbf{x}}, \tilde{t})$  starting from a collision point  $\tilde{\mathbf{x}} = (0, \tilde{p}, 0, \tilde{q})$  with  $m_2$  has physical meaning in the original coordinates if and only if

$$\tilde{q}^2 + \tilde{p}^2 = 8\mu. \quad (41)$$

We introduce the notions of the ejection and collision manifolds for  $m_2$  analogously to Definition 23.

#### 4. Ejection-collision orbits

We now define a level set multiple shooting operator whose zeros correspond to transverse ejection-collision orbits from the body  $m_k$  to the body  $m_l$  for  $k, l \in \{1, 2\}$  in the PCRTBP. Two such orbits in the PCRTBP are illustrated in Figure 3.

Note that the PCRTBP has the form discussed in Example 17, so that a dissipative unfolding is given by the one parameter family of ODEs

$$f_\alpha(x, p, y, q) = f(x, p, y, q) + \alpha(0, p, 0, q), \quad (42)$$

where  $f$  is as defined in Equation (27). Let  $\phi_\alpha(\mathbf{x}, t)$  denote the flow generated by the the vector field of Equation (42). For  $c \in \mathbb{R}$  consider the fixed energy level set  $M$ . Then  $\alpha$  is an unfolding parameter for the mapping

$$R_{\tau, \alpha}(\mathbf{x}) = \phi_\alpha(\mathbf{x}, \tau)$$

from  $M$  to  $M$ . (Here  $R_{\tau, \alpha} : \mathbb{R}^4 \rightarrow \mathbb{R}^4$  for fixed  $\alpha, \tau \in \mathbb{R}$ .)

Define the functions  $P_i : \mathbb{R} \rightarrow \mathbb{R}^4$  for  $i = 1, 2$  by

$$P_i(\theta) := \begin{cases} (0, \sqrt{8(1-\mu)} \cos(\theta), 0, \sqrt{8(1-\mu)} \sin(\theta)) & \text{for } i = 1, \\ (0, \sqrt{8\mu} \cos(\theta), 0, \sqrt{8\mu} \sin(\theta)) & \text{for } i = 2. \end{cases} \quad (43)$$

By Equations (36) and (41) the function  $P_i(\theta)$  parameterizes the collision set for the primary  $m_i$ , with  $i = 1, 2$ . Fix  $k, l \in \{1, 2\}$  and consider level sets  $M_1, \dots, M_6 \subset \mathbb{R}^4$

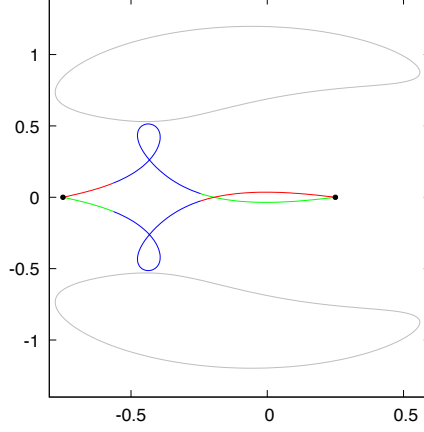


Figure 3: Ejection collision orbits in the PCRTBP when  $\mu = 1/4$  and  $C = 3.2$ . The grey curves at the top and bottom of the figure illustrate the zero velocity curves, i.e. the boundaries of the prohibited Hill's regions, for this value of  $C$ . The black dots at  $x = \mu$  and  $x = -1 + \mu$  depict the locations of the primary bodies. The curves in the middle of the figure represent two ejection-collision orbits:  $m_2$  to  $m_1$  (bottom) and  $m_1$  to  $m_2$  (top). (Recall that  $m_2$  is on the left and  $m_1$  on the right; compare with Figure 2.) These orbits are computed by numerically locating an approximate zero of the function defined in Equation (44). In setting up the BVP we choose to spend  $s = 0.35$  time units in each of the regularized coordinate systems (red and green orbit segments) but this transforms to unequal amounts of time in the original/synodic coordinates. The blue portion of the orbit is in the original coordinates. The curves are plotted by changing all points back to the original coordinates. The entire ejection-collision takes about 2.427 time units in the original/synodic coordinates.

defined by

$$\begin{aligned} M_1 = M_2 &= \{E_k^c = 0\}, \\ M_3 = M_4 &= \{E = c\}, \\ M_5 = M_6 &= \{E_l^c = 0\}. \end{aligned}$$

Choose  $s > 0$ , and for  $i = 1, 2$  recall the definition of the coordinate transformations  $T_i: U_i \setminus \mathcal{C}_i \rightarrow \mathbb{R}^4$  defined in Equations (32) and (39). Taking the maps  $R_{\tau, \alpha}^1, \dots, R_{\tau, \alpha}^5: \mathbb{R}^4 \rightarrow \mathbb{R}^4$  as

$$\begin{aligned} R_{\tau, \alpha}^1(x_1) &= \psi_k^c(x_1, s), \\ R_{\tau, \alpha}^2(x_2) &= T_k(x_2), \\ R_{\tau, \alpha}^3(x_3) &= \phi_\alpha(x_3, \tau), \\ R_{\tau, \alpha}^4(x_4) &= T_l^{-1}(x_4), \\ R_{\tau, \alpha}^5(x_5) &= \psi_l^c(x_5, s), \end{aligned}$$

we let

$$F: \underbrace{\mathbb{R} \times \mathbb{R}^4 \times \dots \times \mathbb{R}^4}_{5 \text{ copies}} \times \mathbb{R} \times \mathbb{R} \times \mathbb{R} \rightarrow \underbrace{\mathbb{R}^4 \times \dots \times \mathbb{R}^4}_{6 \text{ copies}}$$

be defined as

$$F(x_0, x_1, \dots, x_5, x_6, \tau, \alpha) := \begin{pmatrix} P_k(x_0) - x_1 \\ R_{\alpha, \tau}^1(x_1) - x_2 \\ R_{\alpha, \tau}^2(x_2) - x_3 \\ R_{\alpha, \tau}^3(x_3) - x_4 \\ R_{\alpha, \tau}^4(x_4) - x_5 \\ R_{\alpha, \tau}^5(x_5) - P_l(x_6) \end{pmatrix}, \quad (44)$$

where  $x_0, x_6, \tau, \alpha \in \mathbb{R}$  and  $x_1, \dots, x_5 \in \mathbb{R}^4$ . We also write  $(x_k, p_k, y_k, q_k)$  and  $(x_l, p_l, y_l, q_l)$  to denote the regularized coordinates given by the coordinate transformations  $T_k$  and  $T_l$ , respectively.

**Lemma 24.** *Let  $\mathbf{x}^* = (x_0^*, \dots, x_6^*)$  and  $\tau^* > 0$ . If*

$$DF(\mathbf{x}^*, \tau^*, 0)$$

*is an isomorphism and*

$$F(\mathbf{x}^*, \tau^*, 0) = 0,$$

*then the orbit of the point  $x_3^*$  is ejected from the primary body  $m_k$  and collides with the primary body  $m_l$ . (The same is true of the orbit of the point  $x_4^*$ .) Moreover, intersection of the collision and ejection manifolds is transversal on the energy level  $\{E = c\}$  and the time from the ejection to the collision is*

$$\tau^* + 4 \int_0^s \|\pi_{x_k, y_k} \psi_k^c(x_1^*, u)\|^2 du + 4 \int_0^s \|\pi_{x_l, y_l} \psi_l^c(x_5^*, u)\|^2 du. \quad (45)$$

*(Above we use the Euclidean norm.)*

**Proof.** We have  $d_0 = d_6 = k = 1$  and  $d = 4$ , so the condition in Equation (14) is satisfied. We now show that  $\alpha$  is an unfolding parameter for  $R_{\tau, \alpha} = R_{\tau, \alpha}^5 \circ \dots \circ R_{\tau, \alpha}^1$ . Since  $E_i^c$  is an integral of motion for the flow  $\psi_i^c$ , for  $i = 1, 2$ , we see that

$$\begin{aligned} x_1 \in M_1 = \{E_k^c = 0\} & \quad \text{if and only if} & \quad R_{\tau, \alpha}^1(x_1) = \psi_k^c(x_1, s) \in M_2 = \{E_k^c = 0\}, \\ x_5 \in M_5 = \{E_l^c = 0\} & \quad \text{if and only if} & \quad R_{\tau, \alpha}^5(x_5) = \psi_l^c(x_5, s) \in M_6 = \{E_l^c = 0\}. \end{aligned}$$

Also, by Equations (35) and (40) we see that

$$\begin{aligned} x_2 \in M_2 = \{E_k^c = 0\} & \quad \text{if and only if} & \quad R_{\tau, \alpha}^2(x_2) = T_k(x_2) \in M_3 = \{E = c\}, \\ x_4 \in M_4 = \{E = c\} & \quad \text{if and only if} & \quad R_{\tau, \alpha}^4(x_4) = T_l^{-1}(x_4) \in M_5 = \{E_l^c = 0\}. \end{aligned}$$

Moreover  $\alpha$  is an unfolding parameter for the PCRTBP, and hence for

$$R_{\tau, \alpha}^3(x_3) = \phi_\alpha(x_3, \tau).$$

Note that for  $i = 1, 2, 4, 5$ , the maps  $R_{\tau, \alpha}^i$  takes the level sets  $M_i$  into the level set  $M_{i+1}$  and this does not depend on the choice of  $\alpha$ . Then, since  $\alpha$  is an unfolding parameter for  $R_{\tau, \alpha}^3$ , it follows directly from Definition 13 that  $\alpha$  is an unfolding parameter for  $R_{\tau, \alpha} = R_{\tau, \alpha}^5 \circ \dots \circ R_{\tau, \alpha}^1$ .

By applying Lemma 19 to

$$\tilde{F}(x_0, x_6, \tau, \alpha) := R_{\tau, \alpha}(P_k(x_0)) - P_l(x_6)$$

we obtain that  $D\tilde{F}(x_0^*, x_6^*, \tau^*, 0)$  is an isomorphism and that  $\tilde{F}(x_0^*, x_6^*, \tau^*, 0) = 0$ . Since

$$\tilde{F}(x_0^*, x_6^*, \tau^*, 0) = \psi_l^c(T_l^{-1}(\phi(T_k(\psi_k^c(P_k(x_0^*), s)), \tau^*)), s) - P_l(x_6^*),$$

we see that, by Theorem 20 (and its mirror counterpart for the collision with  $m_2$ ) we have an orbit originating at the point  $P_k(x_0^*)$  on the collision set for  $m_k$ , and terminating at the point  $P_l(x_6^*)$  on the collision set for  $m_l$ . The transversality of the intersection between the ejection manifold of  $m_k$  and the collision manifold of  $m_l$  follows from Theorem 16. The time between collisions in Equation (45) follows from Equation (34). ■

**Remark 25 (Additional shooting steps).** We remark that in practice, computing accurate enclosures of flow maps requires shortening the time step. Consider for example the third and fourth component of  $F$  as defined in Equation (44), and suppose that time step of length  $\tau/N$  is desired. By the properties of the flow map, solving the sub-system of equations

$$\begin{aligned} R_{\alpha, \tau}^3(x_3) - x_4 &= \phi_\alpha(x_3, \tau) - x_4 = 0 \\ R_{\alpha, \tau}^4(x_4) - x_5 &= T_l^{-1}(x_4) - x_5 = 0 \end{aligned} \tag{46}$$

is equivalent to solving

$$\begin{aligned} \phi_\alpha(x_3, \tau/N) - y_1 &= 0 \\ \phi_\alpha(y_1, \tau/N) - y_2 &= 0 \\ &\vdots \\ \phi_\alpha(y_{N-2}, \tau/N) - y_{N-1} &= 0 \\ \phi_\alpha(y_{N-1}, \tau/N) - x_4 &= 0 \\ T_l^{-1}(x_4) - x_5 &= 0, \end{aligned}$$

and we can append these new variables and components to the map  $F$  defined in Equation (44) without changing the zeros of the operator. Moreover, by Lemma 19 the transversality result for the operator is not changed by the addition of additional steps. Indeed, by the same reasoning we can (and do) add intermediate shooting steps in the regularized coordinates to reduce the time steps to any desired tolerance.

## 5. Connections between collisions and libration points $L_4, L_5$

For each value of  $\mu \in (0, 1/2]$ , the PCRTBP has exactly five equilibrium solutions. For traditional reasons, these are referred to as libration points of the PCRTBP. Three of these are collinear with the primary bodies, and lie on the  $x$ -axis. These are referred to as  $L_1, L_2$  and  $L_3$ , and they correspond to the co-linear relative equilibrium solutions discovered by Euler. The remaining two libration points are located at the third vertex of the equilateral triangles whose other two vertices are the primary and secondary bodies. These are referred to as  $L_4$  and  $L_5$ , and correspond to the equilateral triangle solutions of Lagrange. Figure 4 illustrates the locations of the libration points in the phase space.

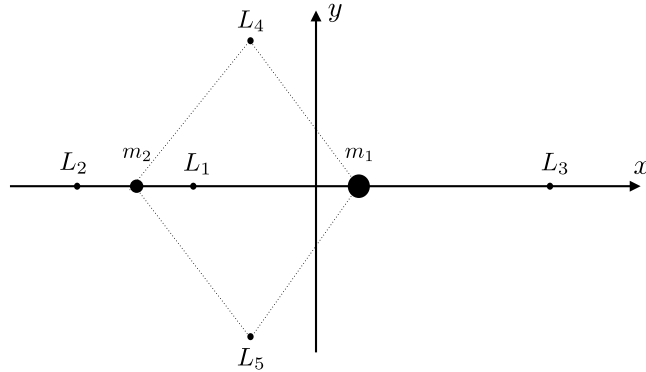


Figure 4: The three collinear libration points  $L_{1,2,3}$  and the equilateral triangle libration points  $L_{4,5}$ , relative to the positions of the primary masses  $m_1$  and  $m_2$ .

For all values of the mass ratio, the collinear libration points have saddle  $\times$  center stability. The center manifolds give rise to important families of periodic orbits known as Lyapunov families. The stability of  $L_4$  and  $L_5$  depend on the mass ratio  $\mu$ . For

$$0 < \mu < \mu_* \approx 0.04,$$

where the exact value is  $\mu_* = 2/(25 + \sqrt{621})$ , the triangular libration points have center  $\times$  center stability. That is, they are stable in the sense of Hamiltonian systems and exhibit the full “zoo” of nearby KAM objects.

When  $\mu > \mu_*$ , the triangular libration points  $L_4$  and  $L_5$  have saddle-focus stability. That is, they have a complex conjugate pair of stable and a complex conjugate pair of unstable eigenvalues. The four eigenvalues then have the form

$$\lambda = \pm\alpha \pm i\beta,$$

for some  $\alpha, \beta > 0$ . In this case, each libration point has an attached two dimensional stable and two dimensional unstable manifold. Since these two dimensional manifolds live in the three dimensional energy level set of  $L_{4,5}$ , there exists the possibility that they intersect the two dimensional collision or ejection manifolds of the primaries transversely. It is also possible that the stable/unstable manifolds of  $L_{4,5}$  intersect one other transversely giving rise to homoclinic or heteroclinic connecting orbits.

In fact, in this paper we prove that both of these phenomena occur and in this section we discuss our method for proving the existence of intersections between a stable/unstable manifold of  $L_{4,5}$ , and an ejection/collision manifold of a primary body. Any point of intersection between these manifolds gives rise to an orbit which is asymptotic to  $L_4$ , but which collides or is ejected from one of the massive bodies. Two such orbits are illustrated in Figure 5.

Let  $\bar{B} \subset \mathbb{R}^2$  denote a closed ball with radius 1. Assume that

$$w_j^\kappa : \bar{B} \rightarrow \mathbb{R}^4 \quad \text{for } j \in \{4, 5\} \text{ and } \kappa \in \{u, s\},$$

parameterize the two dimensional local stable/unstable manifolds of  $L_j$ . We assume that



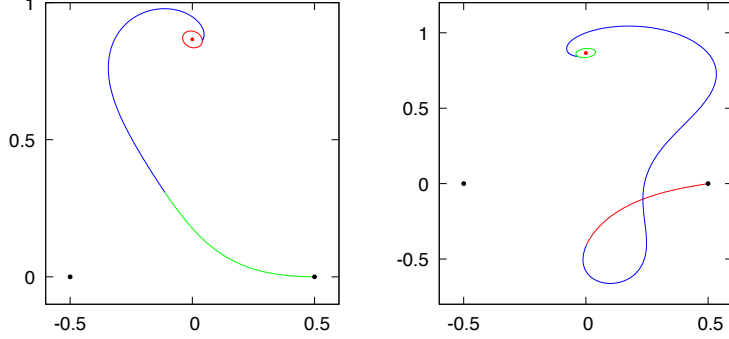


Figure 5: Libration-to-collision and ejection-to-libration orbits for  $\mu = 1/2$  and  $c = 3$  (which is the  $L_4$  value of the Jacobi constant in the equal mass problem). The left frame illustrates an ejection to  $L_4$  orbit, and the right frame an  $L_4$  to collision. In each frame  $m_1$  is depicted as a black dot and  $L_4$  as a red dot. The boundary of a parameterized local unstable manifold for  $L_4$  is depicted as the red circle; stable boundary the green circle. The orbits are found by computing an approximate zero of the map defined in Equation (48). The green portion of the left, and red portion of the right curves are computed in regularized coordinates for the body  $m_1$ , where we have fixed  $s = 0.5$  regularized time units before the change back to original/synodic coordinates. These orbit segments are transformed back to the original coordinates for the plot.

the charts are normalized so that  $w_j^\kappa(0) = L_j$ . Then

$$w_j^\kappa(\bar{B}) = W_{\text{loc}}^\kappa(L_j) \quad \text{for } j \in \{4, 5\}, \kappa \in \{u, s\}.$$

Define the functions

$$P_j^\kappa : \mathbb{R} \rightarrow \mathbb{R}^4 \quad \text{for } j \in \{4, 5\} \text{ and } \kappa \in \{u, s\},$$

by

$$P_j^\kappa(\theta) := w_j^\kappa(\cos \theta, \sin \theta). \quad (47)$$

For  $i \in \{1, 2\}$  consider  $P_i$  as defined in Equation (43).

For

$$\mathbf{x} = (x_0, x_1, x_2, x_3, x_4) \in \mathbb{R}^{14},$$

where  $x_0, x_4 \in \mathbb{R}, x_1, x_2, x_3 \in \mathbb{R}^4$ , and  $j \in \{4, 5\}$  we define

$$F_{i,j}^u, F_{i,j}^s : \mathbb{R}^{16} \rightarrow \mathbb{R}^{16},$$

by the formulas

$$F_{i,j}^u(\mathbf{x}, \tau, \alpha) = \begin{pmatrix} P_j^u(x_0) - x_1 \\ \phi_\alpha(x_1, \tau) - x_2 \\ T_i^{-1}(x_2) - x_3 \\ \psi_i^{c_j}(x_3, s) - P_i(x_4) \end{pmatrix}, \quad F_{i,j}^s(\mathbf{x}, \tau, \alpha) = \begin{pmatrix} P_i(x_0) - x_1 \\ \psi_i^{c_j}(x_1, s) - x_2 \\ T_i(x_2) - x_3 \\ \phi_\alpha(x_3, \tau) - P_j^s(x_4) \end{pmatrix}. \quad (48)$$

Here  $\tau, \alpha \in \mathbb{R}$  and the constant  $c_j$  in  $\psi_i^{c_j}$  is chosen as  $c_j = E(L_j)$ .

Zeros of the operator  $F_{i,j}^u$  correspond to intersections of the unstable manifold of  $L_j$  with the collision manifold of mass  $m_i$ . We also refer to this as a heteroclinic connection

from  $L_j$  to  $m_i$ . Similarly, zeros of the operator  $F_{i,j}^s$  correspond to intersections between the stable manifold of  $L_j$  with the ejection manifold of mass  $m_i$ . In other words, they lead to heteroclinic connections ejected from  $m_i$  and limiting to the libration point  $L_j$  in forward time. This is expressed formally in the following lemma.

**Lemma 26.** *Fix  $i \in \{1, 2\}$ ,  $j \in \{4, 5\}$ , and  $\kappa \in \{u, s\}$ . Suppose there exists  $\mathbf{x}^* = (x_0^*, x_1^*, x_2^*, x_3^*, x_4^*) \in \mathbb{R}^{14}$  and  $\tau^* > 0$  satisfying*

$$F_{i,j}^\kappa(\mathbf{x}^*, \tau^*, 0) = 0,$$

and such that

$$DF_{i,j}^\kappa(\mathbf{x}^*, \tau^*, 0)$$

is an isomorphism. Then we have the following two cases.

1. If  $\kappa = u$ , then the orbit of  $x_1^*$  is heteroclinic from the libration point  $L_j$  to collision with  $m_i$  and the intersection of  $W^u(L_j)$  with the collision manifold of  $m_i$  is transverse with respect to the energy level  $\{E = c_j\}$ .
2. If  $\kappa = s$ , then the orbit of  $x_3^*$  is heteroclinic from the libration point  $L_j$  to ejection with  $m_i$  and the intersection of  $W^s(L_j)$  with the ejection manifold of  $m_i$  is transverse with respect to the energy level  $\{E = c_j\}$ .

**Proof.** The proof follows from an argument similar to the proof of Lemma 24. ■

By a small modification of the operator just defined, we can study orbits homoclinic or heteroclinic to the libration points as well. Such orbits arise as intersections of the stable/unstable manifolds of the libration points, and lead naturally to two point BVPs. Three such orbits, homoclinic to  $L_4$  in the PCRTBP, are illustrated in Figure 6.

Note that homoclinic/heteroclinic connections between equilibrium solutions do not require changing to regularized coordinates as such orbits exist for all forward and backward time and cannot have any collisions. While this claim is mathematically correct, any homoclinic/heteroclinic orbit which passes sufficiently close to a collision with  $m_i$  for  $i \in \{1, 2\}$  becomes difficult to continue numerically. Consequently, these orbits may still be difficult or impossible to validate via computer assisted proof. In this case regularization techniques are an asset even when studying orbits which pass near a collision. The left and center homoclinic orbits in Figure 6 for example are computed entirely in the usual PCRTBP coordinates, while the right orbit was computed using both coordinate systems. With this in mind we express the homoclinic/heteroclinic problem in the framework set up in the previous sections.

Let  $P_j^\kappa : \mathbb{R} \rightarrow \mathbb{R}^4$ , for  $j \in \{4, 5\}$  be the functions defined in Equation (47) and consider

$$\mathbf{x} = (x_0, \dots, x_6) \in \mathbb{R}^{22},$$

where  $x_0, x_6 \in \mathbb{R}$  and  $x_1, \dots, x_5 \in \mathbb{R}^4$ , and fix  $s_1, s_2 > 0$ . Let

$$F_{i,j,k} : \mathbb{R}^{24} \rightarrow \mathbb{R}^{24}, \quad \text{for } j, k \in \{4, 5\}, i \in \{1, 2\},$$

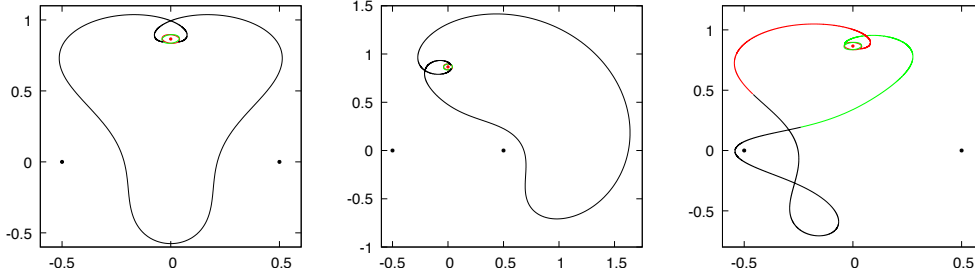


Figure 6: Transverse homoclinic orbits at  $L_4$  for  $\mu = 1/2$  in the  $C = 3$  energy level. Each orbit traverses the illustrated curves in a clockwise fashion. The left and center orbits were known to Stromgren and Szebeheley. The center and right orbits possess no symmetry, and the orbit on the right passes close to collision with  $m_2$ . Each orbit is found by approximately computing a zero of the map defined in Equation (49). The left and center orbits are computed in only the standard coordinate system. In the definition of the shooting template, we allow the orbit to spend  $s_1 = 1.8635$  regularized time units in Levi-Civita coordinates and to flow for  $s_2 = 5$  time units in the original/synodic coordinates before reaching the stable manifold.

be defined as

$$F_{i,j,k}(\mathbf{x}, \tau, \alpha) := \begin{pmatrix} P_j^u(x_0) - x_1 \\ \phi_\alpha(x_1, \tau) - x_2 \\ T_i^{-1}(x_2) - x_3 \\ \psi_i^{c_j}(x_3, s_1) - x_4 \\ T_i(x_4) - x_5 \\ \phi_\alpha(x_5, s_2) - P_k^s(x_6) \end{pmatrix}. \quad (49)$$

One can formulate an analogous result to the Lemmas 24 and 26, so that

$$F_{i,j,k}(\mathbf{x}^*, \tau^*, 0) = 0,$$

together with  $DF_{i,j,k}(\mathbf{x}^*, \tau^*, 0)$  an isomorphism implies that the manifolds  $W^u(L_j)$  and  $W^s(L_k)$  intersect transversally.

Again, the advantage of solving  $F_{i,j,k} = 0$  over parallel shooting in the original coordinates is that one can establish the existence of connections which pass arbitrarily close to a collision  $m_1$  and/or  $m_2$ . Indeed, the operator defined in Equation (49) can be generalized to study homoclinic orbits which make any finite number of flybys of the primaries in any order before returning to  $L_{4,5}$  by making additional changes of variables to regularized coordinates every time the orbit passes near collision.

## 6. Symmetric periodic orbits passing through collision

In this section we show that our method applies to the study of families of periodic orbits which pass through a collision. By this we mean the following. We will prove the existence of a family of orbits parameterized by the value of the Jacobi constant on an interval. As in the introduction, we refer to this as a tube of periodic orbits. For all values in the interval except one, the intersection of the energy level set with the tube is a periodic orbit. For a single isolated value of the energy the intersection of the

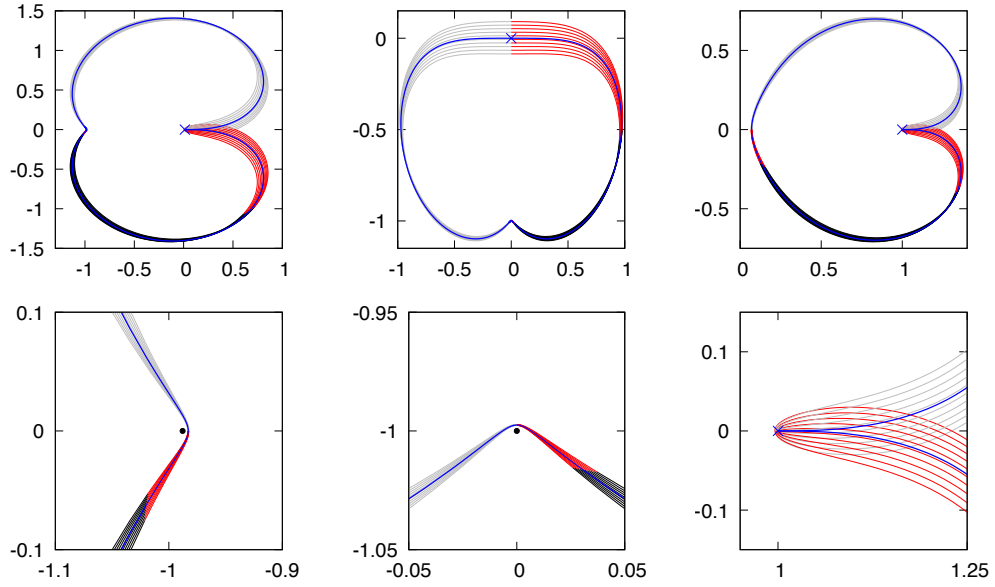


Figure 7: A family of Lyapunov periodic orbits passing through a collision. The left two figures are in the original coordinates, the middle two are in the regularised coordinates at  $m_1$  and the right two are in regularised coordinates at  $m_2$ . (Compare with Figure 2.) The trajectories computed in the original coordinates are in black, and the trajectories computed in the regularized coordinates are in red. The collision with  $m_1$  is indicated by a cross. The mass  $m_2$  is added in the closeup figures as a black dot. The operator (54) gives half of a periodic orbit in red and black. The second half, which follows from the symmetry, is depicted in grey. The plots are for the Earth-moon system.

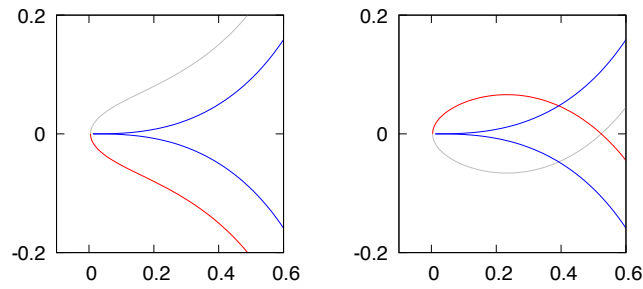


Figure 8: A closeup of a Lyapunov orbit before (left) and after (right) passing through the collision. The plot is in the original coordinates.

energy level set with the tube is an ejection-collision orbit involving  $m_1$ . The situation is depicted in Figure 7.

To establish such a family of periodic orbits we make use of the time reversing symmetry of the PCRTBP. Recall that for

$$S(x, p, y, q) := (x, -p, -y, q)$$

and for the flow  $\phi(\mathbf{x}, t)$  of the PCRTBP we have that

$$S(\phi(\mathbf{x}, t)) = \phi(S(\mathbf{x}), -t). \quad (50)$$

Let us introduce the notation  $\mathcal{S}$  to stand for the set of self  $S$ -symmetric points

$$\mathcal{S} := \{\mathbf{x} \in \mathbb{R}^4 : \mathbf{x} = S(\mathbf{x})\}.$$

The property in Equation (50) is used to find periodic orbits as follows. Suppose  $\mathbf{x}, \mathbf{y} \in \mathcal{S}$  satisfy  $\mathbf{y} = \phi(\mathbf{x}, t)$ . Then by Equation (50), we have

$$\phi(\mathbf{x}, 2t) = \phi(\mathbf{y}, t) = \phi(S(\mathbf{y}), t) = S(\phi(\mathbf{y}, -t)) = S(\mathbf{x}) = \mathbf{x}, \quad (51)$$

meaning that  $\mathbf{x}$  lies on a periodic orbit. Our strategy is then to set up a boundary value problem which shoots from  $\mathcal{S}$  to itself.

The set  $\mathcal{S}$  lies on the  $x$ -axis in the  $(x, y)$  coordinate frame. From the left plot in Figure 7 it is clear that we are interested in points on  $\mathcal{S}$  which will pass through collision with  $m_1$  and close to the collision with  $m_2$ . We therefore consider the set  $\mathcal{S}$  transformed to the regularized coordinates of  $m_1$  and  $m_2$ .

**Lemma 27.** *Let  $\hat{\mathcal{S}}, \tilde{\mathcal{S}} \subset \mathbb{R}^4$  be defined as*

$$\begin{aligned} \hat{\mathcal{S}} &= \{(0, \hat{p}, \hat{y}, 0) : \hat{p}, \hat{y} \in \mathbb{R}\}, \\ \tilde{\mathcal{S}} &= \{(\tilde{x}, 0, 0, \tilde{q}) : \tilde{x}, \tilde{q} \in \mathbb{R}\}. \end{aligned}$$

*Then  $T_1(\hat{\mathcal{S}}) = \mathcal{S}$  and  $T_2(\tilde{\mathcal{S}}) = \mathcal{S}$ .*

**Proof.** The proof follows directly from the definition of  $T_1$  and  $T_2$ . (See Equations (32) and (39).) ■

The intuition behind the choice of  $\hat{\mathcal{S}}, \tilde{\mathcal{S}}$  is seen in Figure 2. From the figure we see that the set  $\hat{\mathcal{S}}$  is the vertical axis  $\{\hat{x} = 0\}$  and  $\tilde{\mathcal{S}}$  is the horizontal axis  $\{\tilde{y} = 0\}$ , which join the primaries in the regularized coordinates.

To find the desired symmetric periodic orbits we fix an energy level  $c \in \mathbb{R}$  and introduce an appropriate shooting operator, whose zero implies the existence of an orbit with energy  $c$ . Slightly abusing notation, let us first define two functions  $\hat{p}, \tilde{q} : \mathbb{R}^2 \rightarrow \mathbb{R}$  as

$$\begin{aligned} \hat{p}(\hat{y}, c) &:= \sqrt{4\hat{y}^6 - 8\mu\hat{y}^4 + 4(\mu - c)\hat{y}^2 + \frac{8\mu\hat{y}^2}{\sqrt{\hat{y}^4 + 1 - 2\hat{y}^2}} + 8(1 - \mu)}, \\ \tilde{q}(\tilde{x}, c) &:= \sqrt{4\tilde{x}^6 - 8(1 - \mu)\tilde{x}^4 + 4((1 - \mu) - c)\tilde{x}^2 + \frac{8(1 - \mu)\tilde{x}^2}{\sqrt{\tilde{x}^4 + 1 - 2\tilde{x}^2}} + 8\mu}. \end{aligned}$$

Observe that from Equations (30) and (38) we have

$$E_1^c(0, \hat{p}(\hat{y}, c), \hat{y}, 0) = 0, \quad (52)$$

$$E_2^c(\tilde{x}, 0, 0, \tilde{q}(\tilde{x}, c)) = 0. \quad (53)$$

Next, we define  $P_1^c, P_2^c : \mathbb{R} \rightarrow \mathbb{R}^4$  by

$$\hat{P}_1^c(\hat{y}) := (0, \hat{p}(\hat{y}, c), \hat{y}, 0),$$

$$\tilde{P}_2^c(\tilde{x}) := (\tilde{x}, 0, 0, \tilde{q}(\tilde{x}, c)),$$

and note that  $P_1^c(\mathbb{R}) \subset \hat{\mathcal{S}}$  and  $P_2^c(\mathbb{R}) \subset \tilde{\mathcal{S}}$ . Taking

$$\mathbf{x} = (x_0, x_1, \dots, x_5, x_6) \in \mathbb{R} \times \underbrace{\mathbb{R}^4 \times \dots \times \mathbb{R}^4}_{5 \text{ copies}} \times \mathbb{R} = \mathbb{R}^{22},$$

we define the shooting operator  $F_c : \mathbb{R}^{24} \rightarrow \mathbb{R}^{24}$  as

$$F_c(\mathbf{x}, \tau, \alpha) = \begin{pmatrix} \hat{P}_1^c(x_0) - x_1 \\ \psi_1^c(x_1, s) - x_2 \\ T_1(x_2) - x_3 \\ \phi_\alpha(x_3, \tau) - x_4 \\ T_2^{-1}(x_4) - x_5 \\ \psi_2^c(x_5, s) - \tilde{P}_2^c(x_6) \end{pmatrix}. \quad (54)$$

We have the following result.

**Lemma 28.** *Suppose that for  $c \in \mathbb{R}$  we have an  $\mathbf{x}(c) \in \mathbb{R}^{22}$  and  $\tau(c) \in \mathbb{R}$  for which*

$$F_c(\mathbf{x}(c), \tau(c), 0) = 0,$$

*then we have one of the following three cases:*

1. *If  $x_0(c) \neq 0$  and  $x_6(c) \neq 0$ , then the orbit through  $T_1(\hat{P}_1^c(x_0(c)))$  is periodic.*
2. *If  $x_0(c) = 0$  and  $x_6(c) \neq 0$ , then the orbit through  $T_1(\hat{P}_1^c(x_0(c)))$  is an ejection-collision with  $m_1$ .*
3. *If  $x_0(c) \neq 0$  and  $x_6(c) = 0$ , then the orbit through  $T_1(\hat{P}_1^c(x_0(c)))$  is an ejection-collision with  $m_2$ .*

**Proof.** The result follows immediately from the definition of  $F_c$  in Equation (54) and from Theorem 20 (or the analogous theorem for  $m_2$ ). We highlight the fact that due to Equations (52)–(53) we have  $E_1^c(\hat{P}_1^c(x_0)) = 0$  and  $E_2^c(\tilde{P}_2^c(x_6)) = 0$ , so the trajectories in the regularized coordinates correspond to the physical trajectories in the physical coordinates of the PCRTBP. ■

We can use the implicit function theorem to compute the derivative of  $\mathbf{x}(c)$  with respect to  $c$ . Let us write  $\mathbf{y}(c) := (\mathbf{x}(c), \tau(c), \alpha(c))$  and suppose  $F_c(\mathbf{y}(c)) = 0$ . (Note that in fact we must also have that  $\alpha(c) = 0$  since  $\alpha$  is unfolding.) Then  $\frac{d}{dc}\mathbf{x}(c)$  is computed from the first coordinates of the vector  $\frac{d}{dc}\mathbf{y}(c)$  and is given by the formula

$$\frac{d}{dc}\mathbf{y}(c) = - \left( \frac{\partial F_c}{\partial \mathbf{y}} \right)^{-1} \frac{\partial F_c}{\partial c}. \quad (55)$$

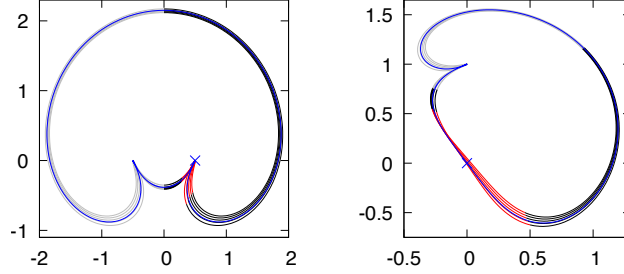


Figure 9: A family of periodic orbits passing through a double collision. The left figure is in the original coordinates and the right figure is in the regularised coordinates at  $m_1$ . The trajectories computed in the original coordinates are in black, the trajectories computed in the regularized coordinates are in red, and the collision orbit is in blue. The second half of an orbit, which follows from the  $R$ -symmetry, is depicted in grey. The plots are for the system with equal masses.

**Theorem 29.** *Assume that for  $c \in [c_1, c_2]$  the functions  $\mathbf{x}(c)$  and  $\tau(c)$  solve the implicit equation*

$$F_c(\mathbf{x}(c), \tau(c), 0) = 0.$$

If

$$x_0(c_1) > 0 > x_0(c_2), \quad (56)$$

$$x_6(c) \neq 0 \quad \text{for all } c \in [c_1, c_2], \quad (57)$$

and

$$\frac{d}{dc}x_0(c) < 0 \quad \text{for all } c \in [c_1, c_2], \quad (58)$$

then there exists a unique energy parameter  $c^* \in (c_1, c_2)$  for which we have an intersection of the ejection and collision manifolds of  $m_1$ . Moreover, for all remaining  $c \in [c_1, c_2] \setminus \{c^*\}$  the orbit of the point  $T_1(\hat{P}_1^c(x_0(c)))$  is periodic.

**Proof.** The result follows directly from the Bolzano theorem and Lemma 28. ■

Theorem 29 is deliberately formulated so that its hypotheses can be validated via computer assistance. Specifically, rigorous enclosures of Equation (55) are rigorously computed and Equations (56)-(58) are rigorously verified using interval arithmetic.

We finish this section with an example of a similar approach, which can be used for the proofs of double collisions in the case when  $m_1 = m_2 = \frac{1}{2}$ . That is, we establish the existence of a family of periodic orbits, parameterized by energy (the Jacobi constant), which are symmetric with respect to the  $y$ -axis, and such that for a single parameter from the family we have a double collision as in Figure 9.

In this case consider  $R : \mathbb{R}^4 \rightarrow \mathbb{R}^4$  defined as

$$R(x, p, y, q) = (-x, p, y, -q).$$

For the case of two equal masses, we have the time reversing symmetry

$$R(\phi(\mathbf{x}, t)) = \phi(R(\mathbf{x}), -t). \quad (59)$$

We denote by  $\mathcal{R}$  the set of all points which are  $R$ -self symmetric, i.e.  $\mathcal{R} = \{\mathbf{x} = R(\mathbf{x})\}$ . An argument mirroring Equation (51) shows that if two points  $\mathbf{x}, \mathbf{y} \in \mathcal{R}$  have  $\mathbf{y} = \phi(\mathbf{x}, t)$ , then these points must lie on a periodic orbit.

To obtain the existence of the family of orbits depicted in Figure 9, define  $p : \mathbb{R}^2 \rightarrow \mathbb{R}$  and  $P_1^c, P_2^c : \mathbb{R} \rightarrow \mathbb{R}^4$  as

$$\begin{aligned} p(y, c) &:= \sqrt{2\Omega(0, y) - c}, \\ P_1^c(y) &:= (0, p(y, c), y, 0), \\ P_2^c(y) &:= (0, -p(y, c), y, 0). \end{aligned}$$

Note that  $P_1^c(y), P_2^c(y) \in \mathcal{R}$  and  $E(P_1^c(y)) = E(P_2^c(y)) = c$  (see Equation (28)). Consider  $x_0, x_7 \in \mathbb{R}$  and  $x_1, \dots, x_6 \in \mathbb{R}^4$ , where

$$x_4 = (s_4, \hat{p}_4, \hat{y}_4, \hat{q}_4) \in \mathbb{R}^4. \quad (60)$$

We emphasize that the first coordinate in  $x_4$  will be used here in a slightly less standard way than in the previous examples. We define also

$$\hat{x}_4 := (0, \hat{p}_4, \hat{y}_4, \hat{q}_4) \in \mathbb{R}^4.$$

We now choose some fixed  $s_2, s_5 \in \mathbb{R}$ ,  $s_2, s_5 > 0$ , and for

$$\mathbf{x} = (x_0, \dots, x_7) \in \mathbb{R} \times \underbrace{\mathbb{R}^4 \times \dots \times \mathbb{R}^4}_6 \times \mathbb{R} = \mathbb{R}^{26}$$

define the operator  $F_c : \mathbb{R}^{26} \times \mathbb{R} \times \mathbb{R} \rightarrow \mathbb{R}^{28}$  as

$$F_c(\mathbf{x}, \tau, \alpha) = \begin{pmatrix} P_1^c(x_0) - x_1 \\ \phi_\alpha(x_1, s_2) - x_2 \\ T_1^{-1}(x_2) - x_3 \\ \psi_1^c(x_3, s_4) - \hat{x}_4 \\ \psi_1^c(\hat{x}_4, s_5) - x_5 \\ T_1(x_5) - x_6 \\ \phi_\alpha(x_6, \tau) - P_2^c(x_7) \end{pmatrix}. \quad (61)$$

Note that in Equation (61) the  $s_2, s_5$  are some fixed parameters, and  $s_4$  is one of the coordinates of  $\mathbf{x}$ . We claim that if  $F_c(\mathbf{x}, \tau, 0) = 0$  and  $\pi_{\hat{y}_4} \mathbf{x} = 0$ , then the orbit of  $x_2$  passes through the collision with  $m_1$ . This is because  $\hat{x}_4 = (0, \hat{p}_4, \hat{y}_4, \hat{q}_4)$ , so that  $F_c = 0$  ensures that the point  $\psi_1^c(x_3, s_4)$  is zero on the  $\hat{x}_4$  coordinate. So, if  $F_c(\mathbf{x}) = 0$  and  $\pi_{\hat{y}_4} \mathbf{x} = 0$ , then  $\pi_{\hat{x}_4, \hat{y}_4} \psi_1^c(x_3, s_4) = 0$  and we arrive at the collision. Moreover, by the  $R$ -symmetry of the system in this case we also establish heteroclinic connections between collisions with  $m_1$  and  $m_2$  (see Figure 9).

If on the other hand  $F_c = 0$  and  $\pi_{\hat{y}_4} \mathbf{x} \neq 0$ , then we have a periodic orbit passing near the collisions with  $m_1$  and  $m_2$ . One can prove a result analogous to Theorem 29 with the minor difference being that instead of using  $x_0$  in Equations (56) and (58) we take  $\hat{y}_4$ . We omit the details in order not to repeat the same argument.



## 7. Computer assisted proofs for collision/near collision orbits

### 7.1. Newton-Krawczyk method

For a smooth mapping  $F : \mathbb{R}^n \rightarrow \mathbb{R}^n$ , the following theorem provides sufficient conditions for the existence of a solution of  $F(x) = 0$  in the neighborhood of a “good enough” approximate solution. The hypotheses of the theorem require measuring the defect associated with the approximate solution, as well as the quality of a certain condition number for an approximate inverse of the derivative. Theorems of this kind are used widely in computer assisted proofs, and we refer the interested reader to the works of [122, 123, 124, 111, 125, 112, 126, 109] for a more complete overview.

Let  $\|\cdot\|$  be a norm in  $\mathbb{R}^n$  and let  $\overline{B}(x_0, r) \subset \mathbb{R}^n$  denote a closed ball of radius  $r \geq 0$  centered at  $x_0$  in that norm.

**Theorem 30 (Newton-Krawczyk).** *Let  $U \subset \mathbb{R}^n$  be an open set and  $F : U \rightarrow \mathbb{R}^n$  be at least of class  $C^2$ . Suppose that  $x_0 \in U$  and let  $A$  be a  $n \times n$  matrix. Suppose that  $Y, Z, r > 0$  are positive constants such that  $\overline{B}(x_0, r) \subset U$  and*

$$\|AF(x_0)\| \leq Y, \quad (62)$$

$$\sup_{x \in \overline{B}(x_0, r)} \|\text{Id} - ADF(x)\| \leq Z. \quad (63)$$

If

$$Zr - r + Y \leq 0, \quad (64)$$

then there is a unique  $\hat{x} \in \overline{B}(x_0, r)$  for which  $F(\hat{x}) = 0$ . Moreover,  $DF(\hat{x})$  is invertible.

**Proof.** The proof is included in [Appendix A](#) for the sake of completeness. ■

The theorem is well suited for applications to computer assisted proofs. To validate the assumptions its enough to compute interval enclosures of the quantities  $F(x_0)$  and  $DF(B)$ , where  $B$  is a suitable ball. These enclosures are done using interval arithmetic, and the results are returned as sets (cubes in  $\mathbb{R}^n$  and  $\mathbb{R}^{n \times n}$ ) enclosing the correct values. A good choice for the matrix  $A$  is any floating point approximate inverse of the derivative of  $F$  at  $x_0$ , computed with standard linear algebra packages. The advantage of working with such an approximation is that there is no need to compute a rigorous interval enclosure of a solution of a linear equation (as in the interval Newton method). In higher dimensional problems, solving linear equations can lead to large overestimation (the so called “wrapping effect”).

In our work the evaluation of  $F$  and its derivative involves integrating ODEs and variational equations. There are well know general purpose algorithms for solving these problems, and we refer the interested reader to [127, 115, 111]. For parameterizing the invariant manifolds attached to  $L_4$  with interval enclosures, we exploit the techniques discussed in [128] (validated integration is also discussed in this reference).

We remark that our implementations use the IntLab laboratory running under Matlab<sup>6</sup> and/or the CAPD<sup>7</sup> C++ library, and recall that the source codes are found at the homepage of MC. See [129] and [113] as references for the usage and the functionality of the libraries.

<sup>6</sup><https://www.tuhh.de/ti3/rump/intlab/>

<sup>7</sup>Computer Assisted Proofs in Dynamics, <http://capd.ii.uj.edu.pl>

7.2. Computer assisted existence proofs for ejection-collision orbits

The methodology of Section 4, and especially Lemma 24, is combined with Theorem 30 to obtain the following.

**Theorem 1.** *Consider the planar PCRTBP with  $\mu = 1/4$  and  $c = 3.2$ . Let*

$$\bar{p} = \begin{pmatrix} -0.564897282072410 \\ 0.978399619177283 \\ -0.099609551141525 \\ -0.751696444982537 \end{pmatrix},$$

$$r = 2.7 \times 10^{-13},$$

and

$$B_r = \{x \in \mathbb{R}^4 : \|x - \bar{p}\| \leq r\},$$

where the norm is the maximum norm on components. Then, there exists a unique  $p_* \in B_r$  such that the orbit of  $p_*$  is ejected from  $m_2$  (at  $x = -1 + \mu, y = 0$ ), collides with  $m_1$  (at  $x = \mu, y = 0$ ), and the total time  $T$  (in synodic/un-regularized coordinates) from ejection to collision satisfies

$$2.42710599795 \leq T \leq 2.42710599796.$$

In addition, the ejection manifold of  $m_2$  intersects the collision manifold of  $m_1$  transversely along the orbit of  $p_*$ , where transversality is relative to the level set  $\{E = 3.2\}$ . Moreover, there exists a transverse  $S$ -symmetric counterpart ejected from  $m_1$  and colliding with  $m_2$ .

**Proof.** The first step in the proof is to define an appropriate version of the map  $F$  in Equation (44), whose zeros correspond to ejection-collision orbits from  $m_2$  to  $m_1$ . In particular we set  $k = 2$  and  $l = 1$ , and choose (somewhat arbitrarily) the parameter  $s = 0.35$  in the definition of the component maps  $R_{\tau,\alpha}^1$  and  $R_{\tau,\alpha}^5$ . The parameter  $s$  determines how long to integrate/flow in the regularized coordinates.

Next we compute an approximate zero  $\bar{x} \in \mathbb{R}^{24}$  of  $F$  using Newton's method. Note that interval arithmetic is not required in this step. The resulting numerical data is recorded in Table 1, and we note that  $\bar{x}_3$  in the table corresponds to  $\bar{p}$  in the hypothesis of the theorem. Note also that we take  $\bar{\alpha}$  in the approximate solution to be zero.

We define  $A$  to be the numerically computed approximate inverse of  $DF(\bar{x})$ , and let

$$B = \bar{B}(\bar{x}, r_*),$$

denote the closed ball of radius

$$r_* = 2 \times 10^{-12},$$

in the maximum norm about the numerical approximation. (The reader interested in the numerical entries of the Matrix can run the accompanying computer program). We note that the choice of  $r_*$  is somewhat arbitrary. (It should be small enough that there is not too much "wrapping", but not so small that there is no  $r \leq r_*$  satisfying the hypothesis of Theorem 30).

$\bar{x}_0 =$	2.945584780500716			
$\bar{x}_1 =$	( 0.0,	-1.387134030283961,	0.0,	0.275425456390970)
$\bar{x}_2 =$	(-0.444581369966432,	-1.038375926396089,	0.112026231721142,	0.449167625710802)
$\bar{x}_3 =$	(-0.564897282072410,	0.978399619177283,	-0.099609551141525,	-0.751696444982537)
$\bar{x}_4 =$	(-0.244097430449606,	0.878139982728136,	-0.025435855606099,	0.543608549989376)
$\bar{x}_5 =$	( 0.018086991443589,	-0.732714475912918,	-0.703153304556756,	1.254598547822042)
$\bar{x}_6 =$	1.459760691418490			
$\bar{\tau} =$	2.051635871465197			
$\bar{\alpha} =$	0.0			

Table 1: Numerical data used in the proof of Theorem 1, giving the approximate solution of  $F = 0$  for the operator (44), whose zeros correspond to the ejection-collision orbits from  $m_2$  to  $m_1$ . We set the mass ratio to  $\mu = 1/4$  and Jacobi constant to  $c = 3.2$ . The resulting orbit is illustrated in Figure 3 (bottom curve).

Using interval arithmetic and validated numerical integration we compute an interval enclosure of the length 24 vector of intervals  $\mathbf{F}$  having

$$F(\bar{x}) \in \mathbf{F},$$

and an interval enclosure of a  $24 \times 24$  interval matrix  $\mathbf{M}$  with

$$DF(x) \in \mathbf{M} \quad \text{for all } x \in B.$$

We then check, again using interval arithmetic, that

$$\|\mathbf{A}\mathbf{F}\| \in 10^{-12} \times [0.0, 0.26850976470521]$$

and that

$$\|\text{Id} - \mathbf{A}\mathbf{M}\| \in 10^{-7} \times [0.0, 0.23119622467860].$$

From these we have

$$\|\mathbf{A}F(\bar{x})\| \leq Y < 0.269 \times 10^{-12}$$

and

$$\sup_{x \in B} \|\text{Id} - \mathbf{A}DF(x)\| \leq Z < 0.232 \times 10^{-7},$$

though the actual bounds stored in the computer are tighter than those just reported (hence the inequality).

We let

$$r = \sup \left( \frac{Y}{1 - Z} \right) \leq 2.7 \times 10^{-13},$$

and note again that the actual bound stored in the computer is smaller than reported here. We then check, using interval arithmetic, that

$$Zr - r + Y \leq -5.048 \times 10^{-29} < 0.$$

We also note that, since  $r \leq r_*$ , we have that  $\bar{B}(\bar{x}, r) \subset B$ , so that

$$\sup_{x \in \bar{B}(\bar{x}, r)} \|\text{Id} - \mathbf{A}DF(x)\| \leq Z,$$

on the smaller ball as well.

From this we conclude, via Theorem 30, that there exists a unique  $x_* \in \overline{B}(\bar{x}, r) \subset \mathbb{R}^{24}$  so that  $F(x_*) = 0$ , and moreover that  $DF(x_*)$  is invertible. Hence, it now follows from Lemma 24 that there exists a transverse ejection-collision from  $m_2$  to  $m_1$  in the PCRTBP.

Note that the integration time in the standard coordinates

$$\bar{\tau} = 2.051635871465197,$$

is one of the variables of  $F$  (we are simply reading this off the table). The rescaled integration time in the regularized coordinates is fixed to be  $s = 0.35$ . Our programs compute validated bounds on the integrals in Equation (45) and provide interval enclosures for the time each orbit spends in the regularized coordinate systems of  $m_1$  and  $m_2$  respectively. This interval enclosure is

$$T_1 + T_2 \in [0.27116751585137, 0.27116751585615] + [0.10430261063473, 0.10430261063793].$$

Since the true integration time  $\tau_*$  is in an  $r$ -neighborhood of  $\bar{\tau}$  it follows that

$$\tau_* \in [2.05163587146492, 2.05163587146547].$$

Interval addition of the three time intervals containing  $T_1$ ,  $T_2$  and  $\tau_*$  provides the desired final bound on the total time of flight given in the theorem.

The connection in the other direction follows from the  $S$ -symmetry of the system (see Equation (50)). The computational part of the proof is implemented in IntLab running under MatLab, and took 21 minutes to run on a standard desktop computer. ■

The orbit whose existence is proven in Theorem 1 is illustrated in Figure 3 (lower orbit of the two orbits illustrated in the figure). The higher orbit follows from the  $S$ -symmetry of the PCRTBP. We remark that our implementation actually subdivides the time steps  $s = 0.35$  in regularized coordinates 50 times, while the time step  $\bar{\tau}$  is subdivided 200 times. This only enlarges the size of the system of equations as discussed in Remark 25.

Validation of the  $50 + 200 + 50 = 300$  steps of Taylor integration, along with the spatial and parametric variational equations, takes most of the computational time for the proof. The choice of the mass  $\mu = 1/4$  and the energy  $c = 3.2$  was more or less arbitrary and the existence of many similar orbits could be proven using the same method.

### 7.3. Connections between ejections/collisions and the libration points $L_4$ , $L_5$

We apply the methodology of Section 5, and especially Lemma 26, in conjunction with Theorem 30 to obtain the following result. The local stable (or unstable) manifolds at  $L_4$  are computed using the methods and implementation of [96]. See Appendix B for a few additional remarks concerning the parameterizations.

**Theorem 2.** *Consider planar PCRTBP with  $\mu = 1/2$  and  $c = 3$  is the energy of  $L_4$ . Let*

$$\bar{p} = \begin{pmatrix} 0.003213450375413 \\ 0.197716496638868 \\ -0.404375730348827 \\ 0.696149210661807 \end{pmatrix},$$

$$r = 8.2 \times 10^{-12},$$

$\bar{x}_0 =$	0.329444389425640			
$\bar{x}_1 =$	(-0.032305434322402,	-0.044152238388004,	0.843244687835647,	0.005057045291404)
$\bar{x}_2 =$	(0.003213450375413,	0.197716496638868,	-0.404375730348827,	0.696149210661807)
$\bar{x}_3 =$	(0.268116630482827,	-0.943915863314079,	-0.754104155383092,	0.671496024758153)
$\bar{x}_4 =$	1.696671399505923			
$\bar{\tau} =$	7.034349085576677			
$\bar{\alpha} =$	0.0			

Table 2: Numerical data providing an approximate zero of the map  $F_{i,j}^u$  defined in Equation (48), for  $i = 1, j = 4, c = 3, \mu = 1/2$  and  $s = 0.5$ . The data is used in the proof of Theorem 2, and results in the existence of the  $L_4$  to collision orbit illustrated in the right frame of Figure 5.

and

$$B_r = \{x \in \mathbb{R}^4 : \|x - \bar{p}\| \leq r\}.$$

Then there exists a unique point

$$p_* \in B_r$$

such that the orbit of  $p_*$  accumulates to  $L_4$  as  $t \rightarrow -\infty$ , collides with  $m_1$  (located at  $x = \mu, y = 0$ ) in finite forward time, and the unstable manifold of  $L_4$  intersects the collision set of  $m_1$  transversely along the orbit of  $p_*$ , where transversality is relative to level set  $\{E = 3\}$ .

**Proof.** The proof is similar to the proof of Theorem 1, and we only sketch the argument. Orbits accumulating to  $L_4$  in backward time and colliding with  $m_1$  are equivalent to zeros of the mapping  $F_{i,j}^u$  defined in Equation (48) with  $j = 4$  and  $i = 1$ . We also set the parameter  $s = 0.5$ , which is the integration time in the regularized coordinates.

The first step is to compute a numerical zero  $\bar{x} = (\bar{x}_0, \bar{x}_1, \bar{x}_2, \bar{x}_3, \bar{x}_4, \bar{\tau}, \bar{\alpha}) \in \mathbb{R}^{16}$  of  $F_{i,j}^u$ . This step exploits Newton's method (no interval arithmetic necessary), and the resulting data is reported in Table 2. Note that  $\bar{x}_1 \in \mathbb{R}^4$  from the table is the initial condition  $\bar{p}$  in the statement of the theorem. We take  $A$  to be a numerically computed approximate inverse of the  $16 \times 16$  matrix  $DF_{i,j}^u(\bar{x})$ . Again, the definition of  $A$  does not require interval arithmetic.

For the next step we compute interval enclosures of  $F(\bar{x})$  and of  $DF_{i,j}^u(x)$  for  $x$  in a cube of radius  $r_* = 5 \times 10^{-9}$  and obtain that

$$\|AF(\bar{x})\| \in 10^{-11} \times [0.0, 0.82147145471154],$$

and that

$$\sup_{x \in B_{r_*}(\bar{x})} \|\text{Id} - ADF_{i,j}^u(x)\| \in [0.0, 0.00151459031904].$$

Using interval arithmetic we compute

$$r = \frac{Y}{1 - Z} \leq 8.3 \times 10^{-12},$$

where the actual value stored in the computer is smaller than reported here (and hence the inequality). We then check, using interval arithmetic, that  $Zr - r + Y < 0$ . Since  $r < r_*$ , we have that there exists a unique  $x_* \in B_r(\bar{x})$  so that  $F_{i,j}^u(x_*) = 0$ . Moreover, transversality follows from the non-degeneracy of the derivative of  $F_{i,j}^u$ .

$\bar{x}_0 =$	1.561515178070094			
$\bar{x}_1 =$	( 0.0,	0.018562030958889,	0.0,	1.999913860896684)
$\bar{x}_2 =$	( 0.191471460280817,	0.959639244531484,	0.805673853857139,	1.170011720749615)
$\bar{x}_3 =$	(-0.112449038686946,	-0.553321424594493,	0.308527098616200,	0.727049637558895)
$\bar{x}_4 =$	5.229765599216696			
$\bar{\tau} =$	4.673109099822270			
$\bar{\alpha} =$	0.0			

Table 3: Numerical data for an approximate zero of the map  $F_{i,j}^s$  defined in Equation (48), with  $i = 1$ ,  $j = 4$  and  $s = 0.5$ . An argument similar to the proof of Theorem 2, using the data in the table, leads to an existence proof for the ejection-to- $L_4$  orbit illustrated in the left frame of Figure 5.

The proof is implemented in IntLab running under MatLab, and took about 30 minutes to run on a standard desktop computer. ■

By replacing the operator  $F_{i,j}^u$  with the operator  $F_{i,j}^s$  defined in Equation (48), again with  $j = 4$  and  $i = 1$ , we obtain a nonlinear map whose zeros correspond to ejection-to- $L_4$  orbits. We compute an approximate numerical zero of the resulting operator (the numerical data is given in Table 3) and repeat a nearly identical argument to that above. This results in the existence of a transverse ejection-to- $L_4$  orbit in the PCRTBP with  $\mu = 1/4$  and  $c = 3$ . The validated error bound for the numerical data has

$$r \leq 1.8 \times 10^{-11},$$

so that the desired orbit passes within an  $r$ -neighborhood of the point

$$\bar{p} = \begin{pmatrix} -0.112449038686947 \\ -0.553321424594493 \\ 0.308527098616200 \\ 0.727049637558896 \end{pmatrix}.$$

In this way we prove the existence of both the orbits illustrated in Figure 5. More precisely, the orbit whose existence is established in Theorem 2 is illustrated in the right frame of the figure, and the orbit discussed in the preceding remarks is illustrated in the left frame.

#### 7.4. Transverse homoclinics for $L_4$ and $L_5$

Combining the methodology of Section 5, and especially Lemma 26, with Theorem 30 we obtain the following result.

**Theorem 3.** *Consider the planar PCRTBP with  $\mu = 1/2$  and  $c = 3$  is the energy level of  $L_4$ . Let*

$$\bar{p} = \begin{pmatrix} -0.037058535628028 \\ -0.007623220519232 \\ 0.873641524369283 \\ 0.033084516464648 \end{pmatrix},$$

and

$$B_r = \{x \in \mathbb{R}^4 : \|x - \bar{p}\| \leq r\},$$

where

$$r = 1.6 \times 10^{-9}.$$

$\bar{x}_0 =$	1.411845524482813			
$\bar{x}_1 =$	(-0.037058535628028,	-0.007623220519232,	0.873641524369283,	0.033084516464648)
$\bar{x}_2 =$	(-0.243792823114517,	-1.231115802740768,	0.191555403283542,	-0.508371511645513)
$\bar{x}_3 =$	(0.536705934592082,	-1.502936895854406,	0.178454709494811,	-0.106295188690239)
$\bar{x}_4 =$	(-0.504618223339967,	-0.258236025635830,	-0.463683951257916,	-1.155517796520023)
$\bar{x}_5 =$	(-0.460363255327369,	-0.431694933697799,	0.467966743350051,	0.748266448178995)
$\bar{x}_6 =$	5.988827136344083			
$\bar{\tau} =$	4.753189987600258			
$\bar{\alpha} =$	0.0			

Table 4: Numerical data for the proof of Theorem 3, which provides an approximate zero of the  $L_4$  homoclinic map  $F_{i,j,k}$  defined in Equation (49), when  $i = k = 4$ ,  $j = 2$ ,  $s_1 = 1.8635$ , and  $s_2 = 5$ . The orbit is depicted on the right plot in Figure 6.

Then there exists a unique  $p_* \in B_r$  so that the orbit of  $p_*$  is homoclinic to  $L_4$  and  $W^s(L_4)$  intersects  $W^u(L_4)$  transversely along the orbit of  $p_*$ , where transversality is relative to the level set  $\{E = 3\}$ .

**Proof.** As in the earlier cases, the argument hinges on proving the existence of a zero of a suitable nonlinear mapping, in this case the map  $F_{i,j,k}$  defined in Equation (49), with  $i = k = 4$  and  $j = 2$ . The integration time parameters are set as  $s_1 = 1.8635$  and  $s_2 = 5$ . These are the flow times in the regularized coordinates and in the original coordinates (the second time) respectively. With these choices, a zero of  $F_{4,2,4}$  corresponds to an orbit homoclinic to  $L_4$  which passes through the Levi-Civita coordinates regularized at  $m_2$ .

The numerical data  $\bar{x} \in \mathbb{R}^{24}$  providing an approximate zero of  $F_{4,2,4}$  is reported in Table 7.4. Note that  $x_1$  corresponds to  $\bar{p}$  in the hypothesis of the theorem. We let  $A$  be a numerically computed approximate inverse of the matrix  $DF_{4,2,4}(\bar{x})$ . The table data and the matrix  $A$  are computed using a numerical Newton scheme, and standard double precision floating point operations.

Using validated numerical integration schemes, validated bounds on the local stable/unstable manifold parameterizations, and interval arithmetic, we compute interval enclosures of  $F_{4,2,4}(\bar{x})$  and of  $DF_{4,2,4}(B_r(\bar{x}))$  with where  $r = 1.659487745915747 \times 10^{-9}$ . We then check that

$$\|AF(\bar{x})\| \in 10^{-8} \times [0.0, 0.16432156145308],$$

and that

$$\sup_{x \in B_r(\bar{x})} \|\text{Id} - ADF_{4,2,4}(B_r(\bar{x}))\| \in [0.0, 0.00980551463848].$$

Finally, we use interval arithmetic to verify that  $Zr - r + Y < 0$  and transversality follows as in the earlier cases which completes the proof. ■

Note that, from a numerical perspective, this is the most difficult computer assisted argument presented so far. This is seen in the fact that  $Z \approx 10^{-2}$  and  $r \approx 10^{-9}$ . That is, these constants are roughly three orders of magnitude less accurate than the previous theorems. On the other hand, the orbit itself is more complicated than those in the previous theorems. We note that the accuracy of the result could be improved by taking smaller integration steps and/or using higher order Taylor approximation. However, this would also increase the required computational time.

Now, by symmetry, the result above gives a transverse homoclinic orbit for  $L_5$  which passes near  $m_1$ . We also observe that each of these transverse homoclinic orbits also satisfy the hypotheses of the theorems of Devaney and Henard discussed in Section 1. In particular, Theorem 3 also proves the existence of a chaotic subsystem in the  $c = 3$  energy level of the PCRTBP near the orbit of  $p_*$ , and a tube of periodic orbits parameterized by the Jacobi constant which accumulate to the homoclinic orbit through  $p_*$ .

We remark that, using similar arguments, we are able to prove also the existence and transversality of the homoclinic orbits in the left and center frames of Figure 6. More precisely, let

$$\bar{p}_1 = \begin{pmatrix} -0.033854025583296 \\ -0.043110876471418 \\ 0.844639632487862 \\ 0.007320747846173 \end{pmatrix}, \quad \bar{p}_2 = \begin{pmatrix} 0.029871559148065 \\ -0.006337684774610 \\ 0.850175365286339 \\ -0.034734413580682 \end{pmatrix},$$

and

$$r_1 = 2.03 \times 10^{-10}, \quad r_2 = 1.84 \times 10^{-8}.$$

Then there exist unique points  $p_*^1 \in B(\bar{p}_1, r_1)$  and  $p_*^2 \in B(\bar{p}_2, r_2)$  so that  $W^{s,u}(L_4)$  intersect transversely along the orbits through these points. It is also interesting to note that  $r_2$  is two orders of magnitude larger than  $r_1$ . This is caused by the fact that the time of flight (integration time) is longer in this case and, more importantly, the fact that the second orbit passes very close to  $m_1$ . Indeed, the error bounds for the second orbit would very likely be improved by changing to regularized coordinates near  $m_1$  and this may even be necessary to validate some homoclinics passing even closer to  $m_1$  or  $m_2$ . Nevertheless, we were able to validate these orbits in standard coordinates so we have not done this here.

The orbit of  $p_*^1$  is illustrated in the left frame of Figure 6 appears to have  $y$ -axis symmetry, however we do not use this symmetry nor do we rigorously prove its existence. The orbit of  $p_*^2$  is illustrated in the center frame of Figure 6 has no apparent symmetry. The orbits illustrated in the left and center frames have appeared previously in the literature, as remarked in Section 1. However, to the best of our knowledge this is the first mathematically rigorous proof of their existence.

### 7.5. Periodic orbits passing through collision

We apply the methodology of section 6, namely Lemma 28 and Theorem 29, with Theorem 30 to obtain the following result. We consider the Earth-Moon mass ratio largely for the sake of variety.

**Theorem 4.** *Consider the Earth-Moon system <sup>8</sup> where  $m_2$  has mass  $\mu = 0.0123/1.0123$  and  $m_1$  has mass  $1 - \mu$ . Let<sup>9</sup>*

$$c_0 = 1.4340459493, \quad \text{and} \quad \delta = 10^{-11}.$$

<sup>8</sup>So named because this is the approximate mass ratio of the Moon relative to the Earth.

<sup>9</sup>In fact, our numerical calculations suggest that a more accurate value of the Jacobi constant for which we have the collision is 1.434045949300768. However, since in the theorem we obtain only interval results, we round  $c_0$  so that digits smaller than the width of the interval are not used.



$\bar{x}_0 =$	0.0			
$\bar{x}_1 =$	( 0.0,	2.8111911379251,	0.0,	0.0)
$\bar{x}_2 =$	( 0.96886794638213,	-0.3219837525934,	-0.52587590839627,	-2.8644348266831)
$\bar{x}_3 =$	( 0.67431017475157,	-0.74811608844773,	-1.0190086228395,	-1.0721803622694)
$\bar{x}_4 =$	(-1.0199016713004,	0.72482377063238,	-0.062207790440189,	1.1639536137604)
$\bar{x}_5 =$	( 0.1377088390491,	-0.32616835939217,	-0.22586709346235,	0.6480010784062)
$\bar{x}_6 =$	0.070375791076957			
$\bar{\tau} =$	2.0972398526268			
$\bar{\alpha} =$	0.0			

Table 5: Numerical data for the proof of Theorem 4, which gives an approximate solution to  $F_c = 0$  for the operator (54), for which we have a collision of the family of Lyapunov orbits with  $m_1$  for the Earth-Moon system (see Figure 7). This occurs for a unique value of the Jacobi constant  $c^* \in \mathbf{c}$ .

There exists a single value  $c^* \in (c_0 - \delta, c_0 + \delta)$  of the Jacobi integral, for which we have an orbit along the intersection of the ejection and collision manifolds of  $m_1$ . Moreover, for every  $c \in [c_0 - \delta, c_0 + \delta] \setminus \{c^*\}$  we have an  $S$ -symmetric Lyapunov orbit, that passes close to the collision with  $m_1$ . In addition, for every  $c \in \{1.2, 1.25, 1.3, \dots, 1.65\}$  there exists a Lyapunov orbit, which passes close the collision with  $m_1$ . (These orbits are depicted in Figure 7.)

**Proof.** The orbits for the Jacobi integral values in  $\mathbf{c} := [c_0 - \delta, c_0 + \delta]$  were established by means of Theorems 29 and 30. We have first pre-computed numerically (through a standard, non-interval, numerical computation) an approximation  $\bar{\mathbf{x}} \in \mathbb{R}^{22}$ ,  $\bar{\tau} \in \mathbb{R}$  for the functions  $\mathbf{x}(c)$  and  $\tau(c)$ , for  $c \in \mathbf{c}$ . (The  $\bar{\mathbf{x}}$  and  $\bar{\tau}$  are written out in Table 5.) We then took  $\bar{x} := (\bar{\mathbf{x}}, \bar{\tau}, 0) \in \mathbb{R}^{24}$ , and a ball  $\bar{B}(\bar{x}, r)$ , in the maximum norm, with  $r = 10^{-11}$ . We established using Theorem 30 that  $\mathbf{x}(c)$  and  $\tau(c)$  satisfying

$$F_c(\mathbf{x}(c), \tau(c), 0) = 0, \quad \text{for } c \in \mathbf{c},$$

are  $r$ -close to  $\bar{\mathbf{x}}$  and  $\bar{\tau}$ . To apply Theorem 30 we have used the matrix  $A$  to be an approximation of  $(DF_c(\bar{\mathbf{x}}, \bar{\tau}, 0))^{-1}$  (computed with standard numerics, without interval arithmetic).

We also checked using interval arithmetic that

$$\begin{aligned} x_0(c_0 - \delta) &\in [3.2261 \cdot 10^{-12}, 5.2262 \cdot 10^{-12}] > 0, \\ x_0(c_0 + \delta) &\in [-4.6229 \cdot 10^{-12}, -2.6228 \cdot 10^{-12}] < 0. \end{aligned}$$

By using Equation (55), we have established the following interval arithmetic bound for the derivative of  $x_0$  with respect to the parameter

$$\frac{d}{dc}x_0(c) \in [-0.53146, -0.25344] < 0 \quad \text{for } c \in \mathbf{c}.$$

We also verified that

$$x_6(c) \in [0.07037579, 0.07037580], \quad \text{for } c \in \mathbf{c},$$

so  $x_6(c) \neq 0$ . This proves all necessary hypotheses of Theorem 29 are satisfied for the interval  $\mathbf{c}$ , which finishes the first part of the proof.

The Lyapunov orbits for  $c \in \{1.2, 1.25, 1.3, \dots, 1.65\}$  were established in a similar way. For each value of the Jacobi constant we have non-rigorously computed an approximation

$\bar{x}_0 =$	2.1500812504263			
$\bar{x}_1 =$	( 0.0,	1.9284591731628,	2.1500812504263,	0.0)
$\bar{y}_1 =$	( 0.69048473611567,	1.7931365837031,	2.0235432631366,	-0.68131264815823)
$\bar{y}_2 =$	( 1.2840491252838,	1.4060903194974,	1.6633024005717,	-1.2578372410208)
$\bar{y}_3 =$	( 1.6975511373876,	0.82331762641153,	1.1255430505039,	-1.635312833307)
$\bar{y}_4 =$	( 1.8749336204161,	0.13626785074409,	0.4974554541058,	-1.7408028751654)
$\bar{y}_5 =$	( 1.7998279644685,	-0.53073278614628,	-0.11297480280335,	-1.5366473737295)
$\bar{y}_6 =$	( 1.5061749347656,	-1.0305902992759,	-0.59342931060715,	-1.0405479042095)
$\bar{y}_7 =$	( 1.0818972907729,	-1.2225719420862,	-0.85102013466618,	-0.34180581034401)
$\bar{y}_8 =$	( 0.65897461363208,	-1.0129455565064,	-0.83705911740279,	0.41484122714387)
$\bar{x}_2 =$	( 0.39363679634804,	-0.35214129843918,	-0.55459777216455,	1.118144276789)
$\bar{x}_3 =$	( 0.47871801188109,	-1.6325298121847,	-0.5792530867862,	0.66259374214967)
$\bar{x}_4 =$	( <b>0.40239981358785</b> ,	-1.0164469492932,	0.0,	1.7224504635177)
$\bar{x}_5 =$	(-0.25865224139372,	-0.43561054122851,	0.51876042853484,	1.7861707478994)
$\bar{x}_6 =$	( 0.29778859976434,	-1.2111468567795,	-0.2683570951738,	-1.0237309759288)
$\bar{x}_7 =$	-0.38367247647373			
$\bar{\tau} =$	0.24444305938687			
$\bar{\alpha} =$	0.0			

Table 6: Numerical data for the proof of Theorem 5 giving an approximate solution to  $F_c = 0$ , for the operator (61), for  $c = 2.05991609689$  for which we have a double collision of a family of  $R$ -symmetric periodic orbits for the equal masses system; see Figure 9. In the bold font we have singled out the first coefficient of  $x_4$ , which is the time  $s_4$  and not the physical coordinate of the collision point, for which we have  $\hat{x} = 0$ . (See Equations (60) and (61).)

of a point for which  $F_c$  is close to zero, and validated that we have  $F_c = 0$  for a point in a given neighbourhood of each approximation by means of Theorem 29. Then each Lyapunov orbit followed from Lemma 28. The proof was conducted by using the CAPD library [113] and took under 4 seconds on a standard laptop. ■

In a similar way we have used the operator in Equation (61) to prove the following result.

**Theorem 5.** *Consider the equal masses system where  $\mu = \frac{1}{2}$ . Let<sup>10</sup>*

$$c_0 = 2.05991609689, \quad \text{and} \quad \delta = 10^{-11}.$$

*There exists a single value  $c^* \in (c_0 - \delta, c_0 + \delta)$  of the Jacobi integral, for which we have two intersections of the ejection and collision manifolds of  $m_1$  and  $m_2$  (a double collision). Moreover, for every  $c \in [c_0 - \delta, c_0 + \delta] \setminus \{c^*\}$  we have an  $R$ -symmetric periodic orbit, that passes close to the collision with both  $m_1$  and  $m_2$ .*

*In addition, for every  $c \in \{2, 2.05, 2.1, 2.15, 2.2\}$  there exists an  $R$ -symmetric periodic orbit, which passes close the collisions with  $m_1$  and  $m_2$ . (See Figure 9.)*

**Proof.** The proof follows along the same lines as the proof of Theorem 4. We do not write out the details of all the estimates since we feel that this brings little added value<sup>11</sup>. In the operator  $F_c$  from Equation (61) we have taken  $s_2 = 3.3$  and  $s_5 = 0.3$ . The fact that  $s_2$  involves a long integration time caused a technical problem for us in obtaining an estimate for  $\frac{d}{dc}\pi_{\hat{y}}\mathbf{x}(c)$ . To get a good enough estimate to establish that  $\frac{d}{dc}\pi_{\hat{y}}\mathbf{x}(c) > 0$  we needed to include additional points  $y_1, \dots, y_m$  in the shooting scheme and extend  $F_c$  to include

$$\phi_\alpha(x_1, s) - y_1, \quad \phi_\alpha(y_1, s) - y_2, \quad \dots \quad \phi_\alpha(y_{m-1}, s) - y_m, \quad \phi_\alpha(y_m, s) - x_2,$$

<sup>10</sup>We believe that a more accurate value of the Jacobi constant for which we have the double collision is 2.059916096889689.

<sup>11</sup>The code for the proof is made available on the personal web page of Maciej Capiński.

where  $s = s_2 / (m + 1)$ . We took  $m = 8$ , and the point  $X_0$  which serves as our approximation for  $F_c = 0$  is written out in Table 6. The proof took under 10 seconds on a standard laptop. ■

**Remark 31 (MatLab with IntLab versus CAPD).** We note that the computer programs implemented in C++ using the CAPD library run much faster than the programs implemented in MatLab using IntLab to manage the interval arithmetic. This is not surprising, as compiled programs typically run several hundred times faster than MatLab programs, and the use of interval arithmetic only complicates things. Moreover, CAPD is a well tested, optimized, general purpose package, while our IntLab codes were written specifically for this project. The CAPD library, due to its efficient integrators, allowed us to perform almost all of the proofs without subdividing the time steps, which was needed for the MatLab code (see Remark 25 and comments at the end of section 7.2), except for the proof of Theorem 5 (see Table 6). In particular, little time has been spent on optimizing these codes. Nevertheless, it is nice to have rigorous integrators implemented in multiple languages, and the codes for validating the 2D stable/unstable manifolds at  $L_4$  were written in IntLab and have not been ported to  $C^{++}$ .

## 8. Acknowledgments

The authors gratefully acknowledge conversations with Pau Martin, Immaculada Baldoma, and Marian Gidea at the 60<sup>th</sup> birthday conference of Rafael de la Llave, *Llavefest* in Barcelona in the summer of 2017. We also offer our sincere thanks to an anonymous referee whose thorough review and thoughtful suggestions greatly improved the quality of the final manuscript.

## Appendix A.

**Proof of Theorem 30.** From Equation (64) and since  $r > 0$  we see that  $Z + \frac{Y}{r} \leq 1$ , which since  $Y, r > 0$  gives

$$Z < 1. \tag{A.1}$$

Now, define the Newton operator

$$T(x) = x - AF(x). \tag{A.2}$$

For  $x_1, x_2 \in \overline{B}(x_0, r)$ , by the mean value theorem and (63), we see that

$$\begin{aligned} \|T(x_1) - T(x_2)\| &\leq \sup_{x \in \overline{B}(x_0, r)} \|DT(x)\| \|x_1 - x_2\| \\ &= \sup_{x \in \overline{B}(x_0, r)} \|\text{Id} - ADF(x)\| \|x_1 - x_2\| \\ &\leq Z \|x_1 - x_2\|, \end{aligned}$$

and since  $Z < 1$  we conclude that  $T$  is a contraction on  $\overline{B}(x_0, r)$ .

To see that  $T$  maps  $\overline{B}(x_0, r)$  into itself, for  $x \in \overline{B}(x_0, r)$  by Equations (62)–(64) we have

$$\begin{aligned} \|T(x) - x_0\| &\leq \|T(x) - T(x_0)\| + \|T(x_0) - x_0\| \\ &\leq \sup_{x \in \overline{B}(x_0, r)} \|DT(z)\| \|x - x_0\| + \|AF(x_0)\| \\ &\leq Zr + Y \\ &\leq r \end{aligned}$$

hence  $T(x) \in \overline{B}(x_0, r)$ .

By the Banach contraction mapping theorem there is a unique  $\hat{x} \in \overline{B}(x_0, r)$  so that

$$T(\hat{x}) = \hat{x}. \quad (\text{A.3})$$

Now observe that for every  $x \in \overline{B}(x_0, r)$ , including  $\hat{x}$ , by Equations (63) and (A.1) we have that

$$\|\text{Id} - ADF(\hat{x})\| \leq Z < 1.$$

Then

$$ADF(\hat{x}) = \text{Id} - (\text{Id} - ADF(\hat{x})) = \text{Id} - B$$

with  $\|B\| < 1$ . By the Neumann series theorem we see that  $ADF(\hat{x})$  is invertible. It therefore follows that both  $A$  and  $DF(\hat{x})$  are also invertible.

From Equations (A.2) and (A.3) we see that  $AF(\hat{x}) = 0$ . But  $A$  is invertible, so it follows that  $F(\hat{x}) = 0$ , as required. ■

## Appendix B.

Here follows a terse description of the local stable/unstable manifold parameterizations used in the proofs in Sections 7.3 and 7.4. Much more complete information is found in [96, 130, 131]. In the present discussion  $f: U \rightarrow \mathbb{R}^d$  denotes the (real analytic) PCRTB vector field, and  $L_j$  is one of the equilateral triangle libration points – so that  $j = 4, 5$ . We are interested in parameter values where  $Df(L_{4,5})$  has complex conjugate stable/unstable eigenvalues

$$\pm\alpha \pm i\beta,$$

with  $\alpha, \beta > 0$ . We write  $\lambda = -\alpha + i\beta$  when considering the stable manifold, and  $\lambda = \alpha + i\beta$  when considering the unstable.

Our goal is to develop a formal series expansion of the form

$$w_j^\kappa(z_1, z_1) = \sum_{m=0}^{\infty} \sum_{n=0}^{\infty} p_{mn} z_1^m z_2^n, \quad (\text{B.1})$$

where  $j = 4$  or  $5$  depending on whether we are based at  $L_4$  or  $L_5$ , and  $\kappa = s$  or  $u$  depending on whether we are considering the stable or unstable manifold. Here  $p_{mn} \in \mathbb{C}^4$  for all  $(m, n) \in \mathbb{N}^2$ . Moreover, we take

$$p_{00} = L_j,$$

where  $j = 4, 5$ , and

$$p_{10} = \xi, \quad \text{and} \quad p_{01} = \bar{\xi},$$

where  $\xi, \bar{\xi} \in \mathbb{C}^4$  are complex conjugate eigenvectors associated with the complex conjugate eigenvalues  $\lambda, \bar{\lambda} \in \mathbb{C}$ .

We use the parameterization method to characterize  $w_j^\kappa$ . While we refer the interested reader to [130, 131] for much more complete discussion of this method, we remark that the main idea is to solve the invariance equation

$$\lambda z_1 \frac{\partial}{\partial z_1} w_j^\kappa(z_1, z_2) + \bar{\lambda} z_2 w_j^\kappa(z_1, z_2) = f(w_j^\kappa(z_1, z_2)), \quad (\text{B.2})$$

subject to the constraints

$$w_j^\kappa(0, 0) = L_j, \quad \frac{\partial}{\partial v} w_j^\kappa(0, 0) = \xi, \quad \text{and} \quad \frac{\partial}{\partial w} w_j^\kappa(0, 0) = \bar{\xi}.$$

$m \setminus n$	0	1	2
0	$\begin{pmatrix} 0.0 \\ 0.0 \\ 0.866 \\ 0.0 \end{pmatrix}$	$\begin{pmatrix} 0.012 + 0.018i \\ -0.025 \\ -0.015 + 0.0067i \\ 0.0034 - 0.019i \end{pmatrix}$	$10^{-3} \begin{pmatrix} -0.050 + 0.076i \\ -0.081 - 0.190i \\ -0.054 - 0.041i \\ 0.140 - 0.051i \end{pmatrix}$
1	$\begin{pmatrix} 0.012 - 0.018i \\ -0.025 \\ -0.015 - 0.0067i \\ 0.0034 + 0.019i \end{pmatrix}$	$10^{-3} \begin{pmatrix} 0.37 \\ -0.47 \\ -0.09 \\ 0.12 \end{pmatrix}$	$10^{-4} \begin{pmatrix} 0.041 + 0.055i \\ -0.130 - 0.070i \\ -0.036 - 0.048i \\ 0.110 + 0.060i \end{pmatrix}$
2	$10^{-3} \begin{pmatrix} -0.050 - 0.076i \\ -0.081 + 0.190i \\ -0.054 + 0.041i \\ 0.140 + 0.051i \end{pmatrix}$	$10^{-4} \begin{pmatrix} 0.041 - 0.055i \\ -0.130 + 0.070i \\ -0.036 + 0.048i \\ 0.110 - 0.060i \end{pmatrix}$	0

$p_{03} = 10^{-5} \begin{pmatrix} -0.14 + 0.18i \\ -0.26 - 0.76i \\ 0.11 + 0.09i \\ -0.47 + 0.11i \end{pmatrix}$	$p_{30} = 10^{-5} \begin{pmatrix} -0.14 - 0.18i \\ -0.26 + 0.76i \\ 0.11 - 0.09i \\ -0.47 - 0.11i \end{pmatrix}$
--	--

Table B.7: Approximate power series coefficients  $p_{mn}$  for the parameterization of the local stable manifold of  $L_4$  for the equal masses case  $\mu = 1/2$ .

It can be show that if  $w_j^\kappa$  solves Equation (B.2) subject to these constraints, then it parameterizes a local stable/unstable manifold at  $L_j$ .

To solve Equation (B.2) numerically we insert the power series ansatz of Equation (B.1), expand the nonlinearities, and match like powers of  $z_1$  and  $z_2$ . This procedure leads to homological equations of the form

$$(Df(p_{00}) - (m\lambda + n\bar{\lambda})\text{Id}) p_{mn} = \mathcal{R}_{mn},$$

describing the power series coefficients  $p_{mn}$  for  $m + n \geq 2$ . Here  $\mathcal{R}_{mn}$  is a nonlinear function of the coefficients of order less than  $m + n$ , whose computation in the case of the PCRTBP is discussed in more detail in [96]. Note that if  $f$  is real analytic, then the coefficients have the symmetry

$$p_{nm} = \overline{p_{mn}},$$

and we obtain the real image of  $\mathcal{P}$  by evaluating on complex conjugate variables  $w = \bar{v}$ .

Since the order zero and order 1 coefficients are determined by  $L_j$  and its eigendata, we can compute  $p_{mn}$  for all  $2 \leq m + n \leq N$  by recursively solving the linear homological equations to any desired order  $N \geq 2$ . We obtain the approximation

$$w_j^{\kappa, N}(z_1, z_2) = \sum_{m+n=0}^N p_{mn} z_1^m z_2^n.$$

For example, in the PCRTBP with  $\mu = 1/2$ , Table B.7 shows approximate coefficients for the stable manifold at  $L_4$ , computed to order  $N = 3$ . The data has been truncated at only two or three significant figures to make it fit in the table. Note that the complex conjugate structure of the coefficients is seen in the table. The table is included to give the reader a sense of the form of the data in these calculations, and could be used to very approximately reproduce some of the results in the present work.

For the calculations in the main body of the text, we take  $N = 12$  and compute the  $p_{mn}$  by recursively solving the homological equations using interval arithmetic. Moreover, using the a-posteriori analysis developed in [116], we obtain a bound of the form

$$\sum_{m+n=13}^{\infty} \|p_{mn}\| \leq 1.4 \times 10^{-13},$$

on the norm of the tail of the parameterization. The analysis is very similar to the a-posteriori analysis of the Newton Krawczyk Theorem 30 promoted in the present work, adapted to the context of Banach spaces of infinite sequences.

Note that this “little ell one” norm bounds the  $C^0$  norm of the truncation error on the unit disk, and that Cauchy bounds can be used to estimate derivatives of the parameterization on any smaller disk. Thus we actually take

$$P_j^\kappa(\theta) = w_j^\kappa(0.9 \cos(\theta) + 0.9 \sin(\theta)i, 0.9 \cos(\theta) - 0.9 \sin(\theta)i),$$

as our local parameterization, where

$$w_j^\kappa(z_1, z_2) = w_j^{\kappa, N}(z_1, z_2) + w_j^{\kappa, \infty}(z_1, z_2),$$

is a polynomial plus a tail which has

$$w_j^{\kappa, \infty}(z_1, z_2) = \sum_{n+m=N+1}^{\infty} p_{mn} z_1^m z_2^n,$$

and

$$\sup_{|z_1|, |z_2| < 1} \|w_j^{\kappa, \infty}(z_1, z_2)\| \leq 1.4 \times 10^{-13}.$$

The 0.9 gives up a portion of the disk, allowing us to bound the derivatives needed in the Newton-Kantorovich argument.

## References

- [1] H. Poincaré, New methods of celestial mechanics. Vol. 1, Vol. 13 of History of Modern Physics and Astronomy, American Institute of Physics, New York, 1993.
- [2] H. Poincaré, New methods of celestial mechanics. Vol. 2, Vol. 13 of History of Modern Physics and Astronomy, American Institute of Physics, New York, 1993.
- [3] H. Poincaré, New methods of celestial mechanics. Vol. 3, Vol. 13 of History of Modern Physics and Astronomy, American Institute of Physics, New York, 1993.
- [4] U. S. R. Association. [Earth’s oldest rock found on the moon](#) [online] (January 2019).
- [5] G. Friedman, The Next Hundred Years, no. ISBN 9780385517058, Doubleday, 2009.
- [6] R. A. Heinlein, The Moon Is A Harsh Mistress, no. ISBN 0312863551, G.P. Putnam’s Sons, 1966.
- [7] J. Llibre, [On the restricted three-body problem when the mass parameter is small](#), Celestial Mech. 28 (1-2) (1982) 83–105. doi:10.1007/BF01230662. URL <https://doi.org/10.1007/BF01230662>
- [8] J. Henrard, [Proof of a conjecture of E. Strömberg](#), Celestial Mech. 7 (1973) 449–457. URL <https://doi-org.ezproxy.fau.edu/10.1007/BF01227510>
- [9] R. L. Devaney, Homoclinic orbits in Hamiltonian systems, J. Differential Equations 21 (2) (1976) 431–438.
- [10] E. Strömberg, Forms of periodic motion in the restricted problem and in the general problem of three bodies, according to the researches executed at the observatory of Copenhagen, Publikationer og mindre Meddelelser fra Kobenhavns Observatorium (39) (1922).
- [11] E. Strömberg, Connaissance actuelle des orbites dans le probleme des trois corps, Bull. Astron. 9 (1934) 87–130.
- [12] V. Szebehely, F. T.V., A family of retrograde orbits around the triangular equilibrium points, The Astronomical Journal 72 (3) (1967) 373–379.
- [13] V. Szebehely, On Moulton’s orbits in the restricted problem of three bodies, Proceedings of the National Academy of (S)ciences of the United States of America 56 (6) (1966) pp. 1641–1645.
- [14] V. Szebehely, Theory of Orbits, Academic Press Inc., 1967.
- [15] A. J. Maciejewski, S. M. Rybicki, [Global bifurcations of periodic solutions of the Hill lunar problem](#), Celestial Mech. Dynam. Astronom. 81 (4) (2001) 279–297. doi:10.1023/A:1013276830424. URL <https://doi.org/10.1023/A:1013276830424>

- [16] A. J. Maciejewski, S. M. Rybicki, [Global bifurcations of periodic solutions of the restricted three body problem](#), *Celestial Mech. Dynam. Astronom.* 88 (3) (2004) 293–324. doi:10.1023/B:CELE.0000017193.10060.ac.  
URL <https://doi.org/10.1023/B:CELE.0000017193.10060.ac>
- [17] E. Pérez-Chavela, S. a. Rybicki, [Topological bifurcations of central configurations in the  \$N\$ -body problem](#), *Nonlinear Anal. Real World Appl.* 14 (1) (2013) 690–698. doi:10.1016/j.nonrwa.2012.07.027.  
URL <https://doi.org/10.1016/j.nonrwa.2012.07.027>
- [18] C. García-Azpeitia, J. Ize, [Global bifurcation of planar and spatial periodic solutions from the polygonal relative equilibria for the  \$n\$ -body problem](#), *J. Differential Equations* 254 (5) (2013) 2033–2075. doi:10.1016/j.jde.2012.08.022.  
URL <https://doi.org/10.1016/j.jde.2012.08.022>
- [19] C. García-Azpeitia, J. Ize, [Global bifurcation of planar and spatial periodic solutions in the restricted  \$n\$ -body problem](#), *Celestial Mech. Dynam. Astronom.* 110 (3) (2011) 217–237. doi:10.1007/s10569-011-9354-2.  
URL <https://doi.org/10.1007/s10569-011-9354-2>
- [20] J. Chazy, [Sur l'allure du mouvement dans le problème des trois corps quand le temps croît indéfiniment](#), *Ann. Sci. École Norm. Sup.* (3) 39 (1922) 29–130.  
URL [http://www.numdam.org/item?id=ASENS\\_1922\\_3\\_39\\_\\_29\\_0](http://www.numdam.org/item?id=ASENS_1922_3_39__29_0)
- [21] F. Moulton, D. Buchanan, T. Buck, F. Griffin, W. Longley, W. MacMillan, *Periodic Orbits*, no. Publication No. 161, Carnegie Institution of Washington, 1920.
- [22] D. G. Saari, [Improbability of collisions in Newtonian gravitational systems](#), *Trans. Amer. Math. Soc.* 162 (1971) 267–271; erratum, *ibid.* 168 (1972), 521. doi:10.2307/1995752.  
URL <https://doi.org/10.2307/1995752>
- [23] D. G. Saari, [Improbability of collisions in Newtonian gravitational systems. II](#), *Trans. Amer. Math. Soc.* 181 (1973) 351–368. doi:10.2307/1996638.  
URL <https://doi.org/10.2307/1996638>
- [24] M. Guardia, V. Kaloshin, J. Zhang, [Asymptotic density of collision orbits in the restricted circular planar 3 body problem](#), *Arch. Ration. Mech. Anal.* 233 (2) (2019) 799–836. doi:10.1007/s00205-019-01368-7.  
URL <https://doi.org/10.1007/s00205-019-01368-7>
- [25] T. Levi-Civita, [Sur la régularisation du problème des trois corps](#), *Acta Math.* 42 (1) (1920) 99–144. doi:10.1007/BF02404404.  
URL <https://doi.org/10.1007/BF02404404>
- [26] A. Celletti, [Basics of regularization theory](#), in: B. Stevens, A. Maciejewski, H. M. (Eds.), *Chaotic Worlds: From Order to Disorder in Gravational N-Body Dynamical Systems*, Springer, Dordrecht, 2006.
- [27] R. L. Devaney, [Singularities in classical mechanical systems](#), in: *Ergodic theory and dynamical systems, I* (College Park, Md., 1979–80), Vol. 10 of *Progr. Math.*, Birkhäuser, Boston, Mass., 1981, pp. 211–333.
- [28] R. McGehee, [Singularities in classical celestial mechanics](#), in: *Proceedings of the International Congress of Mathematicians (Helsinki, 1978)*, Acad. Sci. Fennica, Helsinki, 1980, pp. 827–834.
- [29] R. McGehee, [Triple collision in the collinear three-body problem](#), *Invent. Math.* 27 (1974) 191–227. doi:10.1007/BF01390175.  
URL <https://doi.org/10.1007/BF01390175>
- [30] R. Moeckel, R. Montgomery, [Symmetric regularization, reduction and blow-up of the planar three-body problem](#), *Pacific J. Math.* 262 (1) (2013) 129–189. doi:10.2140/pjm.2013.262.129.  
URL <https://doi.org/10.2140/pjm.2013.262.129>
- [31] E. A. Belbruno, [A new regularization of the restricted three-body problem and an application](#), *Celestial Mech.* 25 (4) (1981) 397–415. doi:10.1007/BF01234179.  
URL <https://doi.org/10.1007/BF01234179>
- [32] R. L. Devaney, [Triple collision in the planar isosceles three body problem](#), *Inventiones mathematicae* 60 (1980) 249–267.
- [33] C. Simó, [Analysis of triple collision in the isosceles problem](#), in: *Classical mechanics and dynamical systems* (Medford, Mass., 1979), Vol. 70 of *Lecture Notes in Pure and Appl. Math.*, Dekker, New York, 1981, pp. 203–224.
- [34] M. S. ElBialy, [Triple collisions in the isosceles three body problem with small mass ratio](#), *Zeitschrift für angewandte Mathematik und Physik ZAMP* 40 (5) (1989) 645–664. doi:10.1007/BF00945869.

- URL <https://doi.org/10.1007/BF00945869>
- [35] E. A. Lacomba, L. Losco, *Triple collisions in the isosceles 3-body problem*, Bull. Amer. Math. Soc. (N.S.) 3 (1, part 1) (1980) 710–714. doi:10.1090/S0273-0979-1980-14802-8. URL <https://doi-org.libproxy.york.ac.uk/10.1090/S0273-0979-1980-14802-8>
- [36] R. MOECKEL, *Orbits near triple collision in the three-body problem*, Indiana University Mathematics Journal 32 (2) (1983) 221–240. URL <http://www.jstor.org/stable/24893242>
- [37] M. Alvarez-Ramírez, E. Barrabés, M. Medina, M. Ollé, *Ejection-collision orbits in the symmetric collinear four-body problem*, Commun. Nonlinear Sci. Numer. Simul. 71 (2019) 82–100. doi:10.1016/j.cnsns.2018.10.026. URL <https://doi.org/10.1016/j.cnsns.2018.10.026>
- [38] E. A. Lacomba, J. Llibre, *Transversal ejection-collision orbits for the restricted problem and the Hill’s problem with applications*, J. Differential Equations 74 (1) (1988) 69–85. doi:10.1016/0022-0396(88)90019-8. URL [https://doi.org/10.1016/0022-0396\(88\)90019-8](https://doi.org/10.1016/0022-0396(88)90019-8)
- [39] J. Delgado Fernández, *Transversal ejection-collision orbits in Hill’s problem for  $C \gg 1$* , Celestial Mech. 44 (3) (1988/89) 299–307. doi:10.1007/BF01235542. URL <https://doi.org/10.1007/BF01235542>
- [40] C. Pinyol, *Ejection-collision orbits with the more massive primary in the planar elliptic restricted three body problem*, Celestial Mech. Dynam. Astronom. 61 (4) (1995) 315–331. URL <https://doi-org.ezproxy.fau.edu/10.1007/BF00049513>
- [41] A. Chenciner, J. Llibre, *A note on the existence of invariant punctured tori in the planar circular restricted three-body problem*, Ergodic Theory Dynam. Systems 8\* (Charles Conley Memorial Issue) (1988) 63–72. doi:10.1017/S0143385700009330. URL <https://doi.org/10.1017/S0143385700009330>
- [42] J. Féjoz, *Averaging the planar three-body problem in the neighborhood of double inner collisions*, J. Differential Equations 175 (1) (2001) 175–187. doi:10.1006/jdeq.2000.3972. URL <https://doi.org/10.1006/jdeq.2000.3972>
- [43] J. Féjoz, *Quasiperiodic motions in the planar three-body problem*, J. Differential Equations 183 (2) (2002) 303–341. doi:10.1006/jdeq.2001.4117. URL <https://doi.org/10.1006/jdeq.2001.4117>
- [44] L. Zhao, *Quasi-periodic almost-collision orbits in the spatial three-body problem*, Comm. Pure Appl. Math. 68 (12) (2015) 2144–2176. doi:10.1002/cpa.21539. URL <https://doi.org/10.1002/cpa.21539>
- [45] S. V. Bolotin, R. S. Mackay, *Periodic and chaotic trajectories of the second species for the  $n$ -centre problem*, Celestial Mech. Dynam. Astronom. 77 (1) (2000) 49–75 (2001). doi:10.1023/A:1008393706818. URL <https://doi.org/10.1023/A:1008393706818>
- [46] S. Bolotin, R. S. MacKay, *Nonplanar second species periodic and chaotic trajectories for the circular restricted three-body problem*, Celestial Mech. Dynam. Astronom. 94 (4) (2006) 433–449. doi:10.1007/s10569-006-9006-0. URL <https://doi.org/10.1007/s10569-006-9006-0>
- [47] S. Bolotin, *Shadowing chains of collision orbits for the elliptic 3-body problem*, in: SPT 2004—Symmetry and perturbation theory, World Sci. Publ., Hackensack, NJ, 2005, pp. 51–58. doi:10.1142/9789812702142\_0007. URL [https://doi.org/10.1142/9789812702142\\_0007](https://doi.org/10.1142/9789812702142_0007)
- [48] J. Font, A. Nunes, C. Simó, *Consecutive quasi-collisions in the planar circular RTBP*, Nonlinearity 15 (1) (2002) 115–142. doi:10.1088/0951-7715/15/1/306. URL <https://doi.org/10.1088/0951-7715/15/1/306>
- [49] J. Font, A. Nunes, C. Simó, *A numerical study of the orbits of second species of the planar circular RTBP*, Celestial Mech. Dynam. Astronom. 103 (2) (2009) 143–162. doi:10.1007/s10569-008-9176-z. URL <https://doi.org/10.1007/s10569-008-9176-z>
- [50] M. Ollé, O. Rodríguez, J. Soler, *Ejection-collision orbits in the RTBP*, Commun. Nonlinear Sci. Numer. Simul. 55 (2018) 298–315. doi:10.1016/j.cnsns.2017.07.013. URL <https://doi.org/10.1016/j.cnsns.2017.07.013>
- [51] M. Ollé, O. Rodríguez, J. Soler, *Analytical and numerical results on families of  $n$ -ejection-collision orbits in the RTBP*, Commun. Nonlinear Sci. Numer. Simul. 90 (2020) 105294, 27. doi:10.1016/j.cnsns.2020.105294.



- URL <https://doi.org/10.1016/j.cnsns.2020.105294>
- [52] M. Ollé, O. Rodríguez, J. Soler, [Transit regions and ejection/collision orbits in the RTBP](#), *Commun. Nonlinear Sci. Numer. Simul.* 94 (2021) 105550, 29. doi:10.1016/j.cnsns.2020.105550.  
URL <https://doi.org/10.1016/j.cnsns.2020.105550>
- [53] T. M. Seara, M. Ollé, O. Rodríguez, J. Soler, [Generalised analytical results on  \$n\$ -ejection-collision orbits in the rtbp: analysis of bifurcations](#), (Submitted) (2022).
- [54] G. H. Darwin, [Periodic Orbits](#), *Acta Math.* 21 (1) (1897) 99–242.  
URL <https://doi-org.ezproxy.fau.edu/10.1007/BF02417978>
- [55] S. B. Edwards, *Hidden Human Computers: the Black Women of NASA*, no. ISBN 978-1680783872, Essential Library, 2017.
- [56] M. L. Shelterly, *Hidden Figures*, no. ISBN 978-0-06-236360-2, William Morrow and Company, 2016.
- [57] A. Selby, *Who is the great Dorthy Vaughn*, no. ISBN 1978491069, Ladies Image Publishing, 2017.
- [58] O. Lutz, [When computers were human](#), NASA JPL, 2016.  
URL <https://www.nasa.gov/feature/jpl/when-computers-were-human>
- [59] J. Walsh, *Human Computers at NASA project*, Digital Commons @ Macalester, 2016.
- [60] A. Celletti, E. Perozzi, *Celestial Mechanics: The Waltz of the Planets*, Springer (in association with Praxis Publishing), 2007.
- [61] E. Belbruno, *Fly me to the moon*, Princeton University Press, Princeton, NJ, 2007, an insider's guide to the new science of space travel, With a foreword by Neil deGrasse Tyson.
- [62] W.-J. Beyn, E. Doedel, [Stability and multiplicity of solutions to discretizations of nonlinear ordinary differential equations](#), *SIAM J. Sci. Statist. Comput.* 2 (1) (1981) 107–120. doi:10.1137/0902009.  
URL <http://dx.doi.org/10.1137/0902009>
- [63] W.-J. Beyn, [The numerical computation of connecting orbits in dynamical systems](#), *IMA J. Numer. Anal.* 10 (3) (1990) 379–405. doi:10.1093/imanum/10.3.379.  
URL <http://dx.doi.org.proxy.libraries.rutgers.edu/10.1093/imanum/10.3.379>
- [64] E. J. Doedel, M. J. Friedman, [Numerical computation of heteroclinic orbits](#), *J. Comput. Appl. Math.* 26 (1-2) (1989) 155–170, continuation techniques and bifurcation problems. doi:10.1016/0377-0427(89)90153-2.  
URL [http://dx.doi.org.proxy.libraries.rutgers.edu/10.1016/0377-0427\(89\)90153-2](http://dx.doi.org.proxy.libraries.rutgers.edu/10.1016/0377-0427(89)90153-2)
- [65] M. J. Friedman, E. J. Doedel, [Computational methods for global analysis of homoclinic and heteroclinic orbits: a case study](#), *J. Dynam. Differential Equations* 5 (1) (1993) 37–57. doi:10.1007/BF01063734.  
URL <http://dx.doi.org.proxy.libraries.rutgers.edu/10.1007/BF01063734>
- [66] E. J. Doedel, M. J. Friedman, B. I. Kunin, [Successive continuation for locating connecting orbits](#), *Numer. Algorithms* 14 (1-3) (1997) 103–124, dynamical numerical analysis (Atlanta, GA, 1995).
- [67] F. J. Muñoz Almaraz, E. Freire, J. Galán, E. Doedel, A. Vanderbauwhede, [Continuation of periodic orbits in conservative and Hamiltonian systems](#), *Phys. D* 181 (1-2) (2003) 1–38. doi:10.1016/S0167-2789(03)00097-6.  
URL [https://doi-org.ezproxy.fau.edu/10.1016/S0167-2789\(03\)00097-6](https://doi-org.ezproxy.fau.edu/10.1016/S0167-2789(03)00097-6)
- [68] E. J. Doedel, B. W. Kooi, G. A. K. van Voorn, Y. A. Kuznetsov, [Continuation of connecting orbits in 3D-ODEs. I. Point-to-cycle connections](#), *Internat. J. Bifur. Chaos Appl. Sci. Engrg.* 18 (7) (2008) 1889–1903. doi:10.1142/S0218127408021439.  
URL <http://dx.doi.org.proxy.libraries.rutgers.edu/10.1142/S0218127408021439>
- [69] E. J. Doedel, B. W. Kooi, G. A. K. Van Voorn, Y. A. Kuznetsov, [Continuation of connecting orbits in 3D-ODEs. II. Cycle-to-cycle connections](#), *Internat. J. Bifur. Chaos Appl. Sci. Engrg.* 19 (1) (2009) 159–169. doi:10.1142/S0218127409022804.  
URL <http://dx.doi.org/10.1142/S0218127409022804>
- [70] R. C. Calleja, E. J. Doedel, A. R. Humphries, A. Lemus-Rodríguez, E. B. Oldeman, [Boundary-value problem formulations for computing invariant manifolds and connecting orbits in the circular restricted three body problem](#), *Celestial Mech. Dynam. Astronom.* 114 (1-2) (2012) 77–106. doi:10.1007/s10569-012-9434-y.  
URL <https://doi-org.ezproxy.fau.edu/10.1007/s10569-012-9434-y>
- [71] G. Gómez, J. Llibre, R. Martínez, C. Simó, [Dynamics and mission design near libration points. Vol. I](#), Vol. 2 of World Scientific Monograph Series in Mathematics, World Scientific Publishing Co., Inc., River Edge, NJ, 2001, fundamentals: the case of collinear libration points, With a foreword by Walter Flury. doi:10.1142/9789812810632\_bmatter.  
URL [https://doi-org.ezproxy.fau.edu/10.1142/9789812810632\\_bmatter](https://doi-org.ezproxy.fau.edu/10.1142/9789812810632_bmatter)

- [72] G. Gómez, C. Simó, J. Llibre, R. Martínez, Dynamics and mission design near libration points. Vol. II, Vol. 3 of World Scientific Monograph Series in Mathematics, World Scientific Publishing Co., Inc., River Edge, NJ, 2001, fundamentals: the case of triangular libration points.
- [73] G. Gómez, A. Jorba, C. Simó, J. Masdemont, Dynamics and mission design near libration points. Vol. III, Vol. 4 of World Scientific Monograph Series in Mathematics, World Scientific Publishing Co., Inc., River Edge, NJ, 2001, advanced methods for collinear points.
- [74] G. Gómez, A. Jorba, C. Simó, J. Masdemont, Dynamics and mission design near libration points. Vol. IV, Vol. 5 of World Scientific Monograph Series in Mathematics, World Scientific Publishing Co., Inc., River Edge, NJ, 2001, advanced methods for triangular points.
- [75] W. S. Koon, M. W. Lo, J. E. Marsden, S. D. Ross, Dynamical systems, the three-body problem and space mission design, in: International Conference on Differential Equations, Vol. 1, 2 (Berlin, 1999), World Sci. Publ., River Edge, NJ, 2000, pp. 1167–1181.
- [76] G. Gómez, W. S. Koon, M. W. Lo, J. E. Marsden, J. Masdemont, S. D. Ross, [Connecting orbits and invariant manifolds in the spatial restricted three-body problem](https://doi-org.ezproxy.fau.edu/10.1088/0951-7715/17/5/002), Nonlinearity 17 (5) (2004) 1571–1606.  
URL <https://doi-org.ezproxy.fau.edu/10.1088/0951-7715/17/5/002>
- [77] W. S. Koon, J. E. Marsden, S. D. Ross, M. W. Lo, [Constructing a low energy transfer between Jovian moons](https://doi-org.ezproxy.fau.edu/10.1090/conm/292/04919), in: Celestial mechanics (Evanston, IL, 1999), Vol. 292 of Contemp. Math., Amer. Math. Soc., Providence, RI, 2002, pp. 129–145.  
URL <https://doi-org.ezproxy.fau.edu/10.1090/conm/292/04919>
- [78] E. Barrabés, J. M. Mondelo, M. Ollé, [Numerical continuation of families of homoclinic connections of periodic orbits in the rtbp](https://dx.doi.org/10.1088/0951-7715/22/12/006) 22 (12) (2009) 2901. doi:10.1088/0951-7715/22/12/006.  
URL <https://dx.doi.org/10.1088/0951-7715/22/12/006>
- [79] E. Barrabés, J. M. Mondelo, M. Ollé, [Numerical continuation of families of heteroclinic connections between periodic orbits in a hamiltonian system](https://dx.doi.org/10.1088/0951-7715/26/10/2747) 26 (10) (2013) 2747. doi:10.1088/0951-7715/26/10/2747.  
URL <https://dx.doi.org/10.1088/0951-7715/26/10/2747>
- [80] B. Kumar, R. L. Anderson, R. de la Llave, [High-order resonant orbit manifold expansions for mission design in the planar circular restricted 3-body problem](https://doi.org/10.1016/j.cnsns.2021.105691), Communications in Nonlinear Science and Numerical Simulation 97 (2021) 105691. doi:<https://doi.org/10.1016/j.cnsns.2021.105691>.  
URL <https://www.sciencedirect.com/science/article/pii/S1007570421000022>
- [81] B. Kumar, R. L. Anderson, R. de la Llave, [Rapid and accurate methods for computing whiskered tori and their manifolds in periodically perturbed planar circular restricted 3-body problems](https://doi.org/10.1007/s10569-021-10057-1), Celestial Mech. Dynam. Astronom. 134 (1) (2022) Paper No. 3, 38. doi:10.1007/s10569-021-10057-1.  
URL <https://doi.org/10.1007/s10569-021-10057-1>
- [82] M. Barcelona, A. Haro, J.-M. Mondelo, [Semi-analytical computation of heteroclinic connections between center manifolds with the parameterization method](https://arxiv.org/abs/2301.08526) (2023). doi:10.48550/ARXIV.2301.08526.  
URL <https://arxiv.org/abs/2301.08526>
- [83] M. Dellnitz, O. Junge, W. S. Koon, F. Lekien, M. W. Lo, J. E. Marsden, K. Padberg, R. Preis, S. D. Ross, B. Thiere, [Transport in dynamical astronomy and multibody problems](https://doi-org.ezproxy.fau.edu/10.1142/S0218127405012545), Internat. J. Bifur. Chaos Appl. Sci. Engrg. 15 (3) (2005) 699–727.  
URL <https://doi-org.ezproxy.fau.edu/10.1142/S0218127405012545>
- [84] G. Arioli, [Branches of periodic orbits for the planar restricted 3-body problem](http://dx.doi.org.ezproxy.fau.edu/10.3934/dcds.2004.11.745), Discrete Contin. Dyn. Syst. 11 (4) (2004) 745–755. doi:10.3934/dcds.2004.11.745.  
URL <http://dx.doi.org.ezproxy.fau.edu/10.3934/dcds.2004.11.745>
- [85] G. Arioli, V. Barutello, S. Terracini, [A new branch of Mountain Pass solutions for the choreographical 3-body problem](http://dx.doi.org.ezproxy.fau.edu/10.1007/s00220-006-0111-4), Comm. Math. Phys. 268 (2) (2006) 439–463. doi:10.1007/s00220-006-0111-4.  
URL <http://dx.doi.org.ezproxy.fau.edu/10.1007/s00220-006-0111-4>
- [86] T. Kapela, P. Zgliczyński, [The existence of simple choreographies for the  \$N\$ -body problem—a computer-assisted proof](http://dx.doi.org.ezproxy.fau.edu/10.1088/0951-7715/16/6/302), Nonlinearity 16 (6) (2003) 1899–1918. doi:10.1088/0951-7715/16/6/302.  
URL <http://dx.doi.org.ezproxy.fau.edu/10.1088/0951-7715/16/6/302>
- [87] T. Kapela, [N-body choreographies with a reflectional symmetry—computer assisted existence proofs](http://dx.doi.org.ezproxy.fau.edu/10.1142/9789812702067_0165), in: EQUADIFF 2003, World Sci. Publ., Hackensack, NJ, 2005, pp. 999–1004. doi:10.1142/9789812702067\_0165.  
URL [http://dx.doi.org.ezproxy.fau.edu/10.1142/9789812702067\\_0165](http://dx.doi.org.ezproxy.fau.edu/10.1142/9789812702067_0165)

- [88] T. Kapela, C. Simó, [Rigorous KAM results around arbitrary periodic orbits for Hamiltonian systems](#), *Nonlinearity* 30 (3) (2017) 965–986. doi:10.1088/1361-6544/aa4ff3.  
URL <http://dx.doi.org.ezproxy.fau.edu/10.1088/1361-6544/aa4ff3>
- [89] T. Kapela, C. Simó, [Computer assisted proofs for nonsymmetric planar choreographies and for stability of the Eight](#), *Nonlinearity* 20 (5) (2007) 1241–1255. doi:10.1088/0951-7715/20/5/010.
- [90] J. Burgos-García, J.-P. Lessard, J. D. Mireles James, [Spatial periodic orbits in the equilateral circular restricted four-body problem: computer-assisted proofs of existence](#), *Celestial Mech. Dynam. Astronom.* 131 (1) (2019) Art. 2, 36. doi:10.1007/s10569-018-9879-8.  
URL <https://doi-org.ezproxy.fau.edu/10.1007/s10569-018-9879-8>
- [91] R. Calleja, C. García-Azpeitia, J.-P. Lessard, J. D. Mireles James, [Torus knot choreographies in the  \$n\$ -body problem](#), *Nonlinearity* 34 (1) (2021) 313–349. doi:10.1088/1361-6544/abcb08.  
URL <https://doi.org/10.1088/1361-6544/abcb08>
- [92] I. Walawska, D. Wilczak, [Validated numerics for period-tupling and touch-and-go bifurcations of symmetric periodic orbits in reversible systems](#), *Commun. Nonlinear Sci. Numer. Simul.* 74 (2019) 30–54. doi:10.1016/j.cnsns.2019.03.005.  
URL <https://doi.org/10.1016/j.cnsns.2019.03.005>
- [93] G. Arioli, [Periodic orbits, symbolic dynamics and topological entropy for the restricted 3-body problem](#), *Comm. Math. Phys.* 231 (1) (2002) 1–24. doi:10.1007/s00220-002-0666-7.  
URL <http://dx.doi.org.ezproxy.fau.edu/10.1007/s00220-002-0666-7>
- [94] D. Wilczak, P. Zgliczynski, [Heteroclinic connections between periodic orbits in planar restricted circular three-body problem—a computer assisted proof](#), *Comm. Math. Phys.* 234 (1) (2003) 37–75. doi:10.1007/s00220-002-0709-0.  
URL <http://dx.doi.org.proxy.libraries.rutgers.edu/10.1007/s00220-002-0709-0>
- [95] M. J. Capiński, [Computer assisted existence proofs of Lyapunov orbits at  \$L\_2\$  and transversal intersections of invariant manifolds in the Jupiter-Sun PCR3BP](#), *SIAM J. Appl. Dyn. Syst.* 11 (4) (2012) 1723–1753. doi:10.1137/110847366.  
URL <http://dx.doi.org/10.1137/110847366>
- [96] S. Kepley, J. D. Mireles James, [Chaotic motions in the restricted four body problem via Devaney’s saddle-focus homoclinic tangle theorem](#), *J. Differential Equations* 266 (4) (2019) 1709–1755. doi:10.1016/j.jde.2018.08.007.  
URL <https://doi-org.ezproxy.fau.edu/10.1016/j.jde.2018.08.007>
- [97] J. Galante, V. Kaloshin, [Destruction of invariant curves in the restricted circular planar three-body problem by using comparison of action](#), *Duke Math. J.* 159 (2) (2011) 275–327. doi:10.1215/00127094-1415878.  
URL <https://doi.org/10.1215/00127094-1415878>
- [98] M. Capiński, M. Guardia, P. Martín, T. M. Seara, P. Zgliczyński, [Oscillatroy motions and parabolic manifolds at infinity in the planar circular restricted three body problem](#), *Journal of Differential Equations* 320 (3) (2022) 316–370.
- [99] M. Capiński, P. Roldán, [Existence of a center manifold in a practical domain around  \$L\_1\$  in the restricted three body problem](#), *SIAM J. Appl. Dyn. Syst.* 11 (1) (2011) 285–318.
- [100] M. Capiński, N. Wodka, [Computer assisted proof of drift orbits along normally hyperbolic manifolds ii: applications to the restricted three body problem](#), (Submitted) (2021).
- [101] M. Capiński, M. Gidea, [Arnold diffusion, quantitative estimates and stochastic behavior in the three-body problem](#), *Communications on Pure and Applied Mathematics* (2018).
- [102] A. Celletti, L. Chierchia, [A computer-assisted approach to small-divisors problems arising in Hamiltonian mechanics](#), in: *Computer aided proofs in analysis* (Cincinnati, OH, 1989), Vol. 28 of IMA Vol. Math. Appl., Springer, New York, 1991, pp. 43–51.  
URL [https://doi-org.ezproxy.fau.edu/10.1007/978-1-4613-9092-3\\_6](https://doi-org.ezproxy.fau.edu/10.1007/978-1-4613-9092-3_6)
- [103] R. de la Llave, D. Rana, [Accurate strategies for K.A.M. bounds and their implementation](#), in: *Computer aided proofs in analysis* (Cincinnati, OH, 1989), Vol. 28 of IMA Vol. Math. Appl., Springer, New York, 1991, pp. 127–146. doi:10.1007/978-1-4613-9092-3\_12.  
URL [http://dx.doi.org/10.1007/978-1-4613-9092-3\\_12](http://dx.doi.org/10.1007/978-1-4613-9092-3_12)
- [104] J.-L. Figueras, A. Haro, A. Luque, [Rigorous computer assisted application of kam theory: a modern approach](#), (Submitted) arXiv:1601.00084 [math.DS] (2016).
- [105] F. Gabern, A. Jorba, U. Locatelli, [On the construction of the Kolmogorov normal form for the Trojan asteroids](#), *Nonlinearity* 18 (4) (2005) 1705–1734. doi:10.1088/0951-7715/18/4/017.  
URL <https://doi.org/10.1088/0951-7715/18/4/017>
- [106] C. Caracciolo, U. Locatelli, [Computer-assisted estimates for Birkhoff normal forms](#), *J. Comput. Dyn.* 7 (2) (2020) 425–460. doi:10.3934/jcd.2020017.

- URL <https://doi.org/10.3934/jcd.2020017>
- [107] O. E. Lanford, III, *Computer-assisted proofs in analysis*, Phys. A 124 (1-3) (1984) 465–470, mathematical physics, VII (Boulder, Colo., 1983). doi:10.1016/0378-4371(84)90262-0. URL [http://dx.doi.org/10.1016/0378-4371\(84\)90262-0](http://dx.doi.org/10.1016/0378-4371(84)90262-0)
- [108] H. Koch, A. Schenkel, P. Wittwer, *Computer-assisted proofs in analysis and programming in logic: a case study*, SIAM Rev. 38 (4) (1996) 565–604. doi:10.1137/S0036144595284180. URL <http://dx.doi.org/10.1137/S0036144595284180>
- [109] J. B. van den Berg, J. Lessard, *Rigorous numerics in dynamics*, Notices Amer. Math. Soc. 62 (9) (2015) 1057–1061.
- [110] J. Gómez-Serrano, *Computer-assisted proofs in PDE: a survey*, SeMA J. 76 (3) (2019) 459–484. doi:10.1007/s40324-019-00186-x. URL <https://doi.org/10.1007/s40324-019-00186-x>
- [111] W. Tucker, *Validated numerics*, Princeton University Press, Princeton, NJ, 2011, a short introduction to rigorous computations.
- [112] M. T. Nakao, M. Plum, Y. Watanabe, *Numerical verification methods and computer-assisted proofs for partial differential equations*, Vol. 53 of Springer Series in Computational Mathematics, Springer, Singapore, [2019] ©2019. doi:10.1007/978-981-13-7669-6. URL <https://doi.org/10.1007/978-981-13-7669-6>
- [113] T. Kapela, M. Mrozek, D. Wilczak, P. Zgliczyński, *CAPD::DynSys: A flexible c++ toolbox for rigorous numerical analysis of dynamical systems*, Communications in Nonlinear Science and Numerical Simulation 101 (2021) 105578. doi:https://doi.org/10.1016/j.cnsns.2020.105578. URL <https://www.sciencedirect.com/science/article/pii/S1007570420304081>
- [114] P. Zgliczynski,  $C^1$  Lohner algorithm, Found. Comput. Math. 2 (4) (2002) 429–465. doi:10.1007/s102080010025.
- [115] D. Wilczak, P. Zgliczynski,  $c^n$ -lohner algorithm, Scheide Informaticae 20 (2011) 9–46.
- [116] J. D. Mireles James, *Validated numerics for equilibria of analytic vector fields: invariant manifolds and connecting orbits*, in: Rigorous numerics in dynamics, Vol. 74 of Proc. Sympos. Appl. Math., Amer. Math. Soc., Providence, RI, 2018, pp. 27–80.
- [117] J. D. M. James, M. Murray, *Computer assisted proof of homoclinic chaos in the spatial equilateral restricted four body problem* (2022). doi:10.48550/ARXIV.2212.00930. URL <https://arxiv.org/abs/2212.00930>
- [118] F. J. Muñoz Almaraz, J. Galán, E. Freire, *Numerical continuation of periodic orbits in symmetric Hamiltonian systems*, in: International Conference on Differential Equations, Vol. 1, 2 (Berlin, 1999), World Sci. Publ., River Edge, NJ, 2000, pp. 919–921.
- [119] E. J. Doedel, R. C. Paffenroth, H. B. Keller, D. J. Dichmann, J. Galán-Vioque, A. Vanderbauwhede, *Computation of periodic solutions of conservative systems with application to the 3-body problem*, Internat. J. Bifur. Chaos Appl. Sci. Engrg. 13 (6) (2003) 1353–1381. doi:10.1142/S0218127403007291. URL <https://doi-org.ezproxy.fau.edu/10.1142/S0218127403007291>
- [120] J. B. van den Berg, A. Deschênes, J.-P. Lessard, J. D. Mireles James, *Stationary coexistence of hexagons and rolls via rigorous computations*, SIAM Journal on Applied Dynamical Systems 14 (2) (2015) 942–979.
- [121] S. Kepley, J. D. Mireles James, *Homoclinic dynamics in a restricted four-body problem: transverse connections for the saddle-focus equilibrium solution set*, Celestial Mech. Dynam. Astronom. 131 (3) (2019) Paper No. 13, 55. doi:10.1007/s10569-019-9890-8. URL <https://doi-org.ezproxy.fau.edu/10.1007/s10569-019-9890-8>
- [122] R. E. Moore, *Interval analysis*, Prentice-Hall Inc., Englewood Cliffs, N.J., 1966.
- [123] A. Neumaier, *Interval methods for systems of equations*, Vol. 37 of Encyclopedia of Mathematics and its Applications, Cambridge University Press, Cambridge, 1990.
- [124] A. Neumaier, S. Zu He, *The Krawczyk operator and Kantorovich’s theorem*, J. Math. Anal. Appl. 149 (2) (1990) 437–443. doi:10.1016/0022-247X(90)90053-I. URL [https://doi.org/10.1016/0022-247X\(90\)90053-I](https://doi.org/10.1016/0022-247X(90)90053-I)
- [125] S. M. Rump, *Verification methods: rigorous results using floating-point arithmetic*, Acta Numer. 19 (2010) 287–449. doi:10.1017/S096249291000005X. URL <http://dx.doi.org/10.1017/S096249291000005X>
- [126] J. B. van den Berg, J.-P. Lessard (Eds.), *Rigorous numerics in dynamics*, Vol. 74 of Proceedings of Symposia in Applied Mathematics, American Mathematical Society, Providence, RI, 2018, aMS Short Course: Rigorous Numerics in Dynamics, January 4–5, 2016, Seattle, Washington. doi:10.1090/psapm/074.

- URL <https://doi.org/10.1090/psapm/074>
- [127] P. Zgliczynski,  $C^1$  Lohner algorithm, *Found. Comput. Math.* 2 (4) (2002) 429–465. doi:10.1007/s102080010025.  
URL <https://doi.org/10.1007/s102080010025>
- [128] J. D. Mireles James, Validated numerics for equilibria of analytic vector fields: invariant manifolds and connecting orbits, (To appear in AMS lecture notes - winter short course series) (2017) 1–55.
- [129] S. Rump, INTLAB - INTerval LABoratory, in: T. Csentes (Ed.), *Developments in Reliable Computing*, Kluwer Academic Publishers, Dordrecht, 1999, pp. 77–104, <http://www.ti3.tu-harburg.de/rump/>.
- [130] X. Cabré, E. Fontich, R. de la Llave, The parameterization method for invariant manifolds. III. Overview and applications, *J. Differential Equations* 218 (2) (2005) 444–515.
- [131] A. Haro, M. Canadell, J.-L. s. Figueras, A. Luque, J.-M. Mondelo, [The parameterization method for invariant manifolds](#), Vol. 195 of Applied Mathematical Sciences, Springer, [Cham], 2016, from rigorous results to effective computations. doi:10.1007/978-3-319-29662-3.  
URL <http://dx.doi.org.ezproxy.fau.edu/10.1007/978-3-319-29662-3>